12-13-2021

Central Respiratory Depression: Insight With Murine Models Of Rett Syndrome And Morphine Overdose

Hao Xing

Recommended Citation
Xing, Hao, "Central Respiratory Depression: Insight With Murine Models Of Rett Syndrome And Morphine Overdose." Dissertation, Georgia State University, 2021.
doi: https://doi.org/10.57709/24829597

CENTRAL RESPIRATORY DEPRESSION : INSIGHT WITH MURINE MODELS OF RETT SYNDROME AND MORPHINE OVERDOSE

by

HAO XING

Under the Direction of Chun Jiang, PhD

A Dissertation Submitted in Partial Fulfillment of the Requirements for the Degree of

Doctor of Philosophy

in the College of Arts and Sciences

Georgia State University

2021

ABSTRACT

Breathing is generated and controlled by brainstem neurons with several sensory feedback loops, where neurotransmission and neuronal membrane excitability play critical roles. Although such a neural control provides stable and dynamic breathing activity, central respiration depression (CRD) can occur in several diseases and drug misuses, which often leads to severe consequences and death. Questions remain open regarding how the neurotransmission and cellular excitability are changed in CRD; what cellular and molecular mechanisms underlie the changes; and whether they can be corrected with pharmacological agents. This dissertation is to address these questions, with two murine models showing characteristic CRD. One is the mouse model of Rett syndrome (RTT), and the other is the rat model of morphine-induced CRD. Experiments were performed in the models where evidence was obtained with *in vivo* plethysmography and *in vitro* recording from brainstem neurons. In the RTT model, we studied the levels of GABAergic and glycinergic signals of neurons in the hypoglossal nucleus (XII) and the dorsal motor nucleus of vagus (DMNV). In the control mice, equal proportions of $GABA_A$ergic and glycinergic synaptic inhibitions was found in the XII/ DMNV neurons. In the RTT model, the deficiency in $GABA_A$ergic neurotransmission was more severe, and these cells relied more on glycinergic synaptic inhibition. In the morphine-induced CRD model, a decrease in cellular excitability was observed in the locus coeruleus (LC) neurons in which the G-protein coupled inwardly rectifying K^+ (GIRK) channels played a role. The GIRK channel is a downstream target of μ opioid receptor (MOR). The activation of MOR by morphine opens the GIRK channels to hyperpolarize LC neurons. Thus, GIRK channel blocker cloperastine (CPS), an antitussive, was tested. We found that CPS alleviated the morphine-induced CRD, and improved morphine-induced inhibition of LC neurons. We also showed that the CPS action

involved inhibitions of GIRK channels in LC neurons, presynaptic glutamatergic neurons, and metabotropic glutamate receptors in the presynaptic terminals. Therefore, several molecular targets regulating neurotransmission and membrane excitability have been demonstrated to be critical for CRD. Pharmacologic targeting on the molecules appears to a novel and promising approach to CRD.

INDEX WORDS: Respiratory depression, Rett syndrome, Hypoglossal nucleus, Dorsal motor nucleus of vagus, GABA, Glycine, Optogenetics, Morphine, μ opioid receptor, GIRK channels, Cloperastine, Glutamate

CENTRAL RESPIRATORY DEPRESSION：INSIGHT WITH MURINE MODELS OF RETT SYNDROME AND MORPHINE OVERDOSE

by

HAO XING

Committee Chair: Chun Jiang

Committee: Deborah Baro

Hang Shi

Electronic Version Approved:

Office of Graduate Studies

College of Arts and Sciences

Georgia State University

August 2021

DEDICATION

To my wife Hongmin Yao, who always support, encourage, and take care of me.

To my mother Xia Sun and my father Shiyan Xing, who love and support me without condition.

To people I love in my hometown and in heaven, I miss you all so much.

ACKNOWLEDGEMENTS

First and foremost, I would like to thank my advisor, Dr. Chun Jiang. He is really a good research advisor and mentor, who has been supporting and pushing me to achieve my Ph.D. degree. Without his guidance and help, I would not be where I am today.

Secondly, I would like to thank my committee members, Dr. Deborah Baro and Dr. Hang Shi for their invaluable suggestions and advice helping me to perform better research and improved my projects.

I would also like to thank some faculty members at GSU. Dr. Bingzhong Xue supplied their valuable advising when I took my qualifying examination. Dr. Paul Ulrich offered me the teaching position and guided my teaching. Dr. Blaustein and Drew helped me be become a qualified teaching assistant by showing me many great teaching skills and providing wonderful teaching guidance. Thanks Dr. Vincent Rehder for sharing the important scholarship information.

I would also like to thank the staff at GSU. LaTesha Warren and Tameka Hudson have been so professional in administrative guidance and assistance. Barry Grant for his help with maintenance and repairs. Members from biology core facility, Ping Jiang, Sonja Young, Gemia Cameron, Hyek-Kyu Seoh and Debby Walthall, have been very helpful in completing the related experiments. Katrina Joyner and Tamiko Brown for their assistance with ordering issues. Department of animal resources staff, especially Joey, Kim, Robert, and Courtney, for their assistance and advice for animal handling and maintaining.

I would also like to thank the colleagues and friends I met in GSU, including but not limited to Dr. Ningren Cui, Dr. Yang Wu, Dr. Lei Yu, Dr. Weiwei Zhong, Dr. Shuang Zhang, and Dr. Christopher M. Johnson.

I acknowledge Brain and Behavior (B&B) Fellowship program for their financial support of my study and research.

TABLE OF CONTENTS

LIST OF TABLES

LIST OF FIGURES

ABBREVIATIONS

5-HT	5-hydroxytryptamine or serotonin
$5\text{-HT}_{1A/2A/3/4A/7}$	serotonin receptor subtype 1A/2A/3/4A/7
Ach	acetylcholine
aCSF	artificial cerebrospinal fluid
AHP	afterhyperpolarization
AMPA	α-amino-3-hydroxy-5-methyl-4-isoxazolepropionic acid
AP_5	(2R)-amino-5-phosphonovaleric acid
Bccl	bicuculline
BötC	Bötzinger complex
ChR	channorodopsin
CNQX	6-cyano-7-nitroquinoxaline-2,3-dione
CNS	central nervous system
CPS	cloperastine
CRD	central respiratory depression
Cre	cre recombinase
cVRG	caudal VRG
DAMGO	(D-Ala^2, N-$MePhe^4$, Gly-ol)-enkephalin
DBH	dopamine beta hydroxylase
DE	delayed excitation
DMNV	dorsal motor nucleus of vagus
DOR	σ opioid receptor
DRG	dorsal respiratory group

DTN	dorsal tegmental nucleus
E2	expiration
Early-I	early inspiration
EEG	electrocardiogram
eGFP	enhanced green fluorescent protein
E_K	K^+ equilibrium potential
EPSCs	excitatory postsynaptic currents
ER	endoplasmic reticulum
f	firing frequency
GABA	γ-aminobutyric acid
$GABA_AR$	$GABA_A$ receptor
$GABA_AR\gamma2$	$GABA_A$ receptor γ2 subunit
$GABA_BR$	$GABA_B$ receptor
GABAR	GABA receptor
GAD	glutamic acid decarboxylase
GFAP	glial fibrillary acidic protein
GIRK	G protein-coupled inwardly rectifying K^+ channels
GlyRβ	glycine receptor β subunit
I	inspiration
IPSCs	inhibitory postsynaptic currents
i.p.	intraperitoneal
KF	Kölliker-Fuse nucleus
K_{ir}	inwardly rectifying K^+ channels

KOR	κ opioid receptor
LC	nucleus of the Locus Coeruleus
LoxP	locus of X-over P1
MECP2	human methyl CpG binding protein 2 gene
MeCP2	methyl CpG binding protein 2
Mecp2	animal methyl CpG binding protein 2 gene
$Mecp2^{-/Y}$	hemizygous male animal with *Mecp2* gene knockout
$Mecp2^{+/-}$	heterozygous female animal with *Mecp2* gene disruption
$Mecp2^{R168X}$	animal *Mecp2* gene with R168X point mutation
mGluR	metabotropic glutamate receptor
mIPSCs	miniature inhibitory postsynaptic currents
MOR	μ opioid receptor
mPB	medial parabrachial nucleus
nAChRs	nicotinic acetylcholine receptors
NE	norepinephrine
NK1R	neurokinin 1 receptor
NMDA	N-methyl-D-aspartate
NOR	Nociceptin receptor
PFC	prefrontal cortex
PiCo	postinspiratory complex
PIR	post-inhibitory rebound
Post-I/E1	post inspiration
preBötC	pre-Bötzinger complex

PV	paravalbumin
RT-PCR	reverse transcription polymerase chain reaction
RTT	Rett Syndrome
rVRG	rostral VRG
SFA	spike frequency adaptation
Stcn	Strychnine
s.c.	subcutaneous
TH	tyrosine hydroxylase
TTX	tetrodotoxin
VRG	ventral respiratory group
XII	hypoglossal nucleus
ZOR	ζ opioid receptor

1 HYPOTHESES AND SPECIFIC AIMS

As a fundamental process supporting all systemic functions, breathing is generated and controlled by brainstem neurons with several sensory feedback loops, where neurotransmission and neuronal membrane excitability are likely to play a critical role. Although such a neural control provides stable and dynamic breathing activity, central respiration can be compromised in several diseases and drug misuses. Such a condition known as central respiration depression (CRD) often leads to severe consequences and death. Despite tremendous investigation of the CRD over past decades, many questions related to the role of neurotransmission and cellular excitability in the CRD remain open. For instance, how does abnormality of brainstem neurons lead to CRD? What cellular mechanisms play a role? What molecules responsible for neurotransmission and neuronal membrane excitability are involved in CRD? Can these molecules be targeted via manipulating neurotransmission and cellular excitability to reverse or alleviate CRD? To answer these questions, this dissertation study was designed and performed with using electrophysiology, optogenetics, and whole-body plethysmography. My **hypothesis** is that CRD is caused by abnormalities of a few molecules responsible for neurotransmission and membrane excitability, finding of which helps not only the understanding of the CRD but also its treatment. Two experimental models were chosen to test the hypothesis. Both display clear CRD. One of them is a mouse model of the genetic disease Rett syndrome (RTT), and the other is opioid overdose. Both involve brainstem neurons that are fully accessible in this lab. Defect in inhibitory neurotransmission plays a role in RTT model of mice, while imbalanced excitatory neurotransmission / neuronal excitability via μ opioid receptor (MOR) are critical in morphine-induced CRD rats. Several molecules are involved including γ aminobutyric acid (GABA), glycine, MOR and G protein coupled inwardly rectifying K^+ (GIRK) channels. There are

pharmacologic tools for manipulating these molecules. Using these animal models, we may be able to shed insight into the common mechanisms involving defects in neurotransmissions and abnormal neuronal excitability in CRD. These may open new fields of research in searching for novel therapeutic treatments of several central respiratory disorders in humans.

Specific Aim: To demonstrate the abnormality of critical molecules that are responsible for neurotransmission and/or membrane excitability and attributable to the CRD, and potential pharmacological correction.

Sub Aim 1*: To determine inhibitory neurotransmission mediated by distinct GABAergic and glycinergic signals in brainstem neurons and their alterations in Mecp2-disrupted mice*.

Experiments were performed in *Mecp2*$^{-/Y}$ mice to answer the questions: How are the inhibitory neurotransmitters GABA and glycine in hypoglossal nucleus (XII) / dorsal motor nucleus of vagus (DMNV) neurons affected after methyl-CpG binding protein 2 gene (*Mecp2*) disruption? How do $GABA_A$-ergic and glycinergic signals account for the inhibitory neurotransmitters in these brainstem neurons of normal mice? Do the changes in $GABA_A$ and glycine signaling in XII/DMNV contribute to the neurotransmission abnormality in *Mecp2*$^{-/Y}$ mice?

Sub Aim 2*: To elucidate GIRK channel-mediated neurotransmission in the rat model of morphine-induced CRD*.

Experiments were performed in morphine-induced CRD rats with several questions to address: Can the blockade of GIRK channels with cloperastine (CPS) alleviate morphine-induced CRD? Can CPS improve survival of the rats with CRD? What is the potency of CPS for GIRK channel inhibition? How does CPS affect LC neuronal excitability and electrophysiological responses to morphine? Are these LC neuronal responses postsynaptic,

presynaptic or both? What presynaptic neurons are involved? How does CPS affect the regulation of neurotransmitter release at synaptic terminals?

2 INTRODUCTION

2.1 Respiration generation and control

Breathing activity is generated and controlled by brainstem neurons in the medulla oblongata and the pons. In the medulla, there are two respiratory centers, i.e., the dorsal respiratory group (DRG) and the ventral respiratory group (VRG). The pontine respiratory center is located in the dorsolateral region in Kölliker-Fuse (KF), medial parabrachial nucleus (mPB), and the LC. Traditionally, the pontine groups are also known as apneustic center and pneumotaxic center. These respiratory groups work as a network by highly elaborate neuronal connections, generating and regulating the breathing activity including breathing frequency and respiratory premotor neuronal output.

2.1.1 Respiration controlling neurons

In the medulla, the DRG is located in the nucleus tractus solitarius (NTS) that contains mainly inspiratory neurons sending promotor signals to the motor neurons of external intercostal muscles and diaphragm. The DRG also receives and integrate sensory afferents from airways and peripheral chemoreceptors (Jordan 2001, Song and Poon 2004). DRG neurons can be stimulated or inhibited by the signals from pontine neurons. The VRG is located around nucleus ambiguus (NA) where there are several subgroups of neurons containing both expiratory and inspiratory signals: the expiratory Bötzinger complex (BötC); inspiratory pre-Bötzinger complex (preBötC); inspiratory rostral VRG (rVRG); and the expiratory caudal VRG (cVRG) (Shannon and Lindsey 1987, Smith, Ellenberger et al. 1991, Schwarzacher, Smith et al. 1995, Gerrits and Holstege 1996). The VRG forms a column in the ventrolateral medulla, also known as the ventral respiratory column (VRC). Motor neurons in the VRC send signals to the pharyngeal/laryngeal muscles through vagus nerve, to diaphragm through phrenic nerve, and to external intercostal

muscles and internal intercostal muscles through the intercostal nerves. The expiratory motor drive in cats, rats and rabbits comes from the cVRG only, projecting to abdominal and internal intercostal muscles. The BötC, also acts as an expiratory neuronal group, mainly sending inhibitory signals to VRG, DRG and phrenic motor neurons (Jiang and Lipski 1990, Bongianni, Mutolo et al. 1997, Schreihofer, Stornetta et al. 1999, Bongianni, Mutolo et al. 2010).

The pontine respiratory groups mostly control the breathing rhythm and patterns. The pneumotaxic centers are located in the dorsolateral pons on the caudal side of the inferior colliculus, while the apneustic center is known to be in the central area of the lower pons (Gautier and Bertrand 1975, Alheid, Milsom et al. 2004). The pneumotaxic centers contain KF nucleus and mPB (Song, Yu et al. 2006), that have both inspiratory, expiratory and phase-spanning cells, and play a role in the switch of respiratory phase from inspiration to expiration and respiration reflex. Currently, how the pneumotaxic center interacts with the apneustic centers is still unclear. The pneumotaxic center is believed to act as an inhibitory center to the apneustic center, sending inhibitory impulses to medullary inspiratory neurons to terminate inspiration and increase the respiratory rate (Dutschmann and Dick 2012). The presence of functional apneustic center was suggested when its connection to pneumotaxic centers was interrupted with the vagus nerves cut, while direct evidence is still lacking. The absence of pneumotaxic center together with vagus nerve produces the prolonged inspiratory gasps interrupted by occasional expirations, a phenomenon known as apneusis.

Certain neurons within these two groups are known to be involved in respiration regulation. LC is a nucleus located in the caudal midbrain and rostral pons near to the lateral floor of the 4th ventricle. As the major pool of noradrenergic signaling in central nervous system (CNS), The LC induces excitatory modulation to most of its projection sites. The LC functions in arousal and

sleep-wake cycle, respiratory regulation, attention, emotion, and anxiety. The excitability of LC neurons is critical for the respiratory regulation in different conditions. The LC neuronal excitability can be affected by respiratory and metabolic acidosis that has been used as a psychiatric diagnostic approach with high CO_2 or intravenous lactate to evoke anxiety/panic attack. The DMNV is a medullary nucleus of the vagus nerve. The DMNV lies in the ventral to the floor of the 4^{th} ventricle. The DMNV motor neurons project to musculus uvulae as well as cardiac and laryngeal/pharyngeal muscles. Muscles in the latter two have respiratory rhythmicity and are responsible for the maintenance of airway dimension and reflex. The XII is found in the dorsal medulla ventral to the DMNV near to the midline of the medulla. The XII contains mostly motor neurons sending signals to control the extrinsic and intrinsic muscles of the tongue, mediating the movement of tongue includes protruding/deviating. These muscles are respiration-modulated and play an important part in sleep apneas. LC, DMNV and XII neurons are modulated by various neurotransmitters or peptides like GABA, glycine, glutamate, acetylcholine (Ach), as well as opioids (Inquimbert, Rodeau et al. 2007, Jin, Cui et al. 2013, Oginsky, Cui et al. 2014, McMenamin, Anselmi et al. 2016, Zhang, Johnson et al. 2016, Quaresma, Teixeira et al. 2020). Thus, their activities are critical during CRD development.

2.1.2 Network control

The neural circuit regulation of respiratory activity is a complicated process. It is known that breathing rhythm generation is produced by combined activity of pacemakers and neuronal interaction in their network. Respiratory neurons in the VRG interact with each other within VRG, also communicating with nuclei in pontine.

The VRG contains both excitatory and inhibitory respiratory neurons. The inhibitory neurons are mostly glycinergic, which is for regulating respiratory pattern; whereas the majority of

excitatory neurons in the preBötC is glutamatergic, who is responsible for rhythmogenesis (Feldman, Del Negro et al. 2013, Janczewski, Tashima et al. 2013), although it has been reported that some of the pacemaker neurons do not participate in rhythmogenesis (Del Negro, Morgado-Valle et al. 2002, Del Negro, Morgado-Valle et al. 2005, Feldman, Del Negro et al. 2013). One quarter of the glycinergic neurons in the preBötC shows properties as inspiratory pacemaker (Morgado-Valle, Baca et al. 2010), and GABAergic neurons are found within the preBötC with inspiratory firing pattern (Kuwana, Tsunekawa et al. 2006). These inhibitory signals within preBötC reduce the respiration rhythm without producing apneas (Janczewski, Tashima et al. 2013), suggesting that rhythmic regulation of respiration involves a postsynaptic inhibition within this region. Both rVRG and cVRG are known to utilize glycine for the phasic inhibition of the respiratory network (Ezure, Tanaka et al. 2003).

Once it was believed that, within the respiratory circuitry, the reciprocal inhibition of these interneurons were required to produce and maintain the respiration cycle. Although direct evidence supporting this scenario is still missing, synaptic inhibitions of these respiratory neurons are still critical for central respiratory activity. In rhythmogenesis circuits, the preBötC and BötC are the major groups within VRG in shaping respiration patterns. In the BötC, more than a half of the neurons is inhibitory, most of which are glycinergic while the rest is GABAergic (Winter, Fresemann et al. 2009). The PreBötC has been considered as the key point of inhibitory interaction site to communicate with other respiration centers to produce the three-phase breathing pattern, i.e., inspiration or I, post-inspiration or post-I/E1 and expiration or E2 (Richter and Smith 2014). The inhibitory communications include: 1) the inhibitory connection among inhibitory neurons, pre-inspiratory/inspiratory preBötC cells and BötC augmenting expiratory cells, 2) direct or indirect inhibitory communications with preBötC early-inspiratory

(early-I) neurons and BötC post-I cells. Some studies reveal that early-I, post-I and E2 neurons are able to form an inhibition ring to regulate respiration (Smith, Abdala et al. 2013).

It is still unclear how the respiratory groups form the excitatory neuronal circuits. Medullary DRG and pontine respiratory groups send excitatory impulses to neurons in BötC, pre-BötC, rVRG and cVRG, and these signals are either phasic or tonic (Smith, Abdala et al. 2013). The excitatory pre-I/I neurons in preBötC give certain projections onto the premotor rVRG and cVRG neurons of phrenic motor neurons, and also project to the motor DMNV/XII neurons. The cVRG premotor neurons project to thoracic and abdominal spinal expiratory motor neurons. Within the spinal cord, the inter-neuronal circuits regulate respiration motor activities. The BötC neurons can be conditionally activated to generate active expiratory activity. Evidence in postnatal animal shows that the BötC neurons give excitatory signals on the preBötC region, and in return, the preBötC sends both excitatory/inhibitory impulses on BötC cells (Tan, Pagliardini et al. 2010, Anderson and Ramirez 2017). Thus, it is reasonable to believe that preBötC acts as an excitation trigger to induce the E2 phase. In addition, a recent study proposes the interaction between the post-I generator post-inspiratory complex (PiCo) and the preBötC (Anderson, Garcia et al. 2016). When applied with $GABA_A$ receptor antagonist, the preBötC and PiCo synchronize their firing pattern into I phase (Anderson, Garcia et al. 2016). This evidence indicates that the inhibition of the neuronal network between PiCo and preBötC is necessary for the breathing rhythm maintenance. After abolishing the inhibitory neurotransmission, a dominant excitatory input from preBötC onto PiCo can emerge. Together, endogenous inhibitory signals overwhelm the excitatory input that originated from preBötC onto PiCo. Even with the evidence, the understandings of the respiration regulating mechanisms are still limited. Further studies are

necessary to elucidate the mechanisms underlying respiration rhythmogenesis in oscillatory networks especially in the CRD condition.

2.2 Central respiratory depression

2.2.1 Symptoms

Respiratory depression also known as hypoventilation, occurs when ventilation is inadequate to perform sufficient respiratory gas exchange due to central and peripheral causes. The latter is often caused by lung/airway injuries, severe obesity, and neuromuscular/developmental diseases. Most cases of respiratory depression are CRD. The causes leading to CRD vary: 1) medical conditions, such as physical injury including trauma to the CNS, 2) accidental or intentional overdose of chemicals/drugs, like opioids, barbiturates, benzodiazepines, and alcohol, 3) voluntary breath-holding like diving training and certain psychiatric diseases, and 4) late stage of CO_2 retention. The normal breathing rate of a healthy adult is 12–20 breaths/minute with tidal volume ~ 500ml, while the symptoms of CRD include slower and shallower breathing with breathing rates lower than 8 breaths/minute and a reduction in the tidal volume shows by over 20% with an increased breathing variation (Barbour, Vandebeek et al. 2004, Hill, Santhakumar et al. 2020). The CRD is not synonymous with respiratory arrest, where breathing activity completely stops, and death occurs within minutes. The CRD causes an increased concentration of CO_2 (hypercapnia) and respiratory acidosis. Moderate elevation of CO_2 stimulates breathing, while extreme hypercapnia inhibits breathing. Besides, the CRD is attributable to systemic hypoxia.

2.2.2 Central dysfunction

CNS depressant drugs, such as barbiturates, benzodiazepines, ethanol, and other sedatives produce CRD when they are overdosed or used in combination. Barbiturate belongs to

nonselective ligands that binding to various ligand-gated ion channels, including serotonin receptor subtype 3 (5-HT_3 receptor), glycine receptor, $GABA_A$ receptor and nicotinic acetylcholine receptor (nAChR). Benzodiazepines binds to the $GABA_A$ receptors as agonists to control the excitability of neurons. The enhanced inhibitory signals within respiration networks are some of the major mechanisms of CRD.

Multiple anti-nociceptive chemicals, include opioids and its derivatives, can also lead to CRD by affecting brainstem neurons including those in the preBötC (Montandon, Qin et al. 2011, Boom, Niesters et al. 2012). The neurokinin-1 receptor r (NK1R)-expressing preBötC neurons are reported sensitive to opioids, which is proved to be responsible for CRD in rats (Montandon, Qin et al. 2011). This opioid-induced CRD is likely mediated through the activation of MORs on the NK1R - expressing preBötC neurons (Montandon, Qin et al. 2011). The CRD can be reversed after the application of serotonin agonists (Manzke, Dutschmann et al. 2009, Boom, Niesters et al. 2012). Thus, one of the potential averting effects against the opioid-induced CRD is to target serotonin receptors in glycinergic preBötC neurons (Manzke, Dutschmann et al. 2009). LC neurons are highly sensitive to opioids as well. There is MOR expression in the LC. Hyperpolarization occurs when the LC is exposed to MOR agonists (Medrano, Santamarta et al. 2017, Enman, Reyes et al. 2019). Therefore, the pharmacological investigation to counteract CRD may involve the LC as well.

2.3 Central respiratory depression in different models

2.3.1 RTT

RTT is a neurodevelopmental disorder mostly associated with gene mutations in the methy-CpG-binding protein 2 (MeCP2) gene on X chromosome, which encodes the MeCP2 transcriptional regulator (Amir, Van den Veyver et al. 1999). It is mainly found in girls with

about 0.01% morbidity rate. Boys inherit mutations in human methy-CpG-binding protein 2 gene (*MECP2*) as well but usually died before birth. As transcriptional repressor and activator, MeCP2 is associated with maturation of the CNS and formation of synaptic connections. Neurological symptoms are firstly observed upon its disruption. The symptoms start from 6 months of age and deteriorate till the death. Typical RTT symptoms include mental and growth retardation, loss of motor function and spoken language, autism-like behaviors, and severe breathing disturbances. The breathing disorders in RTT is attributable to the high rate of sudden infant death (Del Negro, Koshiya et al. 2002). RTT patients exhibit severe hypoventilation interrupted with short hyperventilation (Glaze, Frost et al. 1987). Multiple breathing abnormalities can be observed in both daytime and sleep time (Glaze, Frost et al. 1987, Weese-Mayer, Lieske et al. 2008), like forced breathing, air swallowing, shallow breathing, Biot's breathing, Valsalva's maneuvers, breath holding and apnea (Kerr, Nomura et al. 2001, Weese-Mayer, Lieske et al. 2008), as well as abnormalities of cardiorespiratory integration (Katz, Dutschmann et al. 2009).

Studies in mouse model of RTT also suggest an impaired respiration response to hypercapnia (Zhang, Su et al. 2011). *Mecp2* knockout mice show a reduced sensitivity to mild level of hypercapnia with 1-3% CO_2 while still sensitive to 6-9% CO_2. The affected CO_2 chemo-sensitivity is caused by the abnormal activity of a pH-sensitive K^+ channel. The $K_{ir}4.1$ subunit is overexpressed in the null mice leading to an increase in the proportion of this less pH-sensitive K^+ channel over the more pH sensitive $K_{ir}4.1$/ $K_{ir}5.1$ channel. With the defect, CO_2 cannot be detected by the CNS under mild hypercapnic range (Zhang, Su et al. 2011). Furthermore, neuronal sensitivity to hypoxia may also be involved as the preBötC site-specific restoration of animal *Mecp2* gene generates a normal hypoxic respiratory response (Ward, Arvide et al. 2011).

The hyperexcitation of the KF nucleus and pontine post-I oscillator also been considered as major reasons causing respiratory disorders such as periodic breathing, air swallowing and apneas, since prolonged post-inspirations were observed (Stettner, Huppke et al. 2007, Abdala, Dutschmann et al. 2010). In *Mecp2*-null mice, the occasional central apneas may be due to the dysregulation of post-I activity via disrupting the inspiration initiation. At age of 2-month postnatal, a prolonged expiration phase with apnea was reported in *Mecp2*-null mice, while no significant changes were found during inspiratory phase (Stettner, Huppke et al. 2007, Weese-Mayer, Lieske et al. 2008). This could lead to reduced breathing frequency (Viemari, Roux et al. 2005). In RTT, abnormality of KF neurons contributes an in-coordinated glottal closure during swallowing, which may contribute to breathing apnea (Abdala, Toward et al. 2016). Therefore, these authors believe that the apnea problem in RTT together with upper airway dysregulations may be due to the disrupted central respiratory network: 1) with a decreased excitatory input onto inspiratory neurons, and 2) an overly increased excitatory input onto expiratory neurons.

2.3.2 Opioid-induced CRD

Opioid-induced CRD refers to the breathing depression syndrome that often occurs with opioid overdose or misuse and is the major reason of opioid-induced death. Opioid-induced CRD is a common side effect during opioid drug application. The symptoms of opioid-induced CRD include decreased breathing frequency, reduced respiratory tidal volume and depressed minute ventilation. In human, the respiration rate can be reduced as low as 8 breaths/min, leading low O_2 saturation (<85%) with high arterial CO_2 concentration, accompanied with the decreased ventilatory response to hypercapnia/hypoxia (Boland, Boland et al. 2013). Researchers are interested in identifying how opioid disrupts respiratory rhythmogenesis and respiratory motor outputs as potential mechanisms. Opioid-induced CRD involves the brainstem and carotid

bodies. The brainstem houses respiratory neuronal networks and CO_2 chemoreceptors, while the carotid bodies contain O_2 and proton chemoreceptors. Three potential mechanisms may underlie the opioid-induced CRD: 1) inhibition of the preBötC networks for rhythmic breathing, 2) disruption of respiratory regulation including O_2 and CO_2 chemoreception, and 3) suppression of brainstem premotor output by bulbospinal neurons in the ventral and dorsal respiratory groups. But it is debatable as to which playas a predominant role in the opioid-induced CRD, and whether they can be counteracted with pharmacologic approach.

Currently, naloxone types of MOR antagonists are the only effective therapeutics (Yousefifard, Vazirizadeh-Mahabadi et al. 2020). However, the usage of the MOR antagonists as preventive drugs has problems, as they tend to induce withdrawal responses, and antagonize nociception and other therapeutic objectives. Another option for the treatment of opioid-induced CRD is respiratory stimulants. Dahan et al. (Dahan, van der Schrier et al. 2018) have recently reviewed and analyzed most respiratory stimulants in opioid-induced CRD treatment, including doxapram, GAL021, ampakines, 5-hydroxytryptamine (5-HT) receptor agonists, D1-dopamine receptor agonists, phospodiesterase-4 inhibitors, the endogenous peptide glycyl-glutamine, and thyrotropin-releasing hormone. The authors conclude that none of these experimental drugs are adequate for therapeutic use in opioid-induced CRD (Dahan, van der Schrier et al. 2018). Such a conclusion also points out an alarming reality that there are no therapeutic agents to prevent opioid-induced CRD at all, as naloxone is not suitable for the purpose. Thus, it is necessary to further study these non-opioid CRD reversal agents, and perhaps more importantly to find new ones.

2.4 Cellular mechanism underlying CRD development

Changes in cellular structure can lead to changes in cellular function and ultimately systemic behavior. Before CRD symptoms occur, cellular changes already manifest, some of which may or may not be compensated enough to cover symptoms (Wang, Reyes et al. 2013). Several changes in neuronal morphology include altered dendritic spine morphology, decreased soma size, reduced number of synapses (Armstrong, Dunn et al. 1995). Some are related to transcriptional and translational levels of intracellular skeletal structures (Merriam, Millette et al. 2013). Evidence indicates that chronic treatment with morphine induces a decreased density of dendritic spines (Liao, Lin et al. 2005). Studies also suggest that there is reduced cell volume, even with no increase in cell death (Marchetto, Carromeu et al. 2010), which is attributable to the insufficient brainstem development seen in RTT as well. The reduced cell volume affects dendritic spine morphology, which is related to the expression of α-amino-3-hydroxy-5-methyl-4-isoxazolepropionic acid (AMPA) and n-methyl-d-aspartate (NMDA) receptors together with Ca^{2+} homeostasis in the dendrites (Merriam, Millette et al. 2013).

Studies indicate that impairment of *Mecp2* may impair neuronal differentiation and cell fate by affecting senescence (Kim, Hysolli et al. 2011, Squillaro, Alessio et al. 2012). This suggests that there may be structural abnormalities in the brainstem respiratory neurons of RTT patients. However, reactivation of the *Mecp2* gene during adulthood restored normal function in *Mecp2*-null mice, indicating that the basic structure and connections in the brain appear intact, and only the impairment may be functional (Guy, Gan et al. 2007). Research in opioid-induced CRD reveals that tolerance and withdrawal symptoms may be due to the neuronal structural changes (Mercadante, Arcuri et al. 2019). Substantial tolerance to CRD also occurs, but tolerance to CRD

is lost quickly during withdrawal (Zhilenko, Khoroshilova et al. 1989). Which makes overdose induced CRD occur again in people who misuse opioids in a little while after withdrawal.

2.4.1 Neurophysiology and CRD

Like structural components of neurons, cellular dysfunction has been discovered in various disease models with CRD. Significant concerns about cellular dysfunction are the changes in neuronal intrinsic properties, synaptic activity, and information integration. The output of a neuron depends on normal synaptic connections and intrinsic membrane properties. The neuronal output affects systemic function and behavior. Changes in the neuronal output can lead to abnormal behavior including breathing abnormality. Electrophysiological techniques such as whole-cell patch clamp, are commonly used to study neuronal functions, allowing the study of electrophysiological properties. The electrophysiological properties of neurons contain information of neuronal excitability, synaptic activity, and intrinsic membrane properties. The latter includes passive membrane properties, active membrane properties, and repetitive firing properties.

2.4.2 Neuronal excitability

Neuronal excitability is known as the ability of a neuron to fire action potentials. The more firing, the higher is the excitability. Defected membrane properties with underlying ion channels affect neuronal excitability and are often associated with diseases. Alterations in neural excitability lead to changes in neuronal communication, gene expression, and neuronal plasticity. Studies on pain have shown that there is a group of nerve fibers capable to elicit action potentials with lower threshold of stimulus, contributing to the pain symptom, especially in inflammation and diabetes-associated allodynia (Hong, Morrow et al. 2004, Wang, Strong et al. 2007). Allodynia and hyperalgesia in the streptozocin-induced diabetic rats are associated increased Na^+

currents (Hu, Carrasquillo et al. 2006). Similarly, studies show increased excitability in dorsal root ganglion neurons is associated with inflammatory pain (Hu, Carrasquillo et al. 2006, Tan, Donnelly et al. 2006). Changes in firing patterns towards phasic firing have been implicated in epilepsy. The elevated glutamate level, decreased inhibitory inputs and bias towards hyperexcitation are linked to epilepsy (Treiman 2001, Barker-Haliski and White 2015). The epilepsy mouse model highlights changes that lead to increased hyperpolarization and increased sensitivity to excitatory inputs (Shah, Anderson et al. 2004, Jung, Jones et al. 2007). Pyramidal neurons of hippocampus, that with burst firing properties, shift from 3% to 48% due to changes in Ca^{2+} sensitivity and K^{+} currents (Sanabria, Su et al. 2001). Changes in intrinsic properties have been linked to neuronal output and function (Zhang and Linden 2003). Some well-studied examples of membrane properties changes have been proved to be attributable to pathology symptoms including Alzheimer's disease as well (Mantegazza, Gambardella et al. 2005, Kim, Carey et al. 2007). Many studies have been focused on the mechanisms of changes in neuronal firing patterns. These changes are linked to normal homeostasis as well as pathological states.

The normal regulation of whole-scale oscillations is critical. Neurons need to coordinate all membrane properties and synaptic activity in order to create functional outputs. Variability in electroencephalogram (EEG) waveforms indicating desynchronization has been found in autism spectrum disorders (Sun, Grutzner et al. 2012). Studies demonstrate that the fast phasic firing is important for regulating network timing (Klausberger, Magill et al. 2003), and an increased glutamate together with a reduced GABA leads to the neuronal hyperexcitability in autism spectrum disorders (Purcell, Jeon et al. 2001, Fatemi, Halt et al. 2002).

2.4.3 Intrinsic membrane properties

During the morphine treatment, the membrane property of neurons in KF and preBötC show significantly hypoexcitable (Varga, Reid et al. 2020), with inhibitions of LC, XII and DMNV (May, Dashwood et al. 1989, Hajiha, DuBord et al. 2009). Neuronal overexcitation is very rare in opioid application but not none (Thomas, Corson et al. 2019). Membrane property changes are altered in *Mecp2* mutant mice, resulting a disruption in excitation/inhibition balance underlying CRD development (Calfa, Li et al. 2015, Banerjee, Rikhye et al. 2016). Hyperexcitation in the hippocampus, brainstem, and substantia nigra is the major electrophysiological property change associated with CRD in RTT (Zhang, He et al. 2008, Gantz, Ford et al. 2011). Neuronal excitability changes are regionally different. For example, the forebrain of *Mecp2*-null mice shows hypoexcitation (Dani, Chang et al. 2005). Brainstem neurons include LC and XII cells are hyperexcitable with increased firing activity in response to current injections and increased spontaneous firing activity (Taneja, Ogier et al. 2009, Zhang, Cui et al. 2010, Jin, Cui et al. 2013). Other altered membrane properties include increased action potential threshold and inward rectification, action potential morphology, spike frequency adaptation, delayed excitation, and after hyperpolarization (Zhang, Cui et al. 2010). These changes indicate that basal level of neuronal activity is altered as well as responses to synaptic signals. Mechanisms underlying changes in membrane properties largely depend on changes in protein expression of the corresponding properties.

Passive membrane properties belong to intrinsic membrane properties, which are electrical characteristics of neurons that determine the electrical signaling capabilities. The properties include capacitance, resting membrane potential and input resistance. Capacitance refers to the plasma membrane property as a capacitor that storing electric charge. Observers understand the

size of the cell based on this property, because a large cell has a large capacitance and requires more current to change the resting membrane potential. Input resistance describes the relationship between current and voltage. According to the Ohm's law, V= I×R, an injected current will change the membrane potential of a cell. Similarly, membrane resistance is dependent on the opening/closing status of ion channels, as well as the number of ion channels located on the membrane of the cell. Capacitance and membrane resistance together describe time constant of neurons, which is the time that takes for membrane potential to reach a steady state in response to stimulate.

With the passive membrane properties, a neuron responds to current injection in a linear fashion. Once it passes a certain threshold, the neuron starts to generate action potentials. Then the membrane properties of the cell are described as active membrane properties, which indicate the neuron responses after the neuron starts firing. Active membrane properties include firing frequency (f), afterhyperpolarization (AHP), rheobase, postinhibition rebound (PIR), bursting activity, spike frequency adaptation (SFA) and delayed excitation (DE). The latter three are also known as repetitive firing properties.

2.4.4 Respiration-modulatory neurons

There are multiple neurons involved in respiration regulation in CRD. We here are focused on three specific neurons that are highly correlated in CRD development both in RTT model and opioid-induced CRD model.

2.4.4.1 Neurons in the locus coeruleus

LC is a nucleus located in the posterior area of the rostral pons in the lateral floor of the 4th ventricle. LC neurons project to various regions including cortex, brain stem, cerebellum, hypothalamus, spinal cord, and amygdala. The LC is the major pool of noradrenergic signaling

in CNS that performs excitatory effects on most of its projection sites. Functions of the LC include arousal and sleep-wake cycle, attention, emotion, behavioral and cognitive control, and respiratory regulation.

LC neurons are modulated by GABA, glycine, glutamate, Ach, and opioids. As the source of NE, the excitability of LC and afferent/effect neurotransmissions are critical for respiratory regulation in different conditions. Previous studies from our lab have shown that both the GABAergic inhibition and acetylcholine (Ach) modulation in the LC area are significantly reduced in *Mecp2*-null mice, which lead to neural hyper-excitation (Jin, Cui et al. 2013, Oginsky, Cui et al. 2014). These changes contribute to the impaired norepinephrine (NE) synthesis/release within the LC region and a decreased NE content in the brainstem. Reduced expressions of dopamine beta hydroxylase (DBH) and tyrosine hydroxylase (TH) were observed in LC neurons (Roux, Panayotis et al. 2010, Zhang, Su et al. 2010). Our current study indicates that besides GABA signaling, glycine signaling also shows reduction on LC, and these two neurotransmitters performed a mutual compensatory regulation of LC excitability. Our study also shows that morphine inhibits the firing activity of the LC neurons via modulating membrane properties and altering presynaptic glutamatergic neurons as well as glutamate release from their synaptic terminals, which contribute to opioid-induced CRD. These defects in neurotransmission and LC excitability can be alleviated by blockade of GIRK. After the opioid administration, the increased activity of the LC neurons contributes to the symptoms of withdrawal. The α_2 adrenergic receptor agonist clonidine is used to decrease adrenergic neurotransmission from LC (Devenyi, Mitwalli et al. 1982).

2.4.4.2 Neurons in the dorsal motor nucleus of vagus

The DMNV is a cranial nucleus for the vagus nerve. The DMNV is located in the medulla that lies ventral to the floor of the 4th ventricle. It mostly serves parasympathetic vagal functions in the lungs, airways, heart, gastrointestinal tract, and thoracic/abdominal vagal innervations include broncho-constriction, gland secretion. The DMNV also raises the branchial efferent motor fibers innervating musculus uvulae and laryngeal/pharyngeal muscles activity. Upper airway regulation is critical under the CRD condition. The DMNV shows high expression level of nAChRs (Vivekanandarajah, Waters et al. 2019), and the neuronal excitability is proved to be affected by cholinergic signals (Quaresma, Teixeira et al. 2020). Also, genetic defects of choline acetyltransferase in DMNV neurons leads to over-bronchoconstriction in mice (Lai, Su et al. 2016). Site specific administration of opioid agonist in the DMNV cause clear CRD (May, Dashwood et al. 1989). Besides, decreased serotonin 1A receptor (5-HT_{1A}) and serotonin 2A receptor (5-HT_{2A}) immunoreactivity levels were found in sudden infant death syndrome (SIDS) kids with CRD (Ozawa and Okado 2002). Study also found altered 5-HT innervation and/or uptake in the DMNV contribute to abnormal modulation of respiration in RTT patients (Paterson, Thompson et al. 2005). Inhibitory neurotransmissions including GABA and glycine are critical factors in maintaining DMNV excitability (Inquimbert, Rodeau et al. 2007, McMenamin, Anselmi et al. 2016). Considering the function and various neuronal regulations, the DMNV is a potentially important target in CRD studies.

2.4.4.3 Hypoglossal neurons

The XII is another cranial nerve nucleus in the medulla. It is located between the DMNV and the midline of the medulla. The XII sends motor signals to control the extrinsic and intrinsic muscles of the tongue, mediating the movement of tongue includes protruding/deviating. These

regulations participate in breathing, speaking, swallowing, and talking. Together with DMNV, neuronal excitability of the XII is proved to be affected by cholinergic signals (Quaresma, Teixeira et al. 2020). The XII site specific microinjection of carbachol activates acetylcholine receptors and reverses CRD by increasing respiratory rate (Brandes, Stettner et al. 2011). Another study reveals that the activation of MOR reduces motor output from the XII, and further affects the upper airway function causing breathing disorder (Hajiha, DuBord et al. 2009). Previous studies from our lab have shown that the glycinergic synaptic transmission can be facilitated after activating the α_1-adrenoceptor, and excited XII via both pre- / postsynaptic mechanism (Jin, Cui et al. 2013), while opto-stimulation of NEergic terminals had no effect on XII excitability in *TH-ChR-Mecp2*$^{-/Y}$ double-transgenic mice (Zhang, Johnson et al. 2016). Opioids depress XII motoneuronal output by presynaptic inhibition mechanism, which can be counteracted by AMPA receptor modulator ampakines (Lorier, Funk et al. 2010). Other antagonistic neuropeptides, like methionine-enkephalin, were found reduced in the XII from RTT patients (Saito, Ito et al. 2001). Taken together, the XII is a critical site in regulating respiratory pattern in CRD.

2.5 Molecular substrates underlying CRD

2.5.1 Synaptic transmission / neuronal excitability

Besides the intrinsic membrane properties, changes in synaptic connections also contribute to changes in neuronal excitability in CRD. Classical neurotransmitters such as glutamate, GABA, and glycine can change membrane excitability in receiving cells. The major excitatory neurotransmitter in the CNS is glutamate, which causes excitatory postsynaptic potentials (EPSPs). GABA is the major inhibitory neurotransmitter in the brain causing inhibitory postsynaptic potentials (IPSPs). Similarly, glycine is the other inhibitory neurotransmitter that

plays a more important role in the lower brainstem and the spinal cord, though it can be found in sparse areas of the forebrain (Baer, Waldvogel et al. 2009). All of these three neurotransmitter systems act on ionotropic receptors causing fast responses on the postsynaptic cells. Glutamate also bind to metabotropic glutamate receptor (mGluR) to affect neuronal excitability by presynaptic modulation of neurotransmission. GABA also bind to GABA subtype B ($GABA_B$) receptor. Both mGluR and $GABA_B$ receptors produce their biological effects by opening GIRK channels.

2.5.2 μ-opioid receptor

Opioid receptors are G protein-coupled receptors, which include 5 subtypes: MOR, σ-opioid receptor (DOR), κ-opioid receptor (KOR), ζ-opioid receptor (ZOR) and nociception receptor (NOR). MOR has been considered as the major one that interacts with opioids leading to CRD symptom. MOR is widely expressed in brain, spinal cord, peripheral neurons, and intestinal tract. In the CNS, MOR is found in nucleus accumbens, cortex, nucleus amygdala, olfactory bulb, nucleus of solitary tract, LC, and superficial dorsal horn of spinal cord.

MOR can bind with endogenous opioid peptides like endomorphins, endorphins, dynorphins and enkephalins; also, can be activated by agonists like morphine, fentanyl and D-Ala2, N-MePhe4, Gly-ol]-enkephalin (DAMGO). After activation, MOR leads to various effects include analgesia, sedation, euphoria, pupil constriction, reduced gastrointestinal motility and CRD. The CRD is the major cause of opioid leading death.

Short-term activation of MOR changes neuronal excitability via suppression of presynaptic release of GABA. After the application of fentanyl, a decreasing of glutamate and increasing of GABA release were observed in hypothalamus (Pourzitaki, Tsaousi et al. 2018). These changes in neurotransmissions and the following neuronal excitability alternations are responsible for the

respiratory abnormality in opioid administration. Long-term or high-dose use of opioids leads to mechanisms of tolerance include downregulation of MOR gene expression, which reduces the number of receptors on the cell membrane. As a result, higher concentration of opioids is needed to reach the same level of cellular responses. A sudden stop or reduction of opioids leads to withdrawal symptoms, like drug craving, anxiety, vomiting, diarrhea, and sweating. The withdrawal response is related to the abnormality of norepinephrine system. During the opioid withdrawal, activation of the LC adrenergic neurons is observed, and α_2 agonists can be used to reduce the symptoms (Imani 2011).

Studies have been concentrated on the CRD induced by MOR activation, whereas research on the relationship between MOR and CRD in RTT is limited. One study reveals that MOR gene can be silenced under epigenetic control of *Mecp2*, leaded to the altered expression of MOR in multiple brain regions including cerebellum (Hwang, Song et al. 2009). This could give us a starting point to investigate the MOR signaling under respiratory regulation in RTT. Currently, naloxone is still the most efficient chemical to reverse morphine-induced CRD by binding to MOR to stop the following cellular responses.

2.5.3 Serotonin receptor

5-HT receptors are found in the central and peripheral nervous systems. The 5-HT receptor modulate the release of many neurotransmitters, including GABA, glutamate, epinephrine / norepinephrine, acetylcholine, dopamine, and various hormones. 5-HT receptors can be divided into 7 families of G protein-coupled receptors except for the 5-HT_3 receptor, a ligand-gated ion channel. 5-HT_3 receptors activates an intracellular second messenger cascade to produce an excitatory or inhibitory response. Studies have investigated the activity and manipulation of 5-HT receptors under CRD situation. The 5-HT receptor 7 (5-HT_7) agonist LP-211 improves

specific behavioral including breathing depression in RTT (De Filippis, Nativio et al. 2014). Human study on 11-year-old RTT girl co-treated with 5-HT_{1A} receptor agonist and 5-HT reuptake inhibitor reduced CRD (Ohno, Saito et al. 2016). Animal studies show that 5-HT agonists increase respiration drive force by activating 5-HT_{1A}, 5-HT_7, and 5-HT_{4A} receptors (Oertel, Schneider et al. 2007). But there are no significant effects when using the 5-HT_{1A} receptors agonist buspirone and the 5-HT_{4A} receptors agonist mosapride to counteract opioid-induced CRD in humans (Lotsch, Skarke et al. 2005). The lack of efficiency in human use may be due to a low potency / lower brain concentrations achieved in human (van der Schier, Roozekrans et al. 2014), which indicates 5-HT receptors could still be potential target in treating opioid-induced CRD.

2.5.4 Nicotinic acetylcholine receptor

nAChR are widely found in the central and peripheral nervous system, muscle, and many other tissues of many organisms. It can be activated by acetylcholine and the agonist nicotinic. It serves the motor nerve-muscle communication in neuromuscular junction, also transmits signals between synapsis within sympathetic and parasympathetic nervous system. In CNS, the opening of nAChR allow cations, like Na^+, K^+ and Ca^{2+}, flow cross the pore, which regulate the release of neurotransmitters in classical synaptic transmission so as paracrine transmission (Racke, Juergens et al. 2006). Previous study from our lab shows the α_5-subunit of nAChR was increased as the α_7-subunit was decreased in *Mecp2*-null mice, accompanied with an enhanced nAChR modulated GABA input to the LC (Oginsky, Cui et al. 2014). Activation of $\alpha_4\beta_2$ nAchR by ABT-594 and varenicline counters opioid-induced CRD without affecting analgesia effect (Ren, Ding et al. 2020). These lines of evidence indicate that nicotinic acetylcholine receptor is involved in excitability of respiratory neurons in CRD.

2.5.5 AMPA receptor

AMAP receptor is an ionotropic receptor which is activated by glutamate. The AMPA receptor usually acts as heterotetrameric receptor with the combination of 4 subunits: GluA1, GluA2, GluA3 and GluA4. The AMPA receptor is permeable to cation like Na^+, K^+ and Ca^{2+}. Upon the agonist binding, EPSPs follows to depolarize the postsynaptic cells affecting neural plasticity and synaptic transmission. Both effects are known to be involved in CRD. Within the hippocampus region in RTT mice, an overly increased excitatory signal is found due to the abnormal synaptic trafficking of AMPA receptors (Li, Xu et al. 2016). Human study shows that the defect of AMPA receptor GluA2 subunit disrupts the glutamatergic neurotransmission, leading to RTT-like features with CRD (Salpietro, Dixon et al. 2019). Animal studies show that ampakine CX717 increases the breathing rate by activating the AMPA receptors specifically in the preBötC region. There are studies confirming that ampakine compounds are able to elevate the breathing rate together with the slope of the ventilation responses to carbon dioxide, which eventually raises respiration driving force during opioid-induced CRD (Ren, Poon et al. 2006, Oertel, Felden et al. 2010). Possibly, drugs that interfere with AMPA receptor may prove useful to prevent opioid- and non-opioid-induced CRD.

2.5.6 GABA/glycine in brainstem

The inhibitory neurotransmission includes two neurotransmitters: GABA and glycine. GABA is the predominant transmitter in inhibitory neurons of the brain while glycine typically exists in the spinal cord, brainstem, and retina. After bind to $GABA_A$ receptor and glycine receptor, respectively, IPSPs occur to affect the neuronal excitability. A lot of attention has been given to the involvement of GABA in the shift of excitation/inhibition balance in the development of CRD, whereas studies of glycine are limited. Decreased GABA IPSCs have been found in

Mecp2-null mice in several different nuclei, including, but not limited to the LC, NTS, and KF (Jin, Cui et al. 2013, Abdala, Toward et al. 2016, Chen, Di Lucente et al. 2018). Extensive studies on GABA neurons in RTT models have not been performed, but some studies looking at subclasses of GABA neurons have provided insight into how *Mecp2* disruption affects their activity. One of the primary ways to classify GABA neurons is to examine their expression of GABA receptors, enzymes for GABA synthesis and other coexisting proteins. For instance, a major subgroup of GABA neurons expresses parvalbumin (PV), calcitonin, and somatostatin. The PV neurons appear to be the most widespread throughout the CNS. The PV cells in *Mecp2*-null mice are hyperexcitable (Wydeven, Marron Fernandez de Velasco et al. 2014). Selective deletion of *Mecp2* in either PV or SOM neurons also causes RTT-like phenotypes (Ito-Ishida, Ure et al. 2015). It has been reported that patients taking prescription opioids together with gabapentin have an increased risk of opioid-induced CRD (Gomes, Juurlink et al. 2017). The specific activation of 5-HT_{1A} receptor leads to a dephosphorylation of type α_3 glycine receptors, induces disinhibitions of excitatory and inhibitory neurons to alleviate opioid-induced CRD (Manzke, Niebert et al. 2011).

2.5.7 Glutamate in brainstem

Glutamate is the most abundant excitatory neurotransmitter in the vertebrate nervous system. Glutamate interacts with four types of receptors: AMPA receptor, NMDA receptor, mGluR, and kainate receptors. The last one is similar in respects to AMPA receptor but less abundant. Glutamate also serves as precursor for the metabolic synthesis of GABA, and the activation of NMDA receptor requires co-binding of glycine and glutamate. Considering the role of glutamate in CRD, there is a study proving that glutamate content was decreased in hippocampus region in *Mecp2*-dificient mice, while in LC area, an increased glutamate was observed which was not

correlated with global reductions of GABA (El-Khoury, Panayotis et al. 2014). Another study confirmed a glutamate-induced glutamate release pattern is attributable to abnormal neuronal excitability in *Mecp2*$^{-/Y}$ mice (Balakrishnan and Mironov 2018). It has been reported that the glutamatergic system shows an increased NMDA receptor density in RTT girls younger than 8-year of age, while a reduction of NMDA receptor density was observed in girls older than 10 (Blue, Naidu et al. 1999). Site specific alteration of NMDA receptor expression in RTT mouse models confirms these findings (Blue, Naidu et al. 1999). Esketamine, a non-competitive NMDA receptor antagonist, has been shown to be usable in countering CRD in RTT (Jonkman, van Rijnsoever et al. 2018). The altered synaptic trafficking of AMPA receptors contributes to the hyper-excited synaptic activity in hippocampus in RTT (Li, Xu et al. 2016), and AMPA receptor modulator has been applied to reverse CRD (Ren, Ding et al. 2009, Sultan, Gutierrez et al. 2011). A recent study suggests that the major mechanism underlying opioid-induced CRD involves MOR-mediated inhibition of presynaptic Ca^{2+} channels within the preBötC area (Ramirez, Burgraff et al. 2021). The excitatory neuronal signal to the XII is regulated by AMPA receptors. After activation of the MOR by DAMGO, a reduced inspiratory XII motor output can be observed due to an inhibition of presynaptic excitatory glutamatergic neurotransmission (Lorier, Funk et al. 2010).

2.5.8 GIRK channel

One common ion channel target of GPCRs is the GIRK channel, which is expressed widely throughout the brain. The GIRK channel is a group of K^+ permeable ion channels that are a part of the larger K_{ir} channel family. K_{ir} channels pass inward K^+ currents at membrane voltages below K^+ equilibrium potential (E_K), typically around -90 mV. The inward current is much larger

than the outward K^+ current that passes through the channel above E_K. This is in contrast with other K^+ channels that primarily only allow current to flow outward.

The four isoforms of GIRK channels are GIRK1, GIRK2, GIRK3, and GIRK4. GIRK channels 1-3 are found primarily in the CNS, while GIRK4 is primarily located in the heart. The GIRK channels 1 and 2, often expressed together, are the primary subunits expressed in the brain (Liao, Jan et al. 1996). GIRK channels form tetramers and typically as heterotetramers (Kofuji, Davidson et al. 1995). GIRK2 is the only subunit that can form homotetramers (Lesage, Guillemare et al. 1995). There exist splicing variants of GIRK2, GIRK 2a, b, and c (Wei, Hodes et al. 1998, Luscher and Slesinger 2010). There are also GIRK1 splicing variants, although they have not been studied as well. Splicing variants for GIRK3 and GIRK4 are still unknown.

The subcellular location of GIRK channels depends on the subunit. In pyramidal neurons, GIRK2a and GIRK2c proteins show overlapped expressing locations. Unlike GIRK2c, located throughout the entire neuron, GIRK2a is mostly found on the soma and proximal dendrites (Marron Fernandez de Velasco, Zhang et al. 2017). The GIRK1d splicing variant expression was shown to reduce the currents of other GIRK channels when co-expressed (Steinecker, Rosker et al. 2007). In addition, substantia nigra and VTA neurons do not express GIRK1 channels, but express GIRK2a-GIRK2c and GIRK2a-GIRK3 combinations, which are less sensitive to $G_{\beta\gamma}$ again emphasizing the importance of subunit expression patterns. GIRK channel density in axons, soma, and dendrites differ (Ponce, Bueno et al. 1996). Thus, different GIRK channel isoforms have differential subcellular expression patterns, and that activation of different isoforms could potentially have different cellular effects.

2.5.9 Pre- / postsynaptic modulation of GIRK channel

The GIRK channel has the ability to pass inward K^+ ions, but the main contribution is still efflux of K^+ ions upon activation as most neuronal resting membrane potentials are above the E_K. GIRK channel activation leads to hyperpolarization and inhibition of a neuron. Changes in basic level of GIRK channel activity affects resting membrane potential by 2-8 mV in hippocampal and dorsal raphe neurons (Luscher, Jan et al. 1997, Llamosas, Ugedo et al. 2017). GIRK channels regulate both pre- and postsynaptic cells. The presynaptic regulation of GIRK channels is known in conjunction with auto-receptors, regulating the neurotransmitter release from the releasing cell. These presynaptic auto-receptors bind the neurotransmitter located on axon terminals, where the GIRK channels serve as negative feedback mechanisms, decreasing or inhibiting a further release of the neurotransmitter from the synaptic terminal. Another mechanism by which GIRK channels cause self-inhibition is through dendro-denritic interactions or autaptic transmission (Bacci, Huguenard et al. 2004).

GIRK channel activation on postsynaptic cells leads to inhibition as well. The GIRK channel activation has a slow sustained effect as compared to ionotropic receptor activation. Communication is not always one way though. Postsynaptic cells can inhibit neurotransmitter release from presynaptic cells by activation of GIRK channels via retrograde signaling. Common retrograde signaling molecules include endocannabinoids, nitric oxide, or CO (O'Dell, Hawkins et al. 1991, Wilson and Nicoll 2001). GIRK channels have been implicated in many different physiological phenomena as well as pathophysiological conditions. They play an important role in epilepsy, opioid addiction, and Parkinson’s disease. GIRK2 knockout mice develop seizures and have reduced pain alleviation mediated by opioids (Signorini, Liao et al. 1997, Mitrovic, Margeta-Mitrovic et al. 2003).

CPS is a blocker of GIRK channels. The effects of CPS application can be either excitatory or inhibitory depending on the location of GIRK channels. In additional to GIRK channels, CPS may bind to histamine receptors, sigma receptors, and sodium-glucose transporters (Oranje, Gouka et al. 2019), which may also contribute to the inhibition of the CNS by this drug. If the binding proportions of each type are unbalanced, the effect on one protein may overwhelm the other. After knocking down mRNA expression of GIRK or knocking out GIRK channels, the necessity of GIRK channels during CPS-mediated respiration improvement can be investigated. The LC region has a significant amount of GIRK channel expression (Kawano, Zhao et al. 2004). Therefore, blocking GIRK channels directly on LC cells should stimulate these cells. Opposite effects of GIRK channel inhibition by CPS were found between RTT CRD mice and morphine-induced CRD rats. Previous studies in this lab suggest that the effect of CPS was inhibitory in LC cells in RTT mice, where hyperexcitability is predominant (Johnson, Cui et al. 2020). The CPS-enhanced GABA transmission overwhelms the stimulatory effect of CPS.

In rat model of morphine-induced CRD, hypo excitability is seen in LC neurons. Whereas CPS promotes the glutamate signal to depolarize morphine-inhibited LC neuron in morphine-induced CRD rats in our research. The inhibition of LC cells in RTT mice may help reduce LC excitability and correct the defective NE synthesis via GABA signaling (Johnson, Cui et al. 2020), while it is interesting to know the facilitation effects of CPS on glycinergic signaling to reverse CRD in RTT. In RTT respiratory depression, the excitatory effect of CPS could enhance the glycine signal onto LC by 1) blocking GIRK on presynaptic glycinergic neurons and/or 2) facilitating a pre-presynaptic glutamatergic signaling onto the presynaptic glycinergic cells. Even though multiple targets including GIRK channel have been tested (Ren, Ding et al. 2009, Roozekrans, van der Schrier et al. 2014, Ren, Ding et al. 2015, Liang, Yong et al. 2018, Ren,

Ding et al. 2019, Imam, Kuo et al. 2020), further investigation of GIRK-mediated neuronal excitability and neurotransmission may lead to alternative approaches to brainstem neurons to counteract CRD.

2.6 Therapeutical potentials

2.6.1 Pharmacological approach

Several pharmacological interventions, includes NE reuptake blocker, or the interventions to increase the biogenic amine were able to alleviate the breathing problems in RTT mice (Viemari, Roux et al. 2005, Medrihan, Tantalaki et al. 2008). Study applied the 5-HT_{1A} receptor agonists 8-OH-DPAT and F15599 also correct irregular breathing pattern and reduce apnea by decreasing expiratory neuron activity (Kline, Ramirez-Navarro et al. 2007, Turovsky, Karagiannis et al. 2015). Another approach has been done with the administration of 5-HT re-uptake blockers that is proved to be able to increase the expression level of MeCP2 proteins (Voituron, Menuet et al. 2010). Currently, naloxone types of MOR antagonists are the only effective therapeutics for opioid-induced CRD (Yousefifard, Vazirizadeh-Mahabadi et al. 2020). But several problems cannot be ignored that the usage of the MOR antagonists as preventive drugs tend to antagonize the desired nociception, also induce withdrawal responses. Respiratory stimulants could be a good option for the treatment of opioid-induced CRD. A variety of respiratory stimulants targeting on multiple receptors/pathways have been reviewed and analyzed in opioid-induced CRD treatment, including doxapram, GAL021, ampakines, 5-HT receptor agonists, D1-dopamine receptor agonists, phospodiesterase-4 inhibitors, the endogenous peptide glycyl-glutamine, and thyrotropin-releasing hormone. None of these experimental drugs are adequate for therapeutic use, although they revealed the potentials in opioid-induced CRD treatment (Dahan, van der Schrier et al. 2018).

2.6.2 Genetic manipulation

Beside the pharmacological intervention, genetic strategy is always an option to treat CRD. In RTT, the mutation of *Mecp2* contributes to the CRD symptom. The functions of MeCP2 are activating and repressing various downstream genes. The mutations of *Mecp2* produce abnormal- or un-function MeCP2 proteins. One approach is to stabilize the expression level of MeCP2 protein from the normal *Mecp2* allele by using serotonin re-uptake blockers, which mean to maintain the sufficient amount of normal MeCP2 protein. Another way is taking advantage of the X chromosome inactivation mechanism (Voituron, Menuet et al. 2010). It could be reasonable if we are able to turn off the mutate allele of *MECP2* while turn on the normal one on the other X chromosome, which could reduce the CRD in RTT patients. Genetic therapy for treating CRD in opioid-induced CRD is very limited. One research group found the *Galnt11* gene that transcripts GALNT11, an N-acetylgalactosaminyltransferase, is responsible for exporting of DOR from endoplasmic reticulum (ER) to cell membrane within preBötC complex, and the deletion of *Galnt11* shows a partial reversion of opioid-induced CRD (Bubier, He et al. 2020).

2.6.3 Current clinical management

Respiration stimulants are commonly used in CRD treatment, which mean to stimulate the CNS to enhance the respiration drive with certain level of bronchi-dilating effect. The anti-CRD effect of respiratory stimulants may not be related to the reasons for CRD, but the application of stimulants is mostly accompanied by specific agonists/antagonists. The usage of specific agonists/antagonist is based on the patient history of drug usage, which has been proved efficient. But the situation of CRD patients can be complicated as multiple drugs may be used together to cause CRD, which requires a combination application of various anti-CRD

chemicals. It is possible to worsen the situation due to the side effects from the combination usage of anti-RD medicines. Ventilator is also a clinical option both in emergent CRD and consistent respiration maintaining condition. Ventilator forces air flow in/out of lungs to enable a passive respiration activity in CRD patients, which maintains the adequate intake of O_2 and removal of CO_2.

3 SIGNIFICANCE

CRD is commonly seen in several deadly diseases and drug misusage. The neurobiological mechanisms of the CRD, and its relationship with neurotransmission and neuronal excitability are still poorly understood. Also, it is necessary to demonstrate the CRD in multiple experimental models where different cellular mechanisms may be in action, so that these cellular mechanisms and the identified molecules or cell signaling pathways may be targeted to counteract CRD.

RTT is a neurodegenerative disease, mainly affecting female kids with an incidence rate of 1 out of 10,000 worldwide. CRD including hypoventilation with irregular breathing is the most serious symptom in the RTT patients, attributable to the high rate of sudden death. Mutations of the *MECP2* gene result in more than 90% of RTT cases. It has been reported that a defected GABAergic signal plays a part in the disease, leading to over-excitation of respiratory neurons, which is responsible for the respiratory rhythm disruption in RTT (Medrihan, Tantalaki et al. 2008, El-Khoury, Panayotis et al. 2014, Zhong, Cui et al. 2015). In the brainstem, neurons utilize both GABA and glycine as inhibitory neurotransmitters for neuronal activity regulation. However, whether and how glycine signaling plays a role in RTT CRD remain elusive. We plan to use the *Mecp2*$^{-/Y}$ (*Mecp2*-null) male mouse model and performed *in vitro* electrophysiological recordings from brainstem XII/DMNV neurons to understand the inhibitory neurotransmission changes in RTT. CRD is also a major adverse effect of opioid drug misusage, which causes a loss of large numbers of lives worldwide (Kobelt, Burke et al. 2014). The opioid-induced CRD is primarily mediated by MOR that can be blocked by naloxone types of drugs (Imam, Kuo et al. 2018). However, the usage of them as preventive drugs has problems, as they tend to antagonize the desired opioid effects on reward, nociception, and other therapeutic objectives. Since

naloxone types of drugs are only therapeutics today, there is an urgent need for the understanding of cellular/molecular mechanism underlying CRD in opioid usage condition, so that effective therapeutics may be developed to reverse or alleviate opioid-induced CRD by means of a novel approach other than opioid receptor blockade. MOR is coupled to G-proteins and β-arrestins. The former regulates GIRK channels to affect the neuronal excitability, and the latter is coupled to adenylyl cyclase. GIRK channel targeting avoids the MOR that may induce unwanted side-effects as the MOR is widely expressed in the CNS. As some antitussives act on brainstem mechanisms, it is possible to identify the non-opioid antitussive drugs that act on neuronal excitability via GIRK channels instead of MOR, with relative specificity to the brainstem to suppress the opioid-induced CRD.

Thus, we designed this project to reveal defective patterns of GABAergic and glycinergic inhibitory neurotransmissions in RTT model, and GIRK channel inhibition by an antitussive GIRK channel blocker in regulating brainstem neuronal excitability in morphine-induced CRD.

4 MATERIAL AND METHODS

4.1 Animal

All animal experiments were conducted in accordance with the National Institutes of Health (NIH) Guide for the Care and Use of Laboratory Animals and were approved by the Georgia State University Institutional Animal Care and Use Committee.

4.1.1 Rat

The experiments were performed on WT rats. The wildtype Sprague Dawley rat (Crl: CD, Outbred, Charles River Laboratory, Kingston, NY) were used in this study. Both male and female animals were evenly used in the present study.

4.1.2 Mice

The *GAD-ChR* transgenic mice were generated by cross-breeding the strain of *GAD2-Cre* mice (*Gad2*$^{tm2(cre)Zjh/J}$, Jackson Laboratory SN: 010802) with the *ChR2-eGFP-LoxP* strain (B6;129S-Gt(ROSA)26Sortm32(CAG-COP4*H134R/EGFP)Hze/J, Jackson Laboratory SN: 012569). R168X point mutation: female heterozygous *Mecp2*^{R168X} point mutation mice (strain name: *Mecp2*$^{tm1.1Jtc/SchvJ|B6J}$; 129S6.*Mecp2*^{R168X}, Jackson Laboratory, SN: 024990) were crossbred with wildtype C57BL/6 males to produce the hemizygous *Mecp2*^{R168X} mutant male mice. A genotyping PCR was done to the offspring according to the protocol provided by the Jackson Laboratory. Only male animals were used in the present study.

4.2 Plethysmograph Recording

All rats were 7~8 weeks old and weighed about 170 g. After the pre-injection, on the 3rd day, one conscious and free moving rat was placed into the plethysmography recording chamber. The animal was given a 10-minute settle down time in the recording chamber, then a 20-minute baseline recording was done to have the normal breathing level. The rat was intraperitoneal (*i.p.*)

injected with 10 mg/kg morphine sulfate and put back to recording chamber right away, recorded the breathing for 20~30 minutes, followed by a subcutaneous (*s.c.*) injection with 30 mg/kg CPS and placed the rat back to recording chamber right after the injection. Then a 5-hour recording will be done with a 10-minute break for every 60 minutes. The tidal volume and breathing frequency will be recorded by measuring the pressure changes between the animal chamber and a reference chamber with a force-electricity transducer (PanaVise Products, Inc. Nevada). To have close estimation of the tidal volume (VT), a series of calibration was conducted by converting recorded signals to tidal volume according to a series of measurements with known volumes of air injection to the plethysmograph chamber in a similar time period to each breath. The chambers were perfused with normal air at a flow rate of ~50 ml/min. The variation of tidal volume, variation of breathing frequency and breathing minute ventilation will be calculated. During the 10 minutes break, the recording rat will be put back to the housing cage for food and water intake.

Breathing activity was collected and analyzed with Clampfit software (Molecular Devices) and calculated from at least 100 successive breathing cycles.

4.3 Survival rate

For our survival curve test, all experimental rats were orally pre-treated with cloperastine in drinking water for 7 continuous days. The dosage of oral cloperastine treatment is 30 mg/kg/day, the control group was given with normal drinking water. After 7 days oral treatment of CPS, rats were *i.p.* injected with morphine sulfate on the 8^{th} day and the survival outcomes will be recorded: either the tested animal is survived or dead. A series of doses of morphine sulfate will be injected into animals: 48 mg/kg, 68 mg/kg, 88 mg/kg, 108 mg/kg, 130 mg/kg, 150 mg/kg, and

170 mg/kg. One rat was injected with one dose, and no animal were tested more than one injection regardless of the survival outcomes. The outcomes were recorded as survival or death.

4.4 *In vitro* electrophysiology

Whole cell voltage-clamp and current-clamp studies were performed on cells visualized using a near-infrared charge-coupled device camera. Patch pipettes were pulled with a Sutter pipette puller (model P-97, Novato) with a resistance of 4-6 MΩ. The slices were perfused with the external solution continuously with bubbling of 95% O_2 and 5% CO_2 at 34°C.

For transfected HEK cell patch recording, the pipette solution for voltage clamp recordings contains (in mM) 130 KCl, 20 NaCl, 5 EGTA, 5.46 $MgCl_2$, 2.56 K_2ATP, 0.3 Li_2GTP, 10 HEPES, pH=7.4, mOsm=313. The aCSF contains (in mM) 20 KCl, 140 NaCl, 0.5 $CaCl_2$, 2 $MgCl_2$, 10 HEPES, pH=7.4, 318 mOsm. The eGFP positive cells will be used for patch clamp. The I-V protocol from -120 mV to 100 mV with delta change of +20 mV and a ramp protocol from -100 mV to 100 mV were performed to confirm positive GIRK2 transfection; morphine-increased K^+ current can be used to confirm positive MOR transfection. A continuous recording protocol with -80 mV holding for 1500ms out of 2000ms was recorded to test the K^+ current amplitude level.

For brain slice whole-cell patch recording, the internal (pipette) solution for current clamp recordings contained (in mM): 130 potassium-gluconate, 10 KCl, 10 HEPES, 2 Mg-ATP, 0. 3 Na-GTP, and 0. 4 EGTA (pH 7.30, 285 mOsm. The aCSF solution for current clamp contained (in mM): 124 NaCl, 3 KCl, 1. 3 NaH_2PO_4, 2 $MgCl_2$, 10 d-glucose, 26 $NaHCO_3$, 2 $CaCl_2$, 0.4 ascorbic acid (pH 7.40 bubbled with 95% O_2 and 5% CO_2). The internal (pipette) solution for voltage clamp recordings contained (in mM): 110 Cs_2SO_4, 0.5 $CaCl_2$, 2 $MgCl_2$, 5 EGTA, 5

HEPES, 5 Mg-ATP. The aCSF for brain slice voltage clamp contains (in mM): 124 NaCl, 2.5 KCl, 1.3 $MgSO_4$, 2.4 $CaCl_2$, 1.2 NaH_2PO_4, 11 glucose, 25 $NaHCO_3$.

Whole-cell voltage clamp experiments were performed at a holding potential of −70 mV. To be able to only record AMPA current in brain slice whole-cell voltage clamp experiments, the synaptic currents were blocked with the NMDA receptor antagonist DL-AP_5 (10 μM), the voltage-gated sodium channel blocker TTX (0.5 μM), and the Cl^- current was blocked by bicuculline (20 μM) and strychnine (2 μM). The LY341495 (20 μM) was applied before CPS (20 μM) treatment to block mGluR and increase glutamate release into synapsis; then LY341495 was replaced by CPS to test if there were any further changings of mEPSCs.

A perfusion speed of 5 ml/min was used to make sure the diffusion of chemicals is quick and sufficient. A minimum of 15 min was allowed between each treatment to eliminate any desensitization, and no slice was exposed to the drug more than 2 times. The cell capacitance was measured at the beginning of the recording, and any recordings where the series resistance changed during the experiment were rejected from further analysis. Recordings were amplified with an Axopatch 200B amplifier (Molecular Devices, Union City, CA) with a 2 kHz filter, digitized at 10 kHz, and collected with the Clampex 10.0 software (Molecular Devices).

4.5 Cell culture and GIRK2/MOR double-transfection

Rat G-protein coupled inwardly rectifying K^+ channel subfamily J member 2 (GIRK2) cDNA (GenBank accession No. XM_039088045), rat mu-opioid receptor (MOR) cDNA (GenBank accession No. XM_008758731) and enhanced green fluoresce protein (eGFP) cDNA (GenBank accession No. YP_003162718) were gifted from Dr. Henry A. Lester and Dr. Norman Davidson at California Institute of Technology. These cDNAs were sub-cloned into the eukaryotic

expression vector pcDNA3.1 (Invitrogen) and used for HEK293 expression without cRNA synthesis. Correct construction was confirmed with DNA sequencing (GENEWIZ).

The HEK293 cells were kindly provided by Dr. Deborah Baro (Georgia State University). HEK293 cells were cultured at 37 °C / 5 % CO_2 according to supplier recommendations. For electrophysiological studies of transfected HEK cell: Day 1, cells were cultured in 35mm culture dish for 24 hours to have 50~80% confluence. Day 2, the amount of 5.0 μg target DNA, 0.5 μg GFP DNA and 8 μl Lipofectamine^{TM}Reagent (Gibco BRL, Cat No. 18324-012, 2mg/ml) will be added into 500 μl Opti-MEM medium (Gibco, Cat No. 31985-070, 1X). Add the mixture to the cultured cell and incubated at 37 °C for 4 hours, withdraw the solution and add 2 ml DMEM with 10% FBS, incubated at 37 °C for 18 hours. Day 3, detach the transfected HEK cell and transferred onto 5 X 5 mm glass slice (pre-coated with Ploy-L-Lysine, Sigma, P4832). Cells were cultured for 24~36 hours before patch clamp recording. Succeed transfected HEK cells were confirmed by positive eGFP together with morphine-increased K^+ current.

4.6 Optogenetic stimulation of GAD-expressing neurons

GAD-expressing neurons were detected in brain slices with eGFP expression using fluorescence microscopy in excitation at 470 nm and emission at 535 nm. Opto-stimulation was performed by using a xenon light source with high-speed switcher (Lambda GD-4, Sutter Instruments, Novato, CA). The light source was connected to the incident-light illuminator port of the Zeiss Axioskop 2 microscope (Carl Zeiss AG) and delivered blue light through a 470-490 nm bandpass filter. The 10ms pulse trains were triggered by the Digi-timer D4030 pulse generator (Digitimer Ltd, UK). The latency of light-evoked action potentials was measured from the onset of the light to the onset of opto currents/potentials

4.7 Single-cell reverse transcriptional PCR

Reverse transcription of the single-cell contents obtained from XII or DMNV neurons after each patch clamp recording and put under -20°C freezer until the reverse transcription was performed. The reverse transcription was done within 12 hours after obtained the single-cell contents. The first-strand cDNA synthesis was done using the high-capacity cDNA reverse transcription kit (Applied Biosystems, LOT 00862966) according to the manufacturer's instructions. The reverse transcription product was kept at -20°C until PCR was performed. PCR primers for the target genes were designed with the computer software programs Primer3 and Primer-BLAST (NIH) (Table 5.1). PCR product lengths were ~200bp to not confuse them with primer dimers. Three microliters of reverse transcription product were loaded into an Eppendorf tube with PCR solution containing 10 µl of 5× green GoTaq flexi buffer, 2 µl $MgCl_2$, 1 µl of 10 mM dNTP mix, 1 µl of 10 mM forward and reverse primers, 0.25 µl of GoTaq polymerase, and diluted to 50 µl with nuclease-free water. The thermal cycling program was set to the initial denaturation for 5 min at 95°C for one cycle. The denaturation, annealing, extension cycles were done at 95°C for 45 s, 58°C for 45 s, and 72°C for 1 min, respectively, for 35 cycles. A final extension cycle was done at 72°C for 10 min. Thirty microliters from the second PCR reaction was run on a 2% agarose gel containing ethidium bromide. Gels were imaged using Alpha Innotech Imaging System (Alpha Innotech, Santa Clara, CA). Presence of receptor subunits in the XII / DMNV cell was defined by having a band at the correct size, regardless of strength. Cells that had bands with smearing, possible degradation, or positive glial fibrillary acidic protein band (either one or more of these three) were eliminated from the experiment.

4.8 Data analysis

Clampfit 10.7 software (Molecular Devices) and Mini Analysis Program 6.0.7 (Synaptosoft Inc.) were used to analyze the electrophysiological data. RT-PCR data were analyzed by ImageJ 1.8.0-112 software (National Institutes of Health) based on their average value from all experiments, in each of which 3-4 samples were tested. Statistical analysis was performed using the two-way ANOVA with Fisher's post hoc test, one-way ANOVA with Bonferroni's post hoc test, and/or the two-tailed Student's t-Test (IBM SPSS Statistics 26.0.0.0). The LD_{50} of morphine was calculated by Hill equation, survival histogram comparison was analyzed by Log-rank (Mantel-Cox) test (Graphpad Prism 5.0). Difference was considered significant when $P \leq 0.05$.

5 RESULT 1: CENTRAL INHIBITORY NEURONAL REGULATION OF CRD

Published as "**Xing, H**. Cui, N. Johnson, C. M. Faisthalab, Z. Jiang, C. Dual synaptic inhibitions of brainstem neurons by GABA and glycine with impact on Rett syndrome. *J Cell Physiol*, 2021. 236(5): p. 3615-3628."

5.1 Acknowledgements

This work was supported by the NIH (1R01-NS073875). We thank Nathan Sabate and Zaakir Faisthalab for technical assistance.

5.2 Abstract

RTT is a neurodevelopmental disease caused by mutations in the *MECP2* gene. People with RTT show breathing dysfunction attributable to the high rate of sudden death. Previous studies have shown that insufficient GABA synaptic inhibition contributes to the breathing abnormalities in mouse models of RTT, while it remains elusive how the other inhibitory neurotransmitter, glycine, is affected. We find optogenetic stimulation of GAD-expressing neurons produced GABAergic and glycinergic postsynaptic inhibitions in the XII and the DMNV. By sequential applications of 10μM bicuculline and 1μM strychnine, such inhibition shows ~44% $GABA_A$ergic and ~52% glycinergic in XII, and ~49% GABAAergic and ~46% glycinergic in DMNV in mice without *Mecp2* disruption. Measuring miniature IPSPs (mIPSCs) in these neurons, the $GABA_A$ergic and glycinergic current amplitudes are ~47% and ~49% in XII neurons, and ~48% and ~50% in DMNV neurons, respectively. Single-cell PCR indicated transcripts of $GABA_A$ receptor γ2 subunit ($GABA_AR\gamma2$) and glycine receptor β subunit (GlyRβ) were simultaneously expressed in these cells. In *Mecp2*^{R168X} mice, proportions of $GABA_A$ergic and glycinergic mIPSC amplitudes became ~28% vs. ~69% in XII, and ~31% vs. ~66% in DMNV. Comparing to control counterparts, $GABA_A$ergic and glycinergic mIPSC amplitudes

were significantly decreased in XII / DMNV, so as the transcripts of $GABA_AR\gamma2$ and GlyRβ. These suggest that inhibitory neurons in the medulla produce toughly equal $GABA_A$ergic and glycinergic synaptic inhibitions of XII and DMNV neurons. With *Mecp2* disruption, the XII / DMNV neurons rely more on glycinergic synaptic inhibition.

5.3 Introduction

RTT is a neurodevelopmental disease seen almost exclusively in girls who have 6 to 18 months of apparently normal development after birth, followed by occurrence and progressive deterioration in motor, learning and other behavioral functions (Gold, Krishnarajy et al. 2018). Other symptoms include breathing abnormalities, midline hand position, unusual eye movements, sleep disturbances, seizures, etc. (Mellios, Feldman et al. 2018). The breathing disorders are attributable to the high rate of sudden death.

Mutations in the *MECP2* gene encoding methyl-CpG binding protein 2 underlie almost all cases of RTT and some variant forms of the condition (Enikanolaiye, Ruston et al. 2020). The cytogenetic location of this gene is the long arm of the X chromosome at position 28. The MeCP2 is a critical regulator for activity of various gene (Sbardella, Tundo et al. 2020, Schmidt, Zhang et al. 2020), and exists in cells throughout the body, particularly abundant in neurons (Pejhan, Siu et al. 2020). Mutations in the *MECP2* gene cause disruptions of normal functions of neurons and glia cells in the brain. One of the most common *Mecp2* mutations associated with Rett syndrome is $Mecp2^{R168X}$ point mutation leading to a premature peptide without the methyl-CpG binding domain. In the mouse model of RTT with $Mecp2^{R168X}$, a number of RTT phenotypes have previously been shown, including respiratory, neuromuscular, and behavioral abnormalities resembling those seen in *Mecp2*-null mice (Luoni, Giannelli et al. 2020).

Breathing and several other autonomic functions are generated or controlled by brainstem neurons, including those in the XII and the DMNV. The XII houses somatic motor neurons innervating the extrinsic and intrinsic muscles of the tongue. They control the upper airway dimension, tongue movements, speech, and swallowing. The XII neurons are modulated by respiratory neuronal networks with regular respiratory bursting activity and provide changes in tongue muscular tones according to the breathing rhythm (Petukhova, Ponomareva et al. 2018, Subramaniam, Bawden et al. 2018). The DMNV contains visceral motor neurons constituting the major vagus efferents. It serves for most parasympathetic motor functions in the heart, the gastrointestinal tract, and the urogenital system.

Previous studies in mouse and rat models of RTT have shown that several groups of brainstem neurons are overly excited, including those in the ventral respiratory group (Yamanouchi, Kaga et al. 1993, Calfa, Li et al. 2015, Wu, Zhong et al. 2016, Oginsky, Cui et al. 2017). The hyper-excitability of the brainstem neurons is related to deficiency in GABAergic synaptic inhibition (He, Chen et al. 2014, Abdala, Toward et al. 2016, Anderson, Garcia et al. 2016), which as well as several RTT-types of breathing abnormalities can be improved after the administration of GABA re-uptake blockers or GABA receptor agonists (Fogarty, Smallcombe et al. 2013, Jin, Cui et al. 2013, Zhong, Johnson et al. 2016). Glycine is another inhibitory neurotransmitter playing a role in the spinal cord and the retina (Fogarty, Smallcombe et al. 2013, Poria and Dhingra 2015, Zhou, Han et al. 2016, Petukhova, Ponomareva et al. 2018, Waldvogel, Biggins et al. 2019). Glycine plays an inhibitory role in the brainstem, whereas it is still unclear how the *Mecp2* disruption affects glycine signaling here. More importantly, if neurons adopt both GABAergic and glycinergic synaptic inhibitions, they may gain a survival strategy for system conservation by alternation in the case when one of them becomes defected,

which may occur in the RTT model. To test this hypothesis, we performed these studies. We chose the *Mecp2*^{R168X} mice to study how the GABAergic and glycinergic synaptic inhibitions are affected as this mouse model is closer to human RTT patients than the *Mecp2*-null models. We chose the male mice because: The hemizygous mutant male shows similar symptoms compared to symptomatic heterozygous females (Shah and Bird 2017, Ribeiro and MacDonald 2020). The heterozygous female mice show a large variability in RTT-like symptoms because of the numerous asymptomatic heterozygous females (Johnson, Cui et al. 2015). Also, the hemizygous male are considered as a common model for this disease (Ribeiro and MacDonald 2020).

5.4 Results

5.4.1 Optogenetic stimulation of GAD-expressing neurons inhibit XII / DMNV neurons

Transverse brainstem slices were obtained from *GAD-ChR* mice. GFP-positive neurons were found in several brainstem areas. At the level of the obex (Figure 5.1A & B), these GFP-positive neurons were seen in the area ventrolateral to the XII nucleus (Figure 5.1C, D_1 & D_2). In contrast, cells in the XII and DMNV showed no GFP fluorescence (Figure 5.1D_1 & D_2). In whole-cell voltage clamp, a large outward current was produced in these GFP-positive cells with opto-stimulation (Figure 5.1E_1 & E_2). The current reversed its polarity at near 0mV (Figure 5.1F_1 & F_2), indicating that the current is conducted by cations confirming the expression of ChR in these cells.

Whole-cell recording from the XII / DMNV neurons (Figure 5.2A) showed that the opto-stimulation produced strong hyperpolarization and inhibition of neuronal firing activity (Figure 5.2B_1 & C_1). The hyperpolarization reversed its polarity at near the Cl- reversal potential (Figure 5.2B_2 & B_3). The photo-response was abolished in the presence of TTX (Figure 5.2C_2),

suggesting that the inhibition is post-synaptic after opto-stimulation of ChR-expressing neurons, which is likely to be inhibitory postsynaptic potentials (IPSPs).

5.4.2 The opto-inhibition is eliminated with a joint application of $GABA_A$ & glycine receptor blockers

Because of the Cl^- reversal potential in *GAD-ChR* transgenic mice, we expected that the opto IPSPs recorded in XII and DMNV neurons to be mediated by $GABA_A$ receptors. To our surprise, we found that the IPSPs were not eliminated after application of a high concentration of bicuculline (Bccl, 10 μM) (Figure 5.3A_1 & B_1). The remaining portion of the IPSPs was totally abolished when 1 μM strychnine (Stcn) was added to the perfusion solution (Figure 5.3A_1 & B_1). Similarly, the opto IPSPs were attenuated but not blocked by 1 μM Stcn alone (Figure 5.3A_2 & B_2). They were completely blocked with 10 μM bicuculline added after Stcn (Figure 5.3A_2 & B_2). These results indicate that the ChR-expressing neurons release both GABA and glycine with opto-stimulation, and these neurotransmitters produce postsynaptic inhibitions of XII and DMNV neurons by activations of $GABA_A$ and glycine receptors.

To address the question as to whether XII and DMNV neurons rely on one of the neurotransmitters more than the other, we performed quantitative studies by blocking $GABA_A$ and glycine receptors sequentially. With application of 10 μM Bccl first followed by 1 μM Stcn, the opto IPSPs were suppressed by 49.1 ± 7.4% (means ± s.e.) and 48.2 ± 6.3%, respectively, in XII neurons (Bccl: 5.4±1.1mV, Stcn: 5.2±1.1mV, n=9), and by 51.7 ± 4.0% and 44.4 ± 3.9%, respectively, in DMNV neurons (Bccl: 5.8±1.1mV, Stcn: 4.9±0.8mV, n=9) (Figure 5.3C) (Table 5.2).

With application of 1 μM Stcn first followed by 10 μM Bccl, the opto IPSPs were suppressed by 51.9 ± 3.4% and 44.4 ± 3.9%, respectively, in XII neurons (Stcn: 7.6±1.3mV, Bccl:

5.2±0.8mV, n=8), and by 47.6 ± 2.2% and 47.4 ± 2.2%, respectively, in DMNV neurons (Stcn: 6.2±0.9mV, Bccl: 6.1±1.0mV, n=11) (Figure 5.3D) (Table 5.2).

5.4.3 Miniature IPSCs consisted of $GABA_A$ / glycine components

In voltage clamp, miniature IPSCs were studied in these two groups of neurons after chemical synaptic isolation with AP_5, DNQX and TTX (to remove glutamatergic synaptic excitations and spontaneous firing activity). The cells were recorded at a holding potential near to the E_K with Cs^+ in the pipette solution to get rid of K^+ current and $GABA_B$ receptor contribution. Under this condition, mIPSCs were recorded from XII and DMNV cells (Figures 4 & 5). In the control mice, the baseline amplitude and frequency of these mIPSCs in XII neurons were 33.2 ± 2.2 pA and 8.2 ± 1.2 Hz (n=24), respectively. They were 35.0 ± 3.4 pA and 6.5 ± 0.9 Hz in DMNV cells (n=18), respectively. Neither the mIPSC amplitude nor the frequency was significantly different between the XII and DMNV neurons (Amplitude: XII, mean=33.2±2.2pA, n=24; DMNV, mean=35.0±3.4pA, n=18; P=0.65. Frequency: XII, mean=8.2±1.2Hz, n=24; DMNV, mean=6.5±0.9Hz, n=18; P=0.34. Student's t-Test).

With 10 µM Bccl treatment first followed by 1 µM Stcn, the mIPSC amplitude was reduced by 52.8 ± 1.6% and 43.1 ± 2.4% (Bccl: 18.8±1.6pA, Stcn: 15.5±1.5pA, n=9), the frequency was suppressed by 52.7 ± 6.6% and 46.6 ± 6.7% (Bccl: 7.7±1.4Hz, Stcn: 5.3±0.5Hz, n=9), respectively (Figure 5.4A_1 & C; Table 5.3) in XII neurons. In DMNV with the same sequence of blocker treatments, the mIPSC amplitude was reduced by 46.7 ± 2.0% and 51.4 ± 2.3% (Bccl: 18.4±2.7pA, Stcn: 18.9±2.8pA, n=9), the frequency was reduced by 57.2 ± 1.0% and 41.8 ± 1.1%, respectively (Bccl: 3.7±0.7Hz, Stcn: 2.3±0.5Hz, n=9) (Figure 5.5A_1 & C; Table 5.3). With 1 µM Stcn first followed by 10 µM Bccl, the mIPSC amplitude was reduced in XII neurons by 50.0 ± 2.7% and 46.1 ± 2.4%, respectively (Stcn: 16.0±1.8pA, Bccl: 15.0±1.8pA, n=15),

while the frequency was lowered by 47.0 ± 6.1% and 48.9 ± 6.4%, respectively (Stcn: 2.3±0.5Hz, Bccl: 2.6±0.6Hz, n=15) (Figure 5.4A_2 & D; Table 5.3). In DMNV, the mIPSC amplitude was decreased by 50.8 ± 2.6% and 46.3 ± 2.5% (Stcn: 16.5±2.4pA, Bccl: 15.0±2.3pA, n=9), and the frequency was reduced by 47.6 ± 3.4% and 49.2 ± 3.9%, respectively (Stcn: 3.6±0.7Hz, Bccl: 4.0±0.8Hz, n=9) (Figure 5.5A_2 & D; Table 5.3).

5.4.4 Single cell RT-PCR showed $GABA_A$ / glycine receptor transcriptions

If XII and DMNV neurons adopt both GABAergic and glycinergic synaptic inhibitions, they should express both types of receptors. To test this, we performed single-cell PCR analysis in individual XII and DMNV cells after electrophysiological recording. From the control group, both $GABA_A$R- γ2 and GlyR- β transcripts were detected in XII (8 of 14) and DMNV (11 of 18) neurons (Figure 6A & C). In the other cells, we had either smear band (likely caused by RNA degradation) or GFAP detection (glia contamination), both of which were rejected from data analysis. We did not find a single band of either $GABA_A$R- γ2 or GlyR- β transcripts in any XII or DMNV cells.

In XII neurons, the optical density of $GABA_A$R- γ2 vs GlyR- β was 1.00 vs 1.10 (0.96 ± 0.19, n=8 vs 1.08 ± 0.15, n=8; P=0.18) (Figure 5.6B_1). In DMNV cells, the optical density of $GABA_A$R- γ2 vs GlyR- β = 1.00 vs 1.03 (0.93 ± 0.14, n=11 vs 0.96 ± 0.14, n=11; P=0.73) (Figure 5.6D_1). These results together with our electrophysiological data indicate that GABAergic and glycinergic inhibitions are shared by the XII and DMNV neurons in roughly equal proportions.

5.4.5 Miniature IPSCs in mice with Mecp2-disruption

Previous studies indicate that several group of brainstem neurons are overly excited in animal models of RTT (Chao, Chen et al. 2010, Oginsky, Cui et al. 2017), which may be caused by

inadequate synaptic inhibition by GABA, glycine, or both. Therefore, we studied mIPSCs in XII and DMNV neurons in brain slices obtained from male R168X mice. The baseline mIPSCs (including $GABA_A$ergic and glycinergic mIPSCs) were lower in these neurons than in those from the control mice without *Mecp2* disruption. In XII neurons, the average baseline amplitude and frequency of mIPSCs were 11.6 ± 1.2 pA and 2.9 ± 0.7 Hz, respectively (n=15, Table 5.4), equivalent to 65.0% and 63.9% reductions compared to neurons from control mice. In DMNV neurons, the average baseline amplitude and frequency of mIPSCs were 22.0 ± 2.1 pA and 3.1 ± 0.4 Hz, respectively (n=18; Table 5.4), reduced by 37.1% and 52.3% compared to neurons from control mice.

With 10 μM Bccl exposure first followed by 1 μM Stcn, the mIPSC amplitude of XII neurons was inhibited by 29.2 ± 3.2% and 68.9 ± 3.7% (Bccl: 4.0±0.9pA, Stcn: 8.4±0.9pA, n=9), while the frequency was suppressed by 32.0 ± 6.4% and 64.1 ± 5.9%, respectively (Bccl: 1.3±0.3Hz, Stcn: 2.7±0.7Hz, n=9) (Figure 5.4B_1 & C; Table 5.4). In DMNV neurons, the mIPSC amplitude was inhibited by 30.9 ± 4.5% and 65.5 ± 4.5% (Bccl: 6.9±1.1pA, Stcn: 14.7±2.6pA, n=8), the frequency was reduced by 27.5 ± 1.6% and 50.5 ± 1.5%, respectively (Bccl: 1.5±0.6Hz, Stcn: 1.9±0.4Hz, n=8) (Figure 5.5B_1 & C; Table 5.4).

With 1 μM Stcn first followed by 10 μM Bccl, the mIPSC amplitude of XII neurons was reduced by 69.6 ± 3.9% and 27.4 ± 4.8% (Stcn: 7.2±1.4pA, Bccl: 2.6±0.5pA, n=6), the frequency was suppressed by 72.1 ± 5.6% and 25.5 ± 6.0%, respectively (Stcn: 0.8±0.2Hz, Bccl: 0.3±0.1Hz, n=6) (Figure 5.4B_2 & D; Table 5.4). In DMNV neurons, the mIPSC amplitude was inhibited by 67.4 ± 4.2% and 30.3 ± 4.0% (Stcn: 15.3±2.9pA, Bccl: 5.9±0.7pA, n=8), the frequency was reduced by 65.0 ± 10.8% and 29.9 ± 8.6%, respectively (Stcn: 1.9±0.5Hz, Bccl: 0.7±0.2Hz, n=8) (Figure 5.5B_2 & D; Table 5.4).

Compared to control neurons without *Mecp2* disruption, the $GABA_AR$-γ2 and GlyR-β mRNA levels in both XII & DMNV were lowered in R168X mice (Figure 5.6A & C). The proportion of these two receptor subunits was shifted towards glycine dominancy. In XII neurons, the optical density of $GABA_AR$-γ2 vs GlyR-β was 1.00 vs 1.97 (0.17 ± 0.04 vs. 0.32 ± 0.05, n=24; P=0.006) (Figure 5.6A & B_2). In DMNV cells, the optical density of $GABA_AR$-γ2 vs GlyR-β = 1.00 vs 3.37 (0.22 ± 0.05 vs. 0.73 ± 0.11, n=24; P=0.0003) (Figure 5.6A & D_2).

5.5 Discussion

GABA and glycine are the most important inhibitory neurotransmitters in the developmentally mature mammalian CNS (Ito 2016). In the spinal cord glycine plays a prominent role, while GABA is believed to be the chief player in all other areas of the CNS (Scain, Le Corronc et al. 2010, Ito 2016). Previous studies have shown that GABA and glycine neurotransmitters are co-localized in interneurons in the cerebellar cortex (Crook, Hendrickson et al. 2006, Simat, Parpan et al. 2007) and retina (Koontz, Hendrickson et al. 1993). Co-expression of $GABA_A$ and glycine receptor subunits have also been found in motor neurons in the XII and spinal cord (Carlton and Hayes 1990, Christenson, Shupliakov et al. 1993, Ornung, Shupliakov et al. 1996, Tatetsu, Kim et al. 2012, Waldvogel, Biggins et al. 2019), and GABA / glycine are known to be essential during neuronal development and regeneration, although their functional consequences in regulating medullary neurons are still not clear, especially in RTT. Our observation in the present study strongly suggests that in the medulla oblongata GABA and glycine seem to play equally important roles in the inhibitory neurotransmission, and medullary neurons seem to rely more on glycine signaling in the mouse model of RTT.

Our first evidence was from optogenetic studies in *GAD-ChR* transgenic mice by crossbreeding the *GAD-Cre* mice with *ChR-loxP*-floxed mice. Because the ChR was tandem-

linked to eGFP in the open reading frame, its expression was identified with green fluorescence (Jin, Cui et al. 2013, Zhong, Cui et al. 2015). Functional studies confirmed the expression of ChR based on opto activation of inward cationic currents in voltage clamp and opto depolarization in current clamp in these eGFP-positive neurons. In eGFP-negative XII and DMNV cells opto activation of *GAD-ChR* neurons produces a clear inhibitory post-synaptic potential that has Cl^- reversal potential and disappears in the presence of TTX, indicating that these XII and DMNV neurons are post-synaptic cells. This inhibitory neurotransmission was sensitive to $GABA_A$ receptor antagonist Bccl and glycine receptor antagonist Stcn. It can be suppressed but cannot be totally blocked by either alone. Only can a joint application of both Bccl and Stcn completely eliminate the opto IPSPs. With sequential applications of these blockers, we have found that amplitudes of the GABAergic and glycinergic IPSPs are roughly equal, which were observed in both XII cells and DMNV neurons. This indicates that opto stimulation triggers a release of GABA and glycine from the pre-synaptic GAD expressing neurons.

We have obtained evidence for the inhibitory synaptic transmission via the measurement of mIPSCs with whole cell voltage clamp. This approach allows us to observe spontaneously occurring synaptic currents in a more natural condition without opto-stimulation. The Cl^--mediated inhibitory post-synaptic current was measured after elimination of glutamatergic currents, K^+ currents and neuronal firing activity (Zhong, Cui et al. 2015). Clear mIPSCs have been found from XII / DMNV neurons, which can only partly be inhibited by the application of Bccl or Stcn alone. With a joint application of Bccl / Stcn, the mIPSCs are completely abolished, consistent with our observation with opto stimulation. By quantitative analyzed the data, we have found that $GABA_A$ and glycine currents take equal proportions of the total mIPSCs. These

findings suggest that XII /DMNV neurons receive both GABA and glycine from presynaptic neurons, which are released spontaneously or as a result of firing activity. When we applied the Bccl, Stcn or both, we found that the mIPSC frequency was also reduced, which is likely due to the suppression of the mIPSCs, leading to failure of detection of modest mIPSC events. Supporting the joint contribution of inhibitory synaptic transmission is another evidence from single cell PCR. We picked up a $GABA_A$ receptor subunit and a glycine receptor subunit in our single cell RT-PCR study, which have been previously demonstrated to be reliable markers for GABA and glycine receptor expressions (Haverkamp, Muller et al. 2004, Grudzinska, Schemm et al. 2005, Betz and Laube 2006). Our results from control mice have shown that XII and DMNV neurons have mRNA expressions of both $GABA_A$ receptor γ_2 subunit and glycine receptor β subunit. The transcription levels do not show any significant difference between $GABA_A$Rγ2 and GlyRβ in the XII or DMNV cells, results that are consistent with our electrophysiological findings described above.

Previous studies have shown that in RTT mice with *Mecp2* disruption, the GABA-mediated inhibitory signal is defective, attributable to the development of RTT-like breathing dysfunction (Chao, Chen et al. 2010, Lozovaya, Nardou et al. 2019). In contrast, how glycinergic inhibitory signal is affected in RTT models is poorly studied. A previous study showed that no genomic disturbances were found in glycine receptor α_2 subunit located on the chromosome Xp22.2 where there are several common mutations in RTT patients (Cummings, Dahle et al. 1998). Other studies indicated that the glycine receptor α_3 subunit and glycine transporter 2 may be involved in the breathing abnormalities in RTT models (Hulsmann, Mesuret et al. 2016, Mesuret, Dannenberg et al. 2018). If medullary neurons adopt both GABAergic and glycinergic synaptic inhibitions, functional activity of the glycinergic synaptic inhibition needs to be better

understood in the RTT mice. Indeed, our whole cell voltage clamp study has shown that the amplitude and frequency of mIPSCs in XII and DMNV neurons of the R168X mutation mice are significantly lower than those from control mice. In XII neurons, $GABA_A$ergic and glycinergic mIPSC amplitudes are lowered by ~80% and ~50% when comparing to their counterparts in control mice. In DMNV neurons, $GABA_A$ergic and glycinergic mIPSC amplitudes are lowered by ~62% and ~15% when comparing to control neurons. The proportions of the $GABA_A$ergic to glycinergic mIPSCs (amplitudes) shift from about 1:1 in control to 1:2 in R168X in both types of neurons. Thus, both GABA- and glycine-induced mIPSCs were significantly reduced in *Mecp2*^{R168X} mice. Compared to GABAergic mIPSCs, the deficiency in glycinergic mIPSCs appears less severe, which may allow glycine to contribute more to the remaining inhibitory neuronal communication in XII & DMNV neurons. Our data suggest that the deficiency of GABAergic and glycinergic mIPSCs is more severe in XII neurons than in DMNV cells. This might be due to the functional differences between XII and DMNV neurons as the XII neurons are somatic motor neurons, whereas the DMNV neurons are visceral motor neurons. Functional maintenance of these motor outputs may rely on one of the neurotransmitters more than the other.

We believe that the demonstration of brainstem neuronal adoption of dual inhibitory synaptic transmission is significant, which not only is a novel finding, but also reveals a potentially important mechanism. The brainstem controls several vital functions like respiratory control and cardiovascular control. Thus, additional conservational strategies may be necessary for survival. In comparison to GABAergic synaptic transmission (Wang, Johnston et al. 2005, Chao, Chen et al. 2010), glycinergic signals seem to be less affected in two types of medullary neurons. Although the underlying mechanism for the difference in these two inhibitory neurotransmitter

systems is still not fully understood, the better reserved glycinergic signals might serve to compensate, at a certain degree, the loss of GABA signaling. Therapeutically, the reserved glycinergic signals also could be targeted by promoting the pre-synaptic glycine release, increasing synaptic glycine levels by manipulating re-uptake, or enhancing the function of glycine receptors. These may improve the inhibitory synaptic inputs to medullary neurons alleviating RTT-like symptoms.

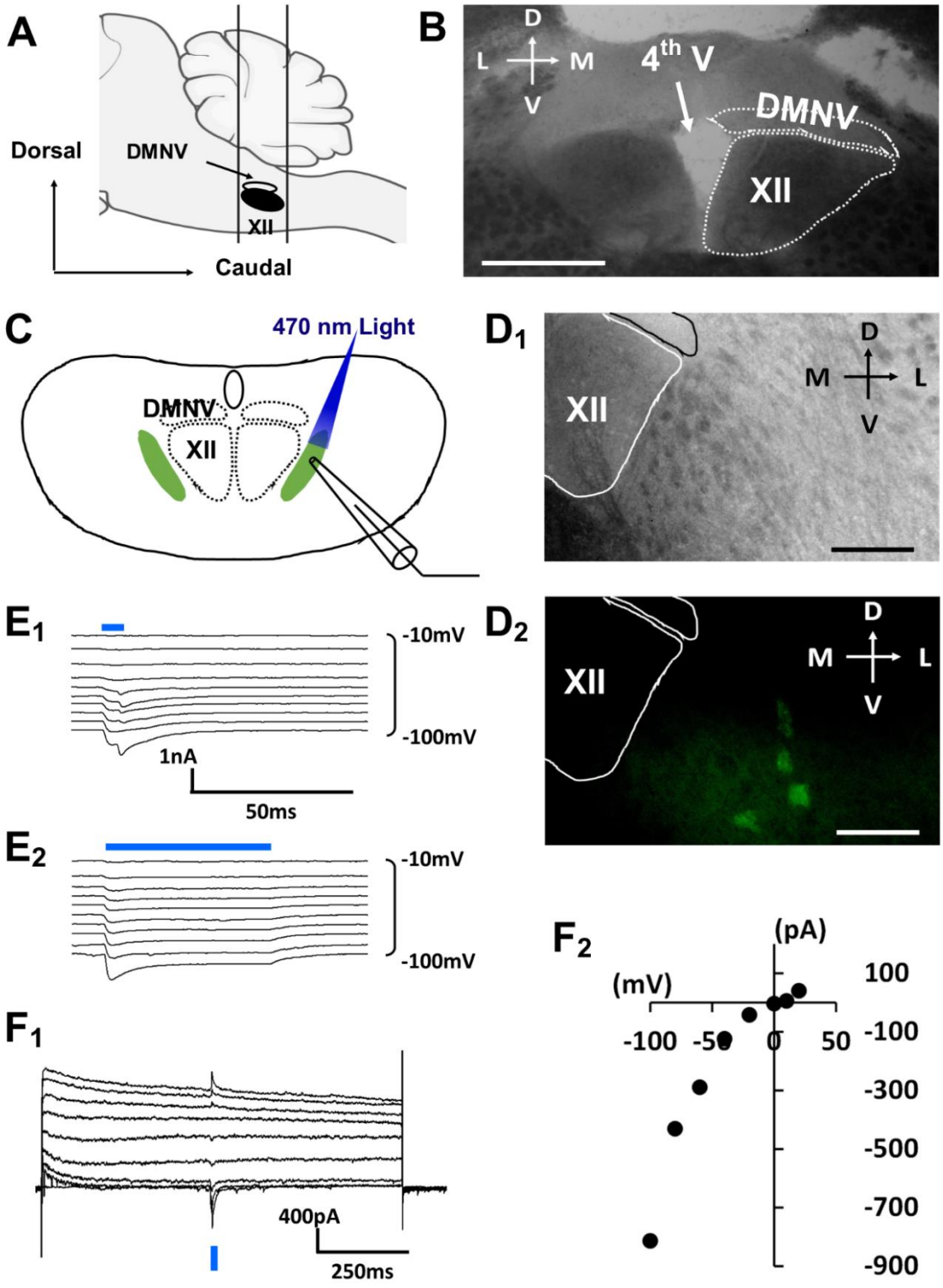
A
Dorsal
DMNV
XII
Caudal
B
D
L
M
V
4th V
DMNV
XII
C
470 nm Light
DMNV
XII
D1
XII
D
M
L
V
D2
XII
D
M
L
V
E1
-10mV
-100mV
1nA
50ms
E2
-10mV
-100mV
F1
400pA
250ms
F2
(pA)
(mV)
100
-100
-300
-500
-700
-900
-100
-50
0
50

Figure 5.1 Optogenetic activation of GAD-expressing neurons.

A. Schematics of sagittal section of the mouse brainstem containing the XII and the DMNV. B. In a coronal section at the obex level in the medulla oblongata, the XII and DMNV are easily identified (scale bar: 800μm). C. Schematics of opto-stimulation and whole-cell recording from GAD-ChR neurons. D. In another coronal section obtained from the medulla of *GAD-ChR* transgenic mice, eGFP positive neurons (D_2) are located ventrolateral to hypoglossal area (D_1). Scale bar: 200μm. E. In voltage clamp recording of GAD-expressing neurons, a clear inward photo current was evoked by 10ms (E_1) and 50ms (E_2) with opto-stimulation. F. In another eGFP positive cell, the photo current reversed its polarity with more depolarization (F_1). The I-V relationship shows the reversal potential of the photo current at 0mV (F_2).

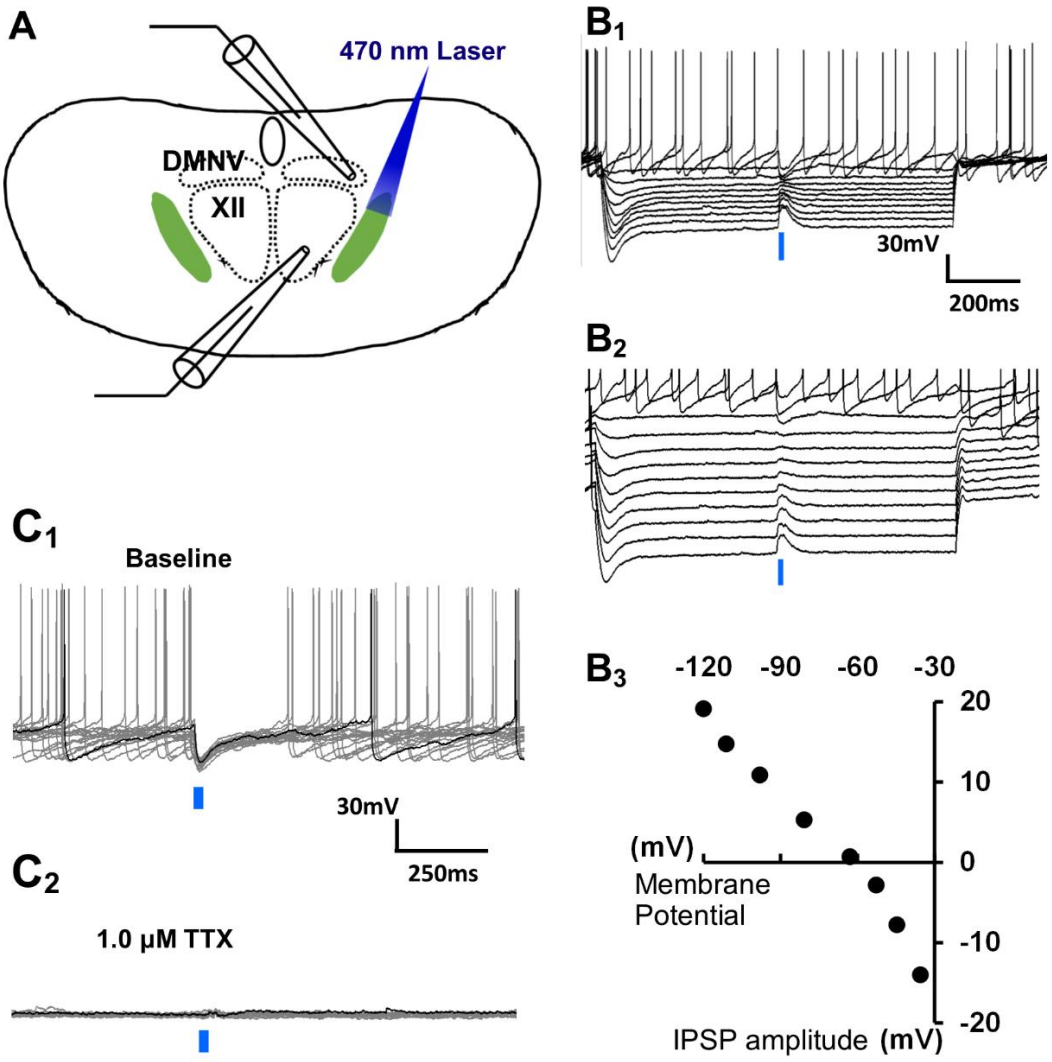

Figure 5.2 Post-synaptic response of XII and DMNV neurons to optogenetic stimulation.

A. Schematics of whole cell recordings from XII and DMNV neurons with opto-stimulation. B_1. The opto-stimulation produced hyperpolarization in a XII neuron without current injection. The hyperpolarization became smaller and smaller with hyperpolarizing current injections, and reversed its polarity with strong hyperpolarizing currents, which is better viewed when the traces are deliberately separated in B_2. B_3. When its amplitude is plotted against membrane potentials created by current injections, a reversal potential at near -60mV is seen, indicating that it is IPSP.

In a DMNV neuron, opto-stimulation produced IPSP and inhibition of spontaneous firing activity (C_1), and the IPSP was eliminated in the presence of 1 μM tetrodotoxin (TTX, C_2).

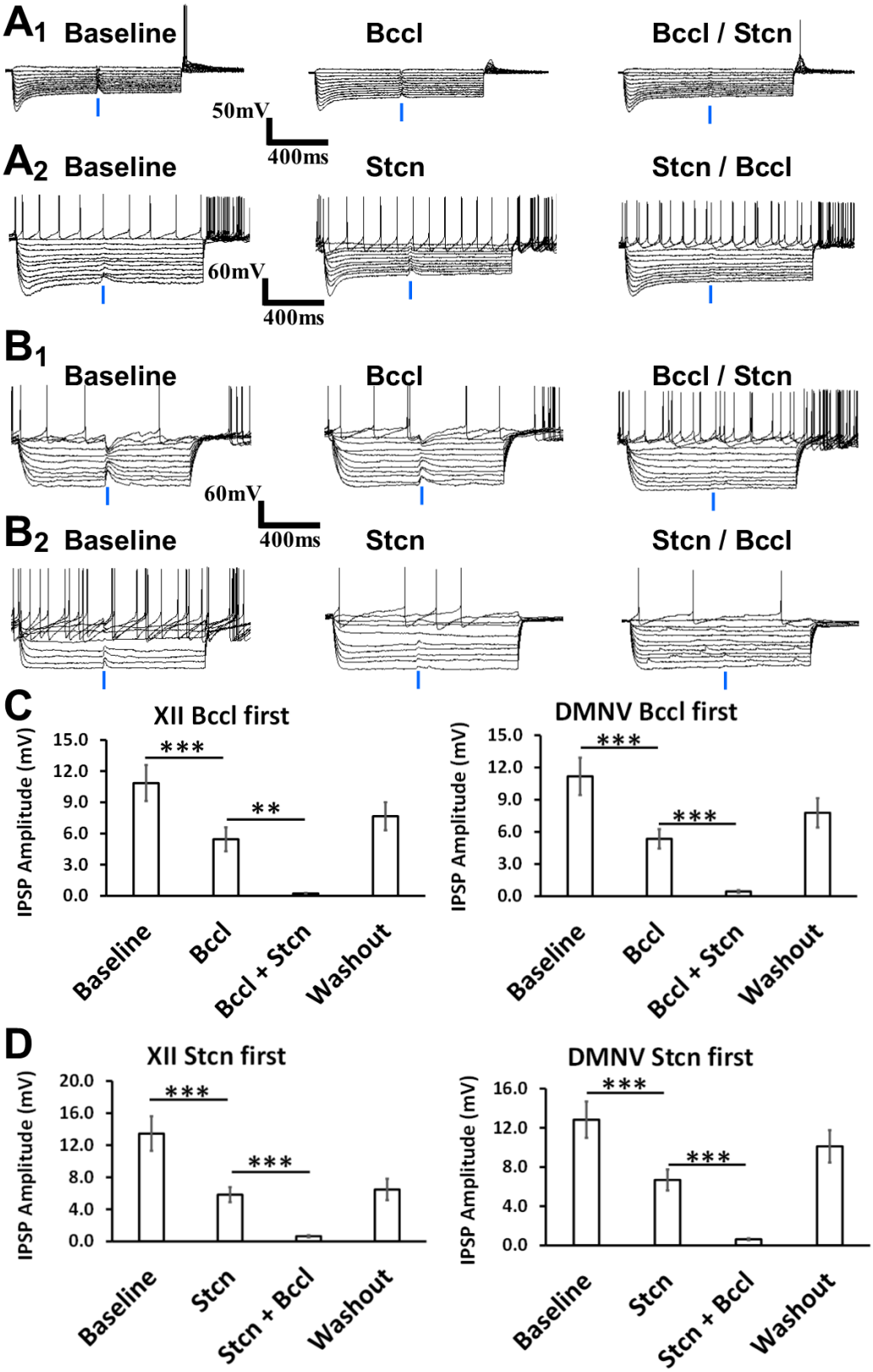
A1 Baseline
Bccl
Bccl / Stcn
50mV
400ms
A2 Baseline
Stcn
Stcn / Bccl
60mV
400ms
B1 Baseline
Bccl
Bccl / Stcn
60mV
400ms
B2 Baseline
Stcn
Stcn / Bccl
C
XII Bccl first
DMNV Bccl first
IPSP Amplitude (mV)
15.0
12.0
9.0
6.0
3.0
0.0
***
**
***
***
Baseline
Bccl
Bccl + Stcn
Washout
D
XII Stcn first
DMNV Stcn first
IPSP Amplitude (mV)
20.0
16.0
12.0
8.0
4.0
0.0
***
***
***
***
Baseline
Stcn
Stcn + Bccl
Washout

Figure 5.3 Involvement of both GABAergic and glycinergic synaptic inhibitions in XII and DMNV neurons.

Whole-cell current clamp was performed before and after blockade of GABA- receptor with 10 μM Bccl and glycine receptor with 1 μM Stcn. A. in XII neurons, opto-stimulation produced IPSPs in the baseline. A_1. The opto IPSP was diminished in the presence of Bccl, and totally abolished after exposures to both Bccl and Stcn. A_2. In another XII cell, the IPSP was also partially blocked by Stcn and completely eliminated with Stcn and Bccl. B. Similar effects were observed in DMNV cells with the same sequences of application of these $GABA_A$ and glycine receptor blockers but neither alone. C, D. Quantitative analysis of the IPSP suppressions by Stcn and Bccl indicates that with application of Bccl first, the opto IPSP was significantly inhibited by 5.4±1.1mV (P=0.0008, n=9) in XII neurons, and by 5.8±1.1mV (P=0.0006, n=9) in DMNV cells; then with Bccl plus Stcn, the opto IPSP was decreased by 5.2±1.1mV (P=0.0015, n=9) in XII and by 4.9±0.8mV (P=0.0003, n=9) in DMNV (C). With Stcn first, the opto IPSP was significantly inhibited by 7.6±1.3mV (P=0.0007, n=8) in XII and by 6.2±0.9mV (P=0.0003, n=11) in DMNV; then with Stcn / Bccl, the opto IPSP was totally eliminated by 5.2±0.8mV (P=0.0004, n=8) in XII and by 6.1±1.0mV (P=0.0004, n=11) in DMNV (D) (**, P<0.01; ***, P<0.001. Student's t-Test).

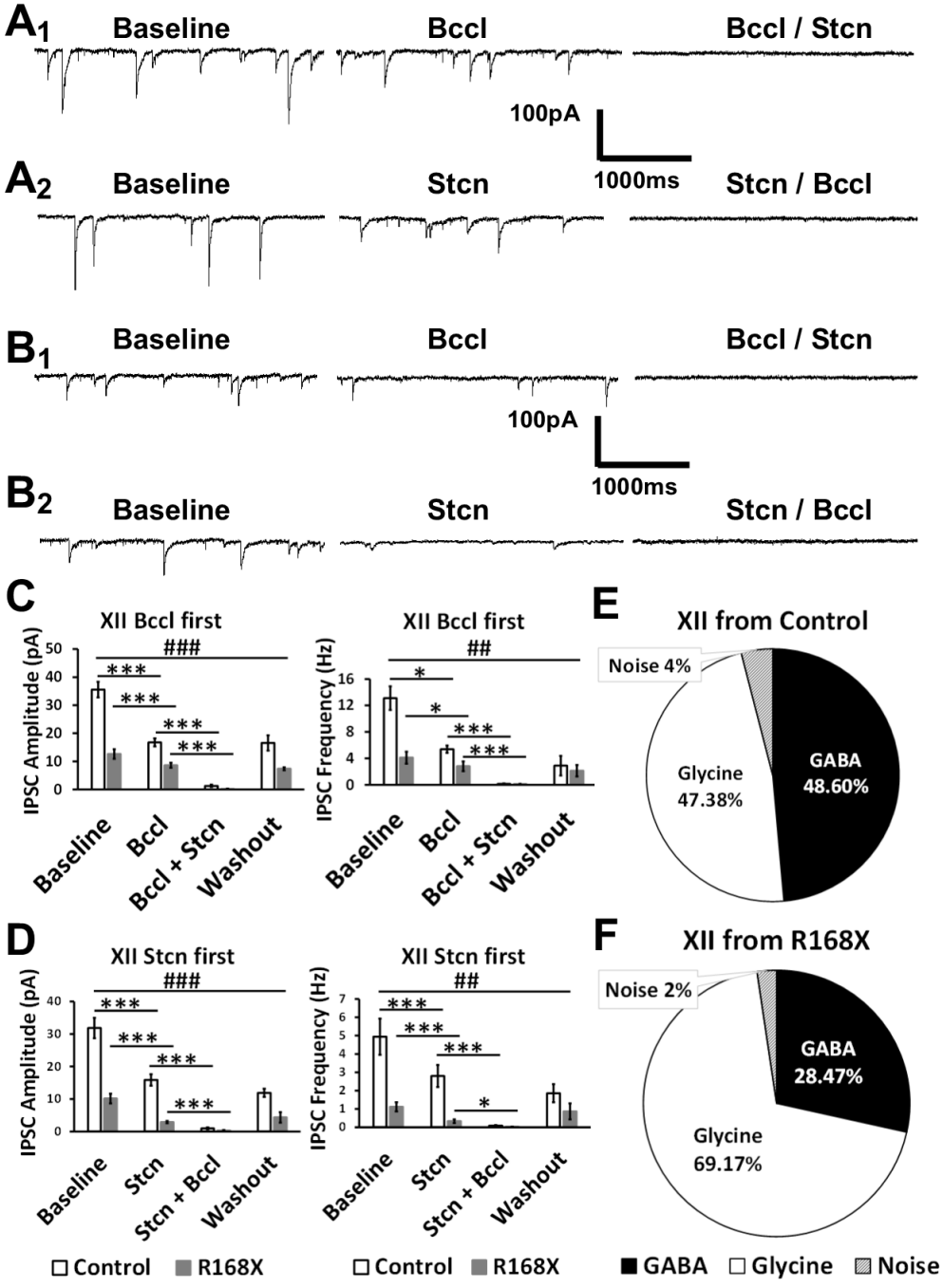
A1
Baseline
Bccl
Bccl / Stcn
100pA
1000ms
A2
Baseline
Stcn
Stcn / Bccl
B1
Baseline
Bccl
Bccl / Stcn
100pA
1000ms
B2
Baseline
Stcn
Stcn / Bccl
C
XII Bccl first
IPSC Amplitude (pA)
Baseline
Bccl
Bccl + Stcn
Washout
XII Bccl first
IPSC Frequency (Hz)
Baseline
Bccl
Bccl + Stcn
Washout
D
XII Stcn first
IPSC Amplitude (pA)
Baseline
Stcn
Stcn + Bccl
Washout
XII Stcn first
IPSC Frequency (Hz)
Baseline
Stcn
Stcn + Bccl
Washout
Control
R168X
Control
R168X
E
XII from Control
Noise 4%
GABA
48.60%
Glycine
47.38%
F
XII from R168X
Noise 2%
GABA
28.47%
Glycine
69.17%
GABA
Glycine
Noise

Figure 5.4 Bicuculline and strychnine sensitivities of miniature IPSCs (mIPSCs) of XII neurons recorded from mice with and without the R168X mutation in *Mecp2*.

A_1. The mIPSCs were studied in a XII neuron from a control mouse with sequential applications of Bccl (10 μM) and then Bccl (10 μM) / Stcn (1 μM). A_2. In another XII cell from a control mouse, the blocker exposure sequence was switched to Stcn (1 μM) first and then Bccl (10 μM) / Stcn (1 μM). The IPSCs were completely eliminated by both blockers but not a single blocker alone. B. Similar experiments were done in XII neurons from mice with the R168X mutation. Under the same condition and blocker exposure sequence, suppressions of the mIPSCs were seen as in the control group of neurons, although the mIPSC amplitude and frequency were lower. C. Treatment with Bccl first significantly decreased the mIPSC amplitude by 18.8±1.6pA (P=0.0007, n=9) and frequency by 7.7±1.4Hz (P=0.025, n=9) in the control group. Such treatment reduced the amplitude by 4.0±0.9pA (P=0.0001, n=9) and frequency by 1.3±0.3Hz (P=0.025, n=9) in R168X group. With Bccl / Stcn, the mIPSC amplitude was suppressed by 15.5±1.5pA (P=0.0002, n=9) and 8.4±0.9pA (P=0.0002, n=9) in the control and R168X groups, respectively, the frequency by 5.3±0.5Hz (P=0.0001, n=9) and 2.7±0.7Hz (P=0.0001, n=9), respectively. D. With Stcn first, the mIPSC amplitude was significantly decreased by 16.0±1.8pA (P=0.0002, n=15), and the frequency by 2.3±0.5Hz (P=0.0002, n=15) in the control group. The same exposures reduced the amplitude by 7.2±1.4pA (P=0.0001, n=6) & frequency by 0.8±0.2Hz (P=0.0002, n=6) in R168X group. Similarly, joint application of Stcn / Bccl inhibited the mIPSC amplitude by 15.0±1.8pA (P=0.0002, n=15) and2.6±0.5pA (P=0.0002, n=6), and the frequency by 2.6±0.6Hz (P=0.0003, n=15) and 0.3±0.1Hz (P=0.021, n=6) in the

control and *R168X* groups, respectively. (*, P<0.05; ***, P<0.001. Fisher's LSD post hoc). For the amplitude of mIPSCs, the main effect of genotype (F = 79.5, df = 1, P = 0.0001), treatment (F = 83.2, df = 3, P = 0.0005) and interactions of genotype × treatment (F = 19.2, df = 3, P = 0.0006) were significant (###, p < 0.001; Two-way ANOVA). As the frequency of mIPSCs, the main effect of genotype (F = 16.2, df = 1, P = 0.0001), treatment (F = 21.0, df = 3, P = 0.0008) and interactions of genotype × treatment (F = 4.3, df = 3, P = 0.007) were significant (##, p < 0.01; Two-way ANOVA). E & F. Proportion of $GABA_A$– and glycine-induced IPSC shifted from 48.6±1.7% vs. 47.4±2.0% (control) to 28.5±2.6% vs. 69.2±2.4% (R168X).

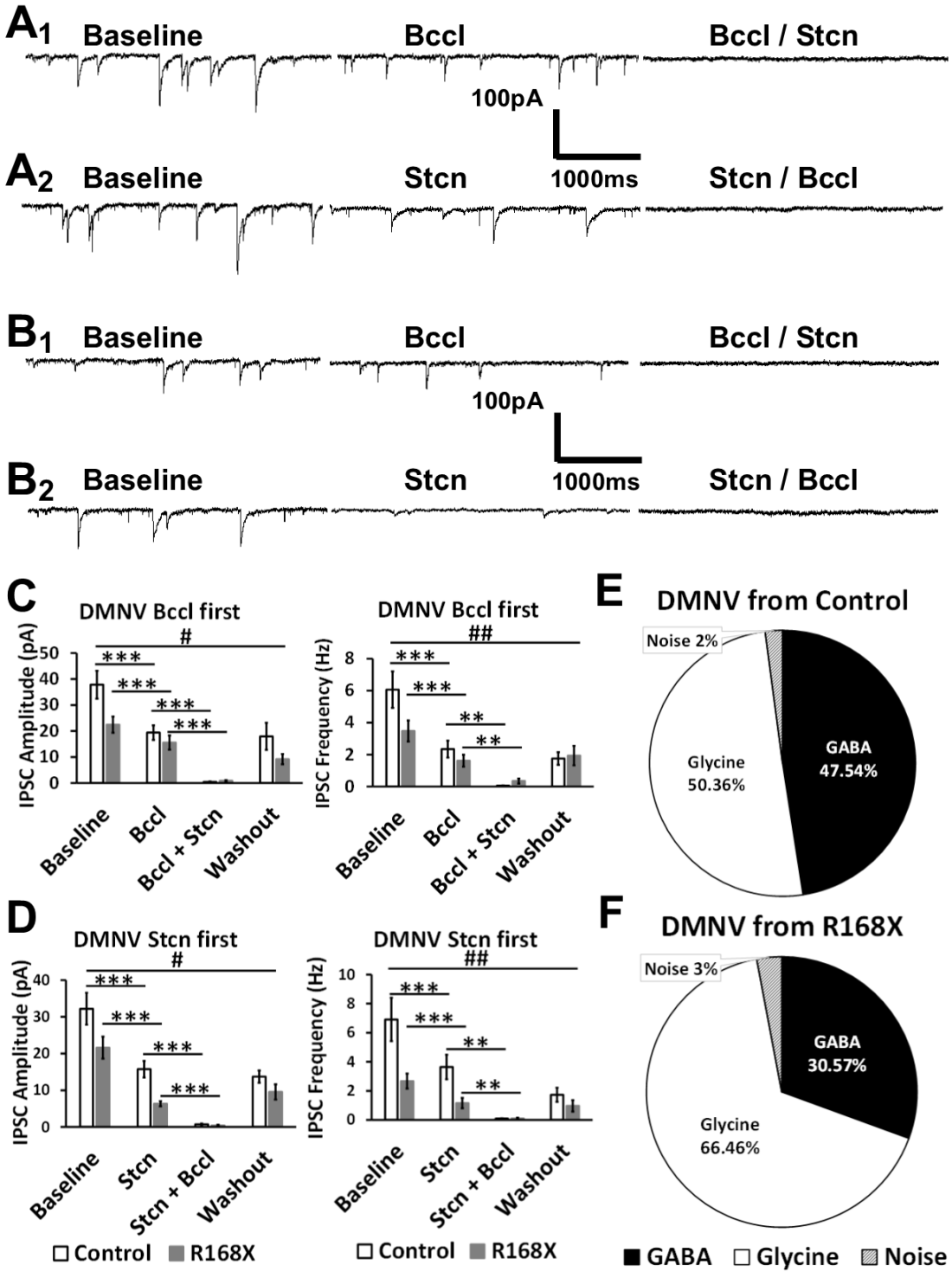
A1 Baseline
Bccl
Bccl / Stcn
100pA
A2 Baseline
Stcn
1000ms
Stcn / Bccl
B1 Baseline
Bccl
Bccl / Stcn
100pA
B2 Baseline
Stcn
1000ms
Stcn / Bccl
C
DMNV Bccl first
IPSC Amplitude (pA)
Baseline
Bccl
Bccl + Stcn
Washout
DMNV Bccl first
IPSC Frequency (Hz)
Baseline
Bccl
Bccl + Stcn
Washout
D
DMNV Stcn first
IPSC Amplitude (pA)
Baseline
Stcn
Stcn + Bccl
Washout
Control
R168X
DMNV Stcn first
IPSC Frequency (Hz)
Baseline
Stcn
Stcn + Bccl
Washout
Control
R168X
E
DMNV from Control
Noise 2%
GABA
47.54%
Glycine
50.36%
F
DMNV from R168X
Noise 3%
GABA
30.57%
Glycine
66.46%
GABA
Glycine
Noise

Figure 5.5 Bicuculline and strychnine sensitivities of miniature IPSCs (mIPSCs) of DMNV neurons recorded from mice with and without the R168X mutation in *Mecp2*.

A, B. The mIPSCs were studied in DMNV neurons under the same condition and the same blocker exposure sequence as shown for XII neurons in Figure 4, with similar results obtained. C. Treatment with Bccl first significantly decreased the mIPSC amplitude by 18.4±2.7pA (P=0.0003, n=9) and frequency by 3.7±0.7Hz (P=0.0009, n=9) in control group. It reduced the amplitude by 6.9±1.1pA (P=0.0003, n=8) and frequency by 1.5±0.6Hz (P=0.0008, n=8) in R168X group. With Bccl / Stcn, the mIPSC amplitude was decreased by 18.9±2.8pA (P=0.0006, n=9) and14.7±2.6pA (P=0.0006, n=8), and the frequency by 2.3±0.5Hz (P=0.001, n=9) and 1.9±0.4Hz (P=0.001, n=8) in the control and R168X groups, respectively. D. Stcn first significantly decreased the mIPSC amplitude by 16.5±2.4pA (P=0.0007, n=9) and 15.3±2.9pA (P=0.0006, n=8), and the frequency by 3.6±0.7Hz (P=0.0002, n=9) and 1.9±0.5Hz (P=0.0003, n=8) in the control and R168X groups, respectively. Joint Stcn / Bccl totally inhibited the mIPSC amplitude by 15.0±2.3pA (P=0.0005, n=9) and 5.9±0.7pA (P=0.0006, n=8), and the frequency by 4.0±0.8Hz (P=0.001, n=9) and 0.7±0.2Hz (P=0.001, n=8) in the control and R168X groups, respectively. (**, P<0.01; ***, P<0.001. Fisher's LSD post hoc). For the amplitude of IPSCs, the main effect of genotype ($F = 12.9$, $df = 1$, $P = 0.001$), treatment ($F = 63.6$, $df = 3$, $P = 0.0001$) and interactions of genotype × treatment ($F = 3.3$, $df = 3$, $P = 0.024$) were significant (#, $p < 0.05$; Two-way ANOVA). As the frequency of IPSCs, the main effect of genotype ($F = 12.1$, $df = 1$, $P = 0.001$), treatment ($F = 27.2$, $df = 3$, $P = 0.0009$) and interactions of genotype × treatment ($F = 4.8$, $df = 3$, $P = 0.004$) were significant (##, $p < 0.01$; Two-way ANOVA). E & F. Proportion of $GABA_A$– and glycine-induced IPSC shifted from 47.5±1.6% vs. 50.4±1.6% (control) to 30.6±2.9% vs. 66.5±2.9% (R168X).

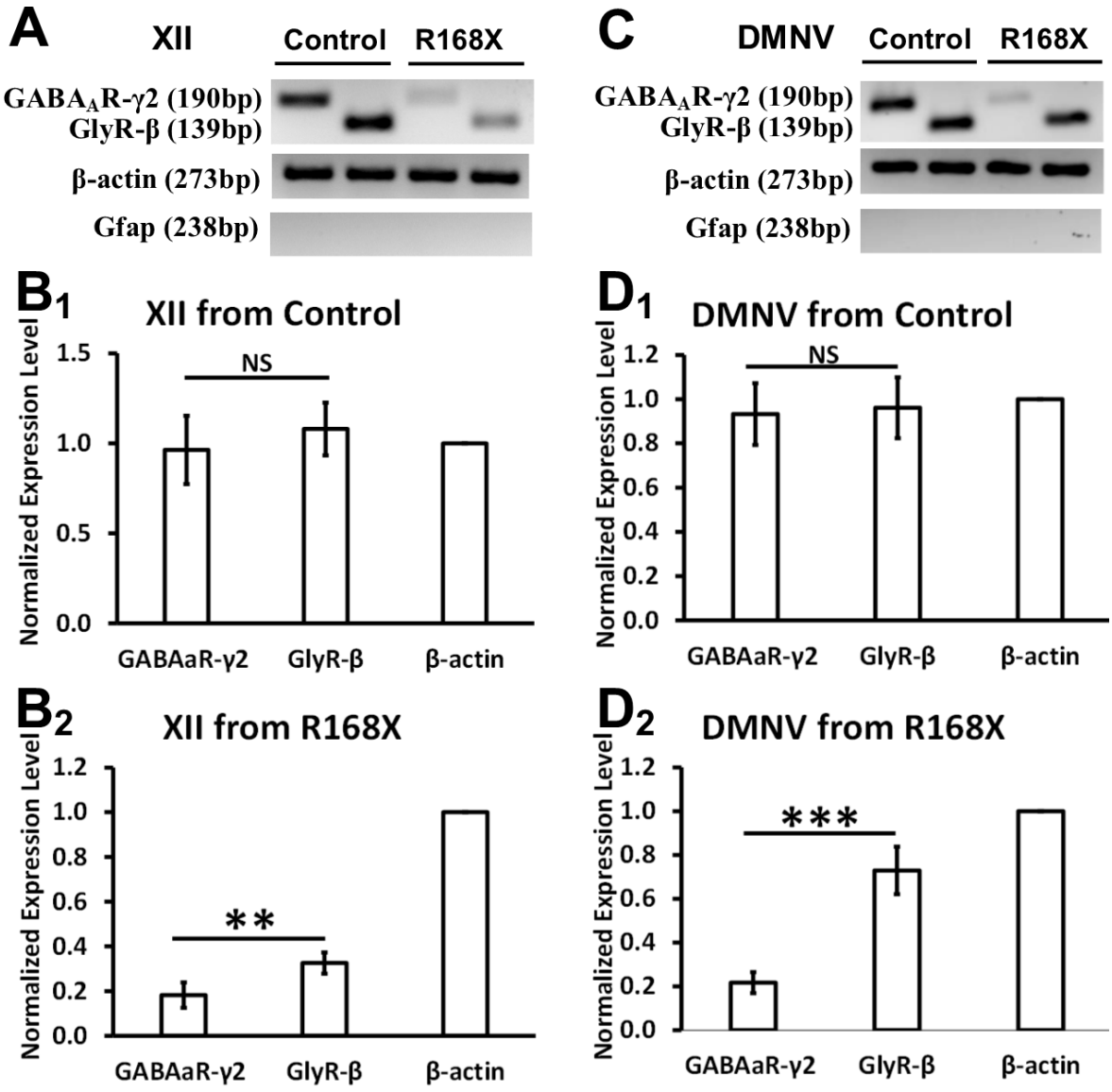

Figure 5.6 Single cell RT-PCR analysis of $GABA_A$ and glycine receptor transcripts in XII & DMNV neurons.

A. in XII neurons, the transcript levels of $GABA_A$ receptor γ_2 subunit ($GABA_AR$-γ2) / glycine receptor β subunit (GlyR-β) are clearly seen, which are also much stronger than those from XII neurons Mecp2 disruptions. In comparison of normalized transcript levels, these two receptor subunits had roughly equal photo-intensity in these two bands ($GABA_AR$-γ2: 0.96±0.19, n=8;

GlyR-β: 1.08±0.15, n=8; P=0.18) (B_1), while GlyR-β photo intensity was much stronger than GABAaR-γ2 in XII neurons with *Mecp2* disruptions ($GABA_AR$-γ2: 0.17±0.04, n=24; GlyR-β: 0.32±0.05, n=24; P=0.006) (B_2). C, D. Similar transcript expression patterns were seen in DMNV (Control: $GABA_AR$-γ2, 0.93±0.14, n=11; GlyR-β, 0.96±0.14, n=11; P=0.73. R168X: $GABA_AR$-γ2, 0.22±0.05, n=24; GlyR-β, 0.73±0.11, n=24; P=0.0003.) (**, P<0.01; ***, P<0.001; NS, not significant; Student's t-Test).

Table 5.1 RT-PCR primers

Target gene	Primer sequence	Accession No.
$GABA_AR$-γ2 FW	TGACAACAAACTTCGACCTGAC	NM 177408
$GABA_AR$-γ2 RV	ATTGCTATTCAACCGGAGAACTT	
GlyR-β FW	GACGCTTGTGCTAAAGAAAAGTC	NM 010298
GlyR-β RV	CCAGCAGCCTGTTCAAGATATTG	
β-actin FW	CACAGTGCTGTCTGGTGGTA	NC 000071.6
β-actin RV	AGGGTATAAAACGCAGCTCAG	
Gfap FW	CCCTGGCTCGTGTGGATTT	NM 001131020
Gfap RV	GACCGATACCACTCCTCTGTC	

Table 5.2 Opto IPSP amplitude (mV)

	Baseline	10 µM Bicuculline first	1 µM Strychnine first	Both antagonists added	Washout	N
XII	10.85 ± 1.73	5.45 ± 1.15		0.24 ± 0.06	7.66 ± 1.35	9
DMNV	11.17 ± 1.74	5.35 ± 0.91		0.44 ± 0.11	7.77 ± 1.37	9
XII	13.45 ± 2.15		5.82 ± 0.94	0.64 ± 0.12	6.47 ± 1.33	8
DMNV	12.83 ± 1.85		6.68 ± 1.07	0.63 ± 0.10	10.11 ± 1.65	11

Table 5.3 mIPSC amplitude (Amp., pA) and frequency (Freq., Hz) from control

		Baseline	10 µM Bicuculline first	1 µM Strychnine first	Both antagonists added	Washout	N
XII	Amp.	35.56 ± 2.78	16.75 ± 1.41		1.26 ± 0.42	16.57 ± 2.72	9
DMNV	Amp.	37.82 ± 5.36	19.39 ± 2.79		0.44 ± 0.16	17.94 ± 5.20	9
XII	Freq.	13.09 ± 1.79	5.37 ± 0.55		0.12 ± 0.07	2.88 ± 1.49	9
DMNV	Freq.	6.07 ± 1.14	2.35 ± 0.53		0.06 ± 0.02	1.76 ± 0.39	9
XII	Amp.	31.85 ± 3.12		15.88 ± 1.77	0.96 ± 0.28	11.90 ± 1.27	15
DMNV	Amp.	32.21 ± 4.34		15.75 ± 2.26	0.73 ± 0.18	13.72 ± 1.66	9
XII	Freq.	5.02 ± 0.98		2.72 ± 0.60	0.09 ± 0.27	1.86 ± 0.49	15
DMNV	Freq.	6.91 ± 1.49		3.64 ± 0.85	0.09 ± 0.02	1.73 ± 0.49	9

Table 5.4 mIPSC amplitude (Amp., pA) and frequency (Freq., Hz) from R168X

		Baseline	10 μM Bicuculline first	1 μM Strychnine first	Both antagonists added	Washout	N
XII	Amp.	12.63 ± 1.74	8.61 ± 0.89		0.18 ± 0.07	7.41 ± 0.51	9
DMNV	Amp.	22.45 ± 3.12	15.57 ± 2.74		0.85 ± 0.26	9.17 ± 1.96	8
XII	Freq.	4.10 ± 0.91	2.80 ± 0.73		0.09 ± 0.03	2.12 ± 0.85	9
DMNV	Freq.	3.48 ± 0.66	2.07 ± 0.34		0.35 ± 0.15	1.94 ± 0.61	8
XII	Amp.	10.15 ± 1.49		2.90 ± 0.36	0.28 ± 0.19	4.35 ± 1.61	6
DMNV	Amp.	21.61 ± 3.00		6.35 ± 0.70	0.41 ± 0.23	9.55 ± 2.09	8
XII	Freq.	1.11 ± 0.25		0.33 ± 0.10	0.02 ± 0.01	0.87 ± 0.44	6
DMNV	Freq.	2.67 ± 0.51		0.78 ± 0.19	0.10 ± 0.04	0.97 ± 0.39	8

6 RESULT 2: CENTRAL EXCITATORY NEURONAL CONTROL OF CRD

Published as "**Hao Xing**, Christopher M Johnson, Chun Jiang. Morphine-induced respiratory depression: behavioral, phrenic and brainstem respiratory neuronal evidence. PCT App. No. US/2020/033360. November 26, 2020."

A manuscript is submitted for publication

Authors: **Hao Xing**, Ningren Cui, Hongmin Yao, Christopher M. Johnson, Chun Jiang. Cloperastine reduces morphine-induced respiratory depression in rats: Potential mechanisms for GIRK channel inhibition in locus coeruleus neurons. *J Cell Physiol.* Submitted.

6.1 Acknowledgements

This work was supported by the NIH (1R01-NS073875).

6.2 Abstract

Respiratory depression is the main cause of death in opioid drug misusage. Currently the only available therapeutic is naloxone drugs that also block certain desired opioid effects. Here we show evidence for alleviating the respiratory depression with the antitussive CPS. Studies were performed in conscious rats *in vivo* and in brains slices *in vitro*. In plethysmography, CPS (30 mg/kg, *s.c.*) alleviated, but not eliminated, morphine-induced breathing depression. CPS oral treatment (30 mg/kg/day, 7-day) shifted LD_{50} of morphine (*i.p.*) from 106 mg/kg to 130 mg/kg. Morphine increased K^+ current in GIRK2/MOR double transfected HEK cells, which was reversed by 5μM CPS. Morphine hyperpolarized locus coeruleus neurons, raised their input resistance and decreased firing activity, all of which can be reversed by CPS. Removal of neuronal firing activity with 0.5 μM TTX reduced the cellular responses of both morphine & CPS. In the presence of 0.5 μM TTX, the morphine-induced hyperpolarization can be eliminated

by CPS, suggesting that both pre- and postsynaptic mechanisms are involved. The presynaptic cells are likely to be AMPA-targeted glutamatergic neurons as CNQX had a similar effect to TTX. The presynaptic mechanisms involved GIRK channels in synaptic terminals, as CPS increased mEPSCs amplitude & frequency in LC cells to the same degree as the metabotropic glutamate receptor blocker LY341495. CPS alleviates morphine-induced breathing depression and improves morphine LD_{50}. In LC neurons, CPS seems to counteract morphine via blocking GIRK channels 1) in LC cells, 2) in presynaptic glutamatergic neurons, and 3) in glutamatergic synaptic terminals. Because these GIRK channels are the major downstream target of MOR, it is possible that CPS interacts with morphine by blocking GIRK signaling.

6.3 Introduction

A major adverse effect of the chronic use of opioid drugs is progressive respiratory depression causing a loss of a large number of lives worldwide (Burke 2016, Jalal, Buchanich et al. 2018). The opioid-induced CRD involves the brainstem respiratory neuronal networks and CO_2 chemoreceptors. Targeting on them, several CRD therapeutics have been developed, including respiratory stimulants (Dahan, van der Schrier et al. 2018) and opioid receptor antagonists (Yousefifard, Vazirizadeh-Mahabadi et al. 2020) . Dahan et al. have recently analyzed most respiratory stimulants in OIRD treatments, including doxapram, GAL021, ampakines, 5-HT receptor agonists, D1-dopamine receptor agonists, phospodiesterase-4 inhibitors, the endogenous peptide glycyl-glutamine, and thyrotropin-releasing hormone. The authors conclude that none of these experimental drugs are adequate for therapeutic use in OIRD (Dahan, van der Schrier et al. 2018). Thus, naloxone types of μ-opioid receptor (MOR) antagonists are the only effective therapeutics (Imam, Kuo et al. 2018). However, the usage of

the MOR antagonists as preventive drugs does not seem practical, as they tend to antagonize therapeutic objectives including nociception relieves.

The GIRK channel, which is a downstream effector of MOR, is known to be involved in the mechanism of OIRD (Luscher and Slesinger 2010, Liang, Yong et al. 2018). Functional GIRK channels in the CNS mainly consist of 2 pairs of heteromeric GIRK1, GIRK2 and GIRK3, or homomeric GIRK2 (Kofuji, Davidson et al. 1995, Lesage, Guillemare et al. 1995, Liao, Jan et al. 1996, Luscher, Jan et al. 1997, Signorini, Liao et al. 1997, Jelacic, Kennedy et al. 2000, Torrecilla, Marker et al. 2002). These GIRK channels are activated by a number of neurotransmitters, such as GABA through GABAB receptors (Takigawa and Alzheimer 1999, Wetherington and Lambert 2002), metabotropic glutamate receptors (Saugstad, Segerson et al. 1996, Knoflach and Kemp 1998), serotonin through 5-HT_{1A} receptors, adenosine through A1 receptors, acetylcholine through M_2 receptors, opioids through μ, δ and κ receptors, and dopamine through D2 receptors (Mansour, Khachaturian et al. 1987, North, Williams et al. 1987, Einhorn and Oxford 1993, Jeong, Han et al. 2001, Wetherington and Lambert 2002, Ivanina, Varon et al. 2004). The activation of these K^+ channels leads to efflux of K^+, hyperpolarization of neurons and a reduction in their excitability, while activation of the GIRK channels in presynaptic terminals inhibits neurotransmitter release from the synaptic terminals.

GIRK channels are activated by several opioid receptor agonists (Mansour, Khachaturian et al. 1987, North, Williams et al. 1987). Treatment of the locus coeruleus neurons with [Met]5-enkephalin induces activation of whole-cell K^+ currents and hyperpolarization (Pepper and Henderson 1980), which are reduced by 40% in GIRK2 knockout mice and by 80% in *GIRK2/GIRK3* double knock-out mice (Torrecilla, Marker et al. 2002). MOR agonists inhibit neurons in the periaqueductal gray and the dorsal root ganglion through activation of GIRK

channels (Williams, Christie et al. 2001, Stotzner, Spahn et al. 2018). GIRK2 and GIRK3 are required for the morphine withdrawal effects, as genetic disruption of these channels in mice markedly attenuates the morphine withdrawal syndrome without affecting morphine analgesia (Cruz, Berton et al. 2008). Pre-treatment with the GIRK channel blocker Tertiapin-Q dose-dependently reverses the fentanyl-induced changes in respiratory rate and inspiratory time (Liang, Yong et al. 2018). MOR agonist suppresses rhythmic breathing in wild-type but not in *GIRK2*-knockout mice (Montandon, Ren et al. 2016). The depression in breathing activity after MOR agonist can be reversed by GIRK channel blocker (Montandon, Ren et al. 2016). The pontine group of respiratory neurons in the KF is hyperpolarized by MOR agonist accompanied by apneusis, effects that can be blocked by GIRK channel inhibitors (Levitt, Abdala et al. 2015).

Theoretically, GIRK channel inhibitors may have widespread effects by acting on multiple brain areas where GIRK channels are expressed. However, some GIRK channel inhibitors appear relatively selective for the brainstem respiratory neuronal networks. By taking such an advantage, some drugs have been developed as central antitussives, such as CPS. CPS is an over-the-counter antitussive approved in several Asian and European countries with excellent safety records (Catania and Cuzzocrea 2011, Soeda, Fujieda et al. 2016). The primary function of CPS in the brainstem is to block GIRK channels leading to inhibitions of the respiratory neuronal networks, although it has σ receptor agonistic and antihistaminic properties as well (Catania and Cuzzocrea 2011, Soeda, Fujieda et al. 2016). . To test the hypothesis that CPS alleviates morphine-induced respiratory depression, we performed these studies. Meanwhile we investigated cellular mechanisms involved in the CPS-morphine interactions.

6.4 Results

6.4.1 CPS alleviated morphine-induced respiratory depression

Breathing activity was measured in whole-body plethysmography. During a 20-min recording the baseline breathing amplitude (tidal volume) averaged 0.35±0.08 ml·100g^{-1} (N=37 rats), and the breathing frequency was 2.0±0.1 Hz (N=37 rats). The calculated minute ventilation (minV = Ti × f) was 41.66±2.53 ml·min^{-1}·100g^{-1} (N=37 rats).

Twenty minutes after CPS injection (30 mg/kg, *s.c.*), the tidal volume, breathing frequency and minute ventilation were 0.38±0.02 ml·100g^{-1}, 1.8±0.0 Hz and 40.92±2.48 ml·min^{-1}·100g^{-1} (N=5 rats), respectively. No significant difference was found statistically (Fig 6.1, Table 6.1).

Drastic changes in these respiratory parameters occurred after morphine injection (10 mg/kg, *i.p.*). Breathing became slow and irregular with frequent apneas. The effects reached the maximum level around 20min after morphine injection and remained at the level for another ~100min. At the plateau level, the tidal volume (0.23±0.08 ml·100g^{-1}, p=0.000134, N=12) breathing frequency (0.5±0.1Hz, p=0.000279, N=12) and minute ventilation (7.36±1.26 ml·min^{-1}·100g^{-1}, p=0.000615, N=12) were all significantly depressed in comparison to the baseline levels. By the time of 240 min after morphine injection, the tidal volume (0.31±0.02 ml·100g^{-1}, p=0.981, N=12), breathing frequency (1.9±0.1Hz, p=0.490, N=12) and minute ventilation (35.29±2.80 ml·min^{-1}·100g^{-1}, p=0.642, N=12) returned to prior morphine levels showing no significant differences from the baseline levels of breathing.

In the time range between 20~60 min after morphine injection, the effects of morphine were rapidly and partially reversed with a dose of CPS injection (Fig 6.1, Table 6.1). A pretreatment with CPS also diminished the effects of following morphine injection. Both were significantly different from the morphine effects (Fig 6.1, Table 6.1).

6.4.2 CPS improved rat survival after morphine overdose

If CPS treatment alleviates morphine-induced respiration depression, such a treatment should improve survival. To test the hypothesis, we studied the death rate at various doses of morphine in two groups of rats. One group was treated with CPS in the drinking water (30 mg/kg/day for 7 continuous days), and the other was given normal drinking water for 7 continuous days. On the 8th day, each rat received a single dose of morphine injection (*i.p.*). None of these rats had previous exposure to any other agents.

The survival rate was calculated as number of survival / total (survival + death), the survival histogram was drawn as morphine dose vs. survival rate for each group. We also tried to describe their relationship with Hill equation, the LD_{50} of morphine treatment for control group is 106 mg/kg (*i.p.*). For CPS group (30mg/kg/day, 7-days), LD50 of morphine located around 130 mg/kg (*i.p.*). The CPS oral administration significantly shifted the survival curve of morphine treatment rightward ($\chi 2$ (1, N=130) = 5.335, p = 0.0209, Mantel-Cox test. Fig 6.2, Table 6.2).

6.4.3 CPS counteracted GIRK channel activation after morphine exposure

The opioid-induced respiration depression is mainly mediated by the μ opioid receptor. Activation of these receptors leads to activation of the GIRK channels and hyperpolarization. In the CNS, these channels are made of heteromeric GIRK1-GIRK3 or homomeric GIRK2 (Corey, Krapivinsky et al. 1998). Thus, we co-transfected HEK cells with GIRK2 and μ opioid receptor. Whole-cell voltage clamp was performed in the HEK cells 2 days after transfection. The GIRK channels mediated K^+ currents were seen in the transfected HEK cells, which showed inward rectification and were strongly inhibited by Ba^{2+} (100 μM). The current amplitude increased markedly when the cell was exposed to morphine (10 μM) (Fig 6.3 A_1, A_2; Table 6.3). In the

plateau of the morphine activated currents, CPS (5μM) reversed the currents to nearly the baseline level (Fig 6.3 A_1, A_2; Table 6.3).

When applied before morphine, CPS suppressed the amplitude of baseline K^+ current from 215.2±24.1pA to 67.8±7.5pA. Under this condition, the same contraction of morphine (10 μM) produced only modest current activation from 67.8±7.5pA to 176.5±26.7pA (Fig 6.3 B_1, B_2; Table 6.3). Statistical analysis indicated that the morphine effects on GIRK2 current activation were significantly reduced by CPS applied either before or after morphine treatment.

6.4.4 CPS diminished morphine-induced inhibition of LC neurons

CPS is a central antitussive acting in the CNS, likely on the brainstem neuronal networks. Neurons in the LC are known to be a part of such neuronal networks, play an important role in breathing regulation, and form a major target of opioid drugs (Medrano, Santamarta et al. 2017). Hence, we chose the LC neurons for the study of potential CPS-morphine interaction.

Consistent with previous reports (Torrecilla, Quillinan et al. 2008), exposure of LC neurons to morphine (5 μM) in the brain slice preparation produced strong hyperpolarization of the cells together with an increase in the input resistance and a decrease in spontaneous firing (Fig 6.4 A_1, A_2, A_3, A_4; Table 6.4).

With the continuing presence of morphine, application of CPS (20 μM) to the perfusion solution led to fast reversal, though not complete, of the morphine effects (Fig 6.4 A_1, A_2, A_3, A_4; Table 6.4). A pretreatment of the LC neurons with CPS produced small but significant depolarization and increased firing rate, while cellular responses to following morphine treatment were significantly reduced (Fig 6.4 B_1, B_2, B_3, B_4; Table 6.4).

6.4.5 Pre-/post synaptic mechanisms in regulating LC excitability

To understand whether the CPS-morphine interaction occurs within the LC neurons or involves presynaptic cells. Experiments were performed in the presence of TTX (0.5 μM) to block synaptic transmissions. Under this condition, morphine hyperpolarized the LC cells to much smaller degree (Fig 6.5 A_1, A_2, A_3; Table 6.4). Similarly, the input resistance was decreased from 562.0±15.5ΩM to 465.7±15.7ΩM, significantly less than without TTX (Fig 6.5 A_1, A_2, A_3; Table 6.4). In the presence of TTX, CPS produced smaller depolarization of the LC neurons and raised their input resistance to a less degree, which were seen before and after morphine exposure (Fig 6.5 B_1, B_2, B_3; Table 6.4). These results suggest that although both CPS and morphine act on postsynaptic LC neurons, these cells are not the only target and presynaptic mechanisms are involved as well.

The observations above indicate that CPS has excitatory effects on the LC neurons, while the morphine effects are inhibitory. If presynaptic mechanisms are involved, they should be mediated by excitatory neurons rather inhibitory neurons. This is due to the fact that dis-inhibition requires firing of two inhibitory neurons and cannot take place in the presence of TTX. Therefore, we performed whole-cell current clamp with 20μM CNQX to block the AMPA receptor. Similar to the TTX experiments, the inhibitory effects of morphine and excitatory effects of CPS were both significantly diminished (Fig 6.6 A_1, A_2, A_3, A_4; Table 6.4). When compared to their levels after TTX treatment, there was no significant difference in LC neuronal response between TTX and CNQX treatments (Fig 6.6 A_1, A_2, A_3, A_4; Table 6.4), suggesting that presynaptic glutamatergic neurons are involved.

In addition to the GIRK channels in soma and dendrites, CPS may act on GIRK channels in the presynaptic terminals. Blockade of these GIRK channels may prevent the feedback

regulation of glutamate release mediated by the metabotropic glutamate receptors. Thus, we carried out voltage clamp measuring glutamatergic miniature EPSCs (mEPSCs) in the LC neurons. We found that CPS exposure raised the amplitude of the mEPSCs from 14.0±1.8pA to 18.6±2.1pA, and increased mEPSCs frequency from 2.6±0.1Hz to 4.0±0.4Hz (Fig 6.7 A_1, A_2, A_3; Table 6.5). The effects of CPS were likely to be mediated by the presynaptic metabotropic glutamate receptors, because LY341495, a selective blocker of these receptors, had similar effects, and because CPS had no additional effects on the mEPSCs after LY341495 treatment (Fig 6.7 B_1, B_2, B_3; Table 6.5).

6.5 Discussion

GIRK channels are one of the two downstream targets of MOR, which is involved in the regulation of brainstem respiratory neurons (Williams, Christie et al. 2001, Stotzner, Spahn et al. 2018). GIRK channels are a group of K^+ channels whose activation relies on the direct interaction with the $G_{\beta\gamma}$ subunit of G proteins. GIRK channels are expressed widely in most tissues and cells, where they participate in the regulation of various cellular activity. In the CNS, GIRK channels are activated by a number of neurotransmitters (Einhorn and Oxford 1993, Saugstad, Segerson et al. 1996, Knoflach and Kemp 1998, Takigawa and Alzheimer 1999, Jeong, Han et al. 2001, Wetherington and Lambert 2002, Ivanina, Varon et al. 2004). Opioids through μ, σ and κ receptors are also key mechanism to activate GIRK channels (Mansour, Khachaturian et al. 1987, North, Williams et al. 1987). The activation of these K^+ channels leads to hyperpolarization of postsynaptic cells reducing their excitability, while activation of the GIRK channels in presynaptic terminals inhibits neurotransmitter release from the synaptic terminals. Treatment of the locus coeruleus neurons with MOR agonist induces activation of whole-cell K^+ currents and hyperpolarization, which are reduced in *GIRK* knock-out mice

(Pepper and Henderson 1980, Torrecilla, Marker et al. 2002). MOR agonists inhibit neurons in the periaqueductal gray and the dorsal root ganglion through activation of GIRK channels.

Inhibition of the GIRK channels has excitatory effects on neuronal firing activity and breathing (Levitt, Abdala et al. 2015, Liang, Yong et al. 2018). The respiratory depression induced by DAMGO, a peptide MOR agonist, can be reversed by the GIRK channel blocker Tertiapin-Q (Montandon, Ren et al. 2016). Tertiapin-Q is a synthesized bee venom peptide, and a useful tool for laboratory research. It blocks multiple types of K^+ channels and needs to be applied by local injection in a brain area (Montandon, Ren et al. 2016). In contrast, CPS is an oral antitussive, and can pass through blood brain barrier. Thus, our finding in the current studies has apparently advanced the research for potential treatment and prevention of CRD.

CPS blocks GIRK channels, while morphine activates them, by producing depolarization and hyperpolarization, respectively. Although these apparently opposite effects can take place in a cell, it is necessary to demonstrate whether CPS and morphine share some common cellular processes, and where the potential interaction occurs.

If the CPS interacted with morphine in LC neurons by postsynaptic mechanism only, on the one hand, elimination of presynaptic input would not affect the levels of excitation and inhibition produced by CPS and morphine. If the interaction were solely presynaptic, on the other hand, both effects would be abolished after blockade of synaptic transmission. Testing the possibilities, we used TTX to block firing activity of all neurons. Under this condition, we have found that the effects of morphine and CPS on LC neurons cannot be maintained, neither eliminated. Instead, LC neurons show intermediate levels of inhibition and excitation by morphine and CPS, respectively. The remaining inhibitory effect of morphine can be totally blocked by CPS, a finding that supports the existence of postsynaptic interaction of CPS with morphine in LC cells.

In addition to the reduction of morphine and CPS effects in the presence of TTX, our results show that CPS does not completely eliminate the morphine-induced LC neuronal inhibition when presynaptic inputs remain intact, which also supports the presence of presynaptic interaction. CPS could produce excitatory effects by inhibition of GIRK channels in presynaptic glutamatergic neurons, or by excitation of a pre-presynaptic inhibitory neuron that inhibits another presynaptic inhibitory neuron. This is known as disinhibition. Our results do not support such a mechanism, as firing activity required for disinhibition cannot be brought about in the presence of TTX. Consistent with such a scenario, we have found that blockade of AMPA receptors with CNQX has an identical effect as TTX. Thus, it is likely that the presynaptic interaction of CPS with morphine occurs in glutamatergic neurons.

Besides these post- and presynaptic cellular mechanisms, CPS may also block GIRK in the presynaptic terminals. When applying a metabotropic glutamate receptor blocker LY341495, we have found that glutamatergic mEPSCs are augmented, indicating the presence of feedback regulation of glutamate release from the presynaptic terminals by the metabotropic glutamate receptors. A similar increase in the mEPSCs has been observed when we applied CPS. Therefore, these results suggest that CPS depolarizes LC neurons by blocking GIRK channels in 1) soma and/or dendrites of LC cells, 2) presynaptic glutamatergic neurons, and 3) presynaptic glutamatergic terminals.

It is worth noting that our currents studies are not providing evidence of cellular mechanisms of CPS-morphine interaction. Our *in vivo* studies have shown that CPS treatment significantly shifts the LD_{50} of morphine (*i.p.*) rightward. This as well as the fact that CPS is an over-the-counter antitussive in several Asian and European countries suggests that further studies in preclinical and clinical trials are highly possible.

Although our findings are encouraging, several questions remain open: It is known that CPS interacts with not only GIRK channels, but also σ receptors and histamine receptors, and these interactions may have additional effects either favorable or unfavorable in the regulation of brainstem neuron activity during CRD. In our previous studies CPS (30 mg/kg. *i.p.*) was used without any detectable adverse side effects in mice. We found that with a higher concentration of CPS (≥30 mg/kg) injected intraperitoneally caused suspicious seizure in 2 of 7 rats after high dose morphine treatment (≥10mg/kg, *i.p.*), while none of the other 5 rats with CPS (30 mg/kg. *i.p.*) showed similar symptom. Because of this, no data of these 7 rats were used in current study. Subsequently, we tried subcutaneous application of the same dose of CPS (30 mg/kg). No rats showed any abnormalities. Clearly, further pharmacokinetic studies of CPS are needed to determine the difference of different methods of application as well as species difference between rats and mice. GIRK channels are expressed in various tissues and cells. As an antitussive medicine, CPS affects the activity of GIRK channel, works on the brainstem cough center to suppress cough. But if brainstem the only or main target of CPS, and how other brain areas are affected by CPS is unknown. Furthermore, *in vivo* studies of phrenic nerve activity, and activity of neurons in pons & medullary respiratory groups are necessary with parallel comparison to neurons in forebrain areas.

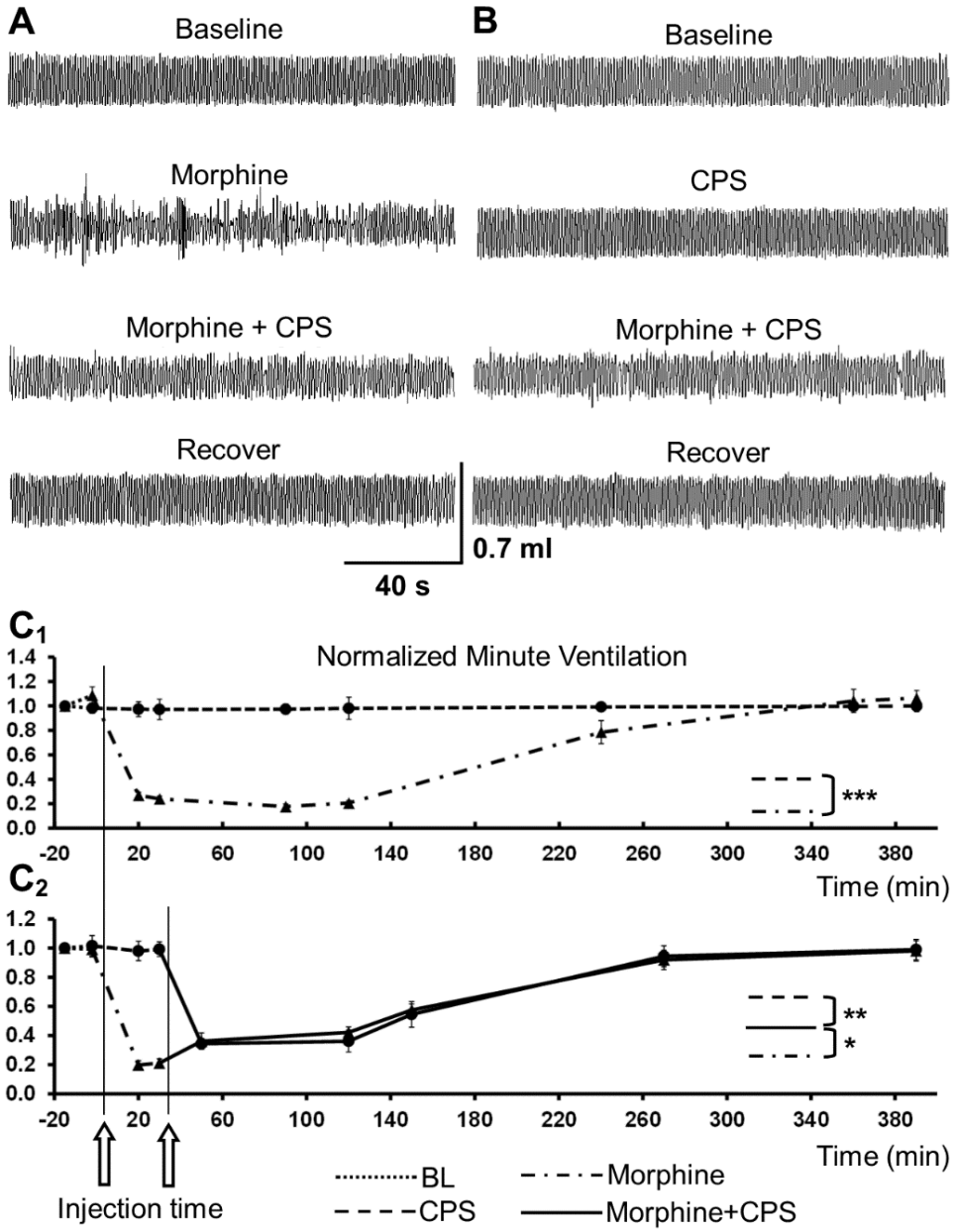

Figure 6.1 Effects of morphine / CPS on whole-body breathing activity.

A, Morphine injection before CPS. B, Cloperastine injection before morphine. C, Analyzed drugs effects. During a 20-min baseline recording the tidal volume was 0.35±0.08 ml·100g^{-1} (N=37), the breathing frequency was 2.0±0.1 Hz (N=37), and the minute ventilation was 41.66±2.53 ml·min^{-1}·100g^{-1} (N=37). When we only injected rat with CPS, the tidal volume was

0.38±0.02 ml·100g-1 (N=5), the breathing frequency was 1.8±0.0 Hz (N=5), and the minute ventilation was 40.92±2.48 $ml \cdot min^{-1} \cdot 100g^{-1}$ (N=5). All the tidal volume (p=0.610), breathing frequency (p=0.827) and minute ventilation (p=0.653) of CPS treatment shown no significant difference with baseline breathing. As we only injected rat with morphine, 20min till 120min after morphing injection, the tidal volume (0.23±0.08 $ml \cdot 100g^{-1}$, p=0.000134, N=12) breathing frequency (0.5±0.1 Hz, p=0.000279, N=12) and minute ventilation (7.36±1.26 $ml \cdot min^{-1} \cdot 100g^{-1}$, p=0.000615, N=12) were all significantly depressed than baseline. By the time of 240 min after morphine injection, the tidal volume (0.31±0.02 ml·100g-1, p=0.981, N=12), breathing frequency (1.9±0.1 Hz, p=0.490, N=12) and minute ventilation (35.29±2.80 $ml \cdot min^{-1} \cdot 100g^{-1}$, p=0.642, N=12) had no significant differences with baseline breathing. Based on the average data from 20~60 min time range, as we give CPS together with morphine, we found the tidal volume (0.28±0.03 $ml \cdot 100g^{-1}$, N=11) was better than morphine maximum effect (p=0.0158), but still depressed than CPS treatment (p=0.00952); the breathing frequency (1.2±0.0 Hz, N=11) was better than morphine treatment (p=0.0294) but still depressed than CPS treatment (p=0.00432); the minute ventilation (20.24±0.76 $ml \cdot min^{-1} \cdot 100g^{-1}$, N=11) was better than morphine treatment (p=0.0228) but depressed than CPS treatment (p=0.00259). There were statistically significant differences between group means as determined by one-way ANOVA: $F(3, 91) = 95.50$, $p = 0.000110$. (*, $p \leq 0.05$; **, $p \leq 0.01$; ***, $p \leq 0.001$; Bonferroni's post hoc test).

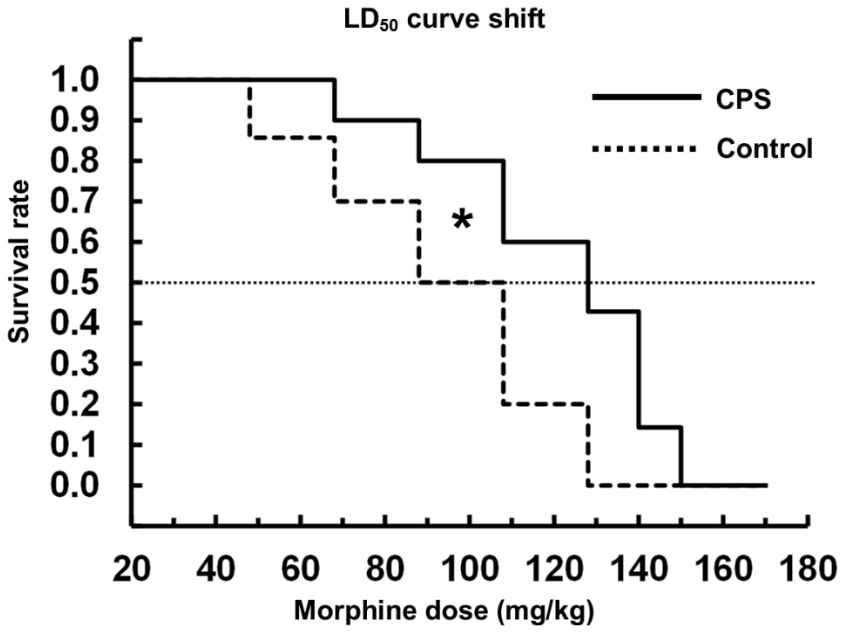

Figure 6.2 CPS shifted the survival curve of morphine rightward.

The survival percentage at difference morphine doses were: at morphine dose 48mg/kg, all rats from CPS and control groups were survived (N=7 rats per group); at morphine dose 68mg/kg, CPS survival rate was 100.0% (N=7), control group survival rate was 85.7% (6 survived, 1 died, N=7); at morphine dose 88mg/kg, CPS survival rate was 90.0% (9 survived, 1 died, N=10), and control group survival rate was 70.0% (7 survived, 3 died, N=10); at reported morphine LD_{50} dose 108mg/kg, CPS survival rate was 80.0% (8 survived and 2 died, N=10), control group survival rate was 50.0% (5 survived and 5 died, N=10); at the morphine dose 128mg/kg, CPS survival rate was 60.0% (6 survived and 4 died, N=10), and control group survival rate was 20.0% (2 survived and 8 died, N=10); at the morphine dose 140mg/kg, survival rate of CPS group was 42.9% (3 survived and 4 died, N=7), and control group survival rate was 0% (7 died, N=7); at the morphine dose 150mg/kg, CPS survival rate was 14.3% (1 survived and 6 died, N=7), survival rate of control group was 0% (7 died, N=7); at the morphine dose

170mg/kg, all tested rats from both groups were died (N=7 rats per group). The 30mg/kg/day, 7-days CPS oral administration significantly shifted the survival curve of *i.p.* morphine treatment rightward ($\chi 2$ (1, N=130) = 5.335, p = 0.0209, Mantel-Cox test).

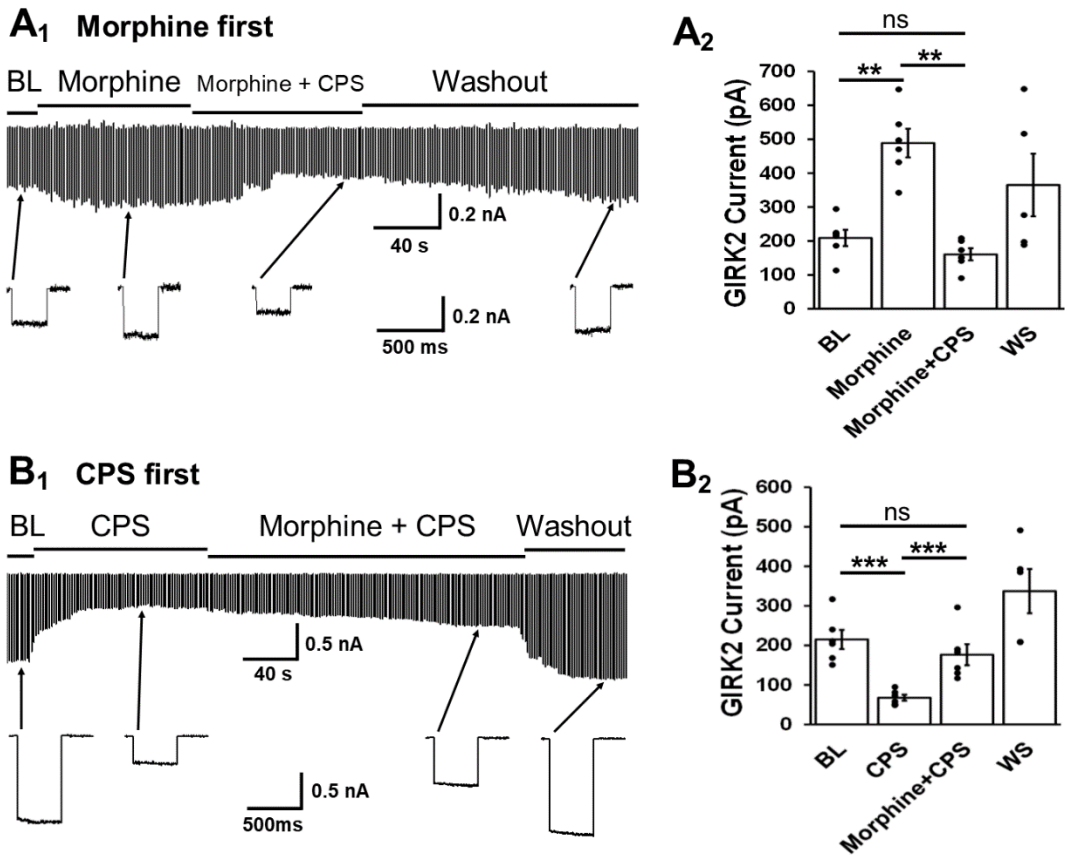

Figure 6.3 Effects of morphine/CPS on K^+ current in GIRK2/MOR transfected HEK Cells.

A, morphine treatment before CPS. B, CPS treatment before morphine. A_1, B_1, recording traces of K^+ current with drug treatment. A_2, B_2, analyzed amplitude of GIRK2 current. When we gave morphine before CPS, the morphine treatment increased K^+ current amplitude from 208.8±24.1pA to 488.7±42.1pA, with a changing level of 279.8±33.8pA (p=0.00144); then we gave morphine together with CPS, the amplitude of K^+ current reduced from 488.7±42.1pA to 160.5±17.7pA, with a changing level of 328.2±44.6pA (p=0.00517, N=6). When we applied CPS before morphine, CPS reduced the amplitude of K^+ current from 215.2±24.1pA to 67.8±7.5pA, with a changing level of 147.3±23.2pA (p=0.000418); then morphine & CPS were applied together, the amplitude of K^+ current increased from 67.8±7.5pA to 176.5±26.7pA, with a changing level of 108.7±22.9pA (p=0.000727, N=6). There were statistically significant

differences between group means as determined by one-way ANOVA: $F(3, 32) = 53.11$, $p = 0.0101$. (*, $p \leq 0.05$; **, $p \leq 0.01$; ***, $p \leq 0.001$; Bonferroni's post hoc test).

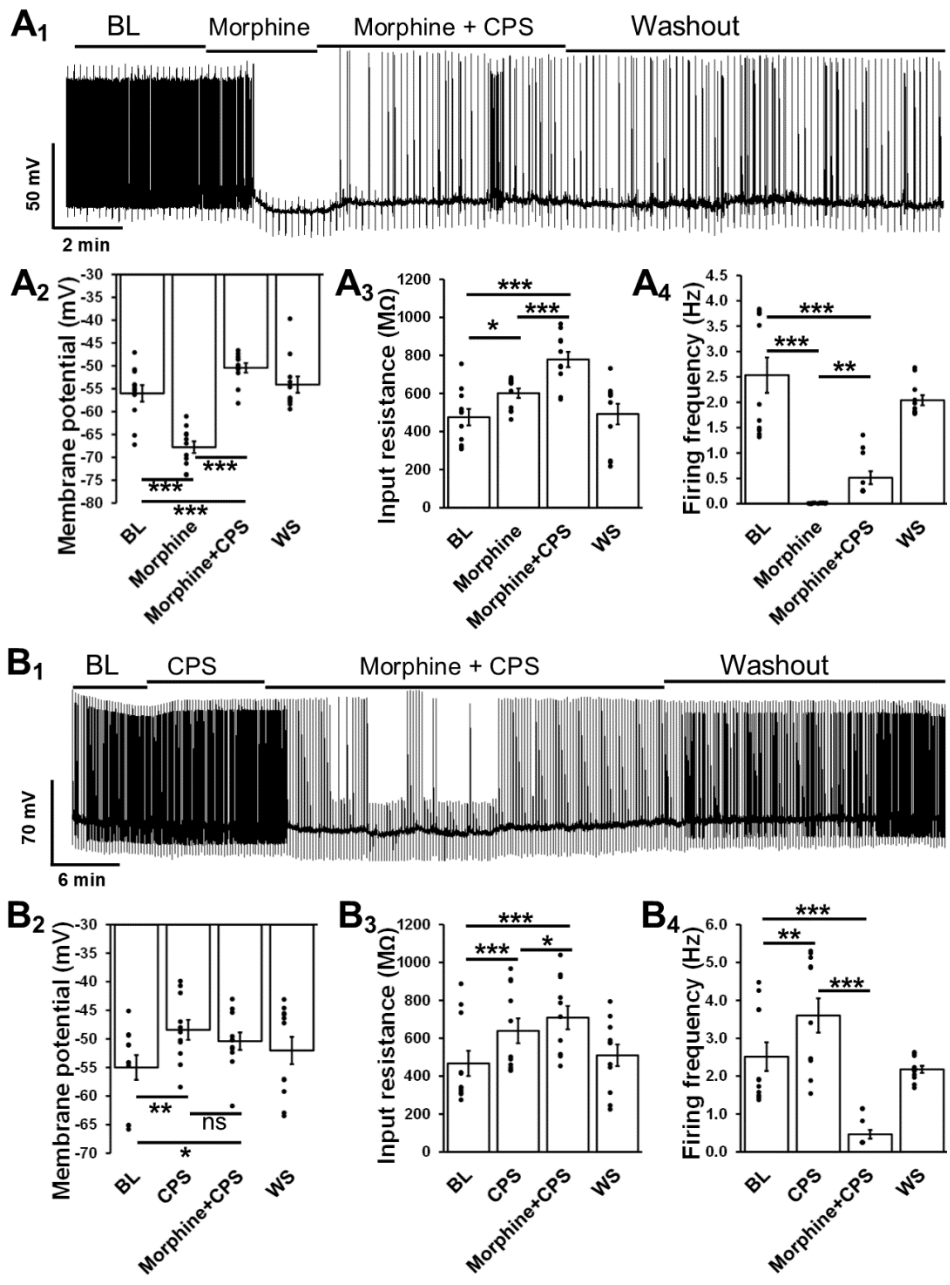

Figure 6.4 Morphine / CPS affected the firing activity of LC neuron.

A_1, B_1, whole-cell current clamp recording traces of drug treatment. A_2, A_3, A_4, B_2, B_3, B_4, analyzed membrane properties. Morphine hyperpolarized LC membrane from -56.0±1.8mV to -67.8±1.3mV, with a changing level of 11.8±1.4mV (p=0.000954); increased input resistance from 475.9±43.5ΩM to 601.7±25.0ΩM, with a changing level of 125.9±47.0ΩM (p=0.0232);

decreased firing frequency from 2.5±0.4Hz to 0 Hz, with a changing level of 2.5±0.4Hz (p=0.000276). Then we applied CPS with morphine, the membrane potential changed from -67.8±1.3mV to -50.4±1.1mV, with a changing level of 17.4±1.1mV (p=0.000203); input resistance changed from 601.7±25.0ΩM to 778.6±40.1ΩM, with a changing level of 176.8±32.3ΩM (p=0.000272); spontaneous firing frequency changed from 0Hz to 0.5±0.1Hz, with a changing level of 0.5±0.1Hz (p=0.00239, N=11). With CPS treatment before morphine: CPS depolarized LC neuron membrane potential from -55.0±2.2mV to -48.4±1.8mV, with a changing level of 6.6±1.6mV (p=0.00178); increased input resistance from 467.2±66.7ΩM to 639.3±65.7ΩM, with a changing level of 172.2±31.6ΩM (p=0.000284); firing frequency was increased from 2.5±0.4Hz to 3.6±0.5Hz, with a changing level of 1.1±0.2Hz (p=0.00131). As we applied morphine+CPS after then, membrane potential was hyperpolarized from -48.4±1.8mV to -50.4±1.5mV, with a changing level of 3.3±0.5mV (p=0.0669); input resistance increased from 639.3±65.7ΩM to 708.7±61.8ΩM, with a changing level of 69.4±28.3ΩM (p=0.0342); firing frequency decreased from 3.6±0.5Hz to 0.5±0.1Hz, with a changing level of 3.1±0.4Hz (p=0.000116, N=11). There were statistically significant differences between group means as determined by one-way ANOVA: $F(3, 51) = 7.192$, $p = 0.000413$. (*, $p \leq 0.05$; **, $p \leq 0.01$; ***, $p \leq 0.001$; Bonferroni's post hoc test).

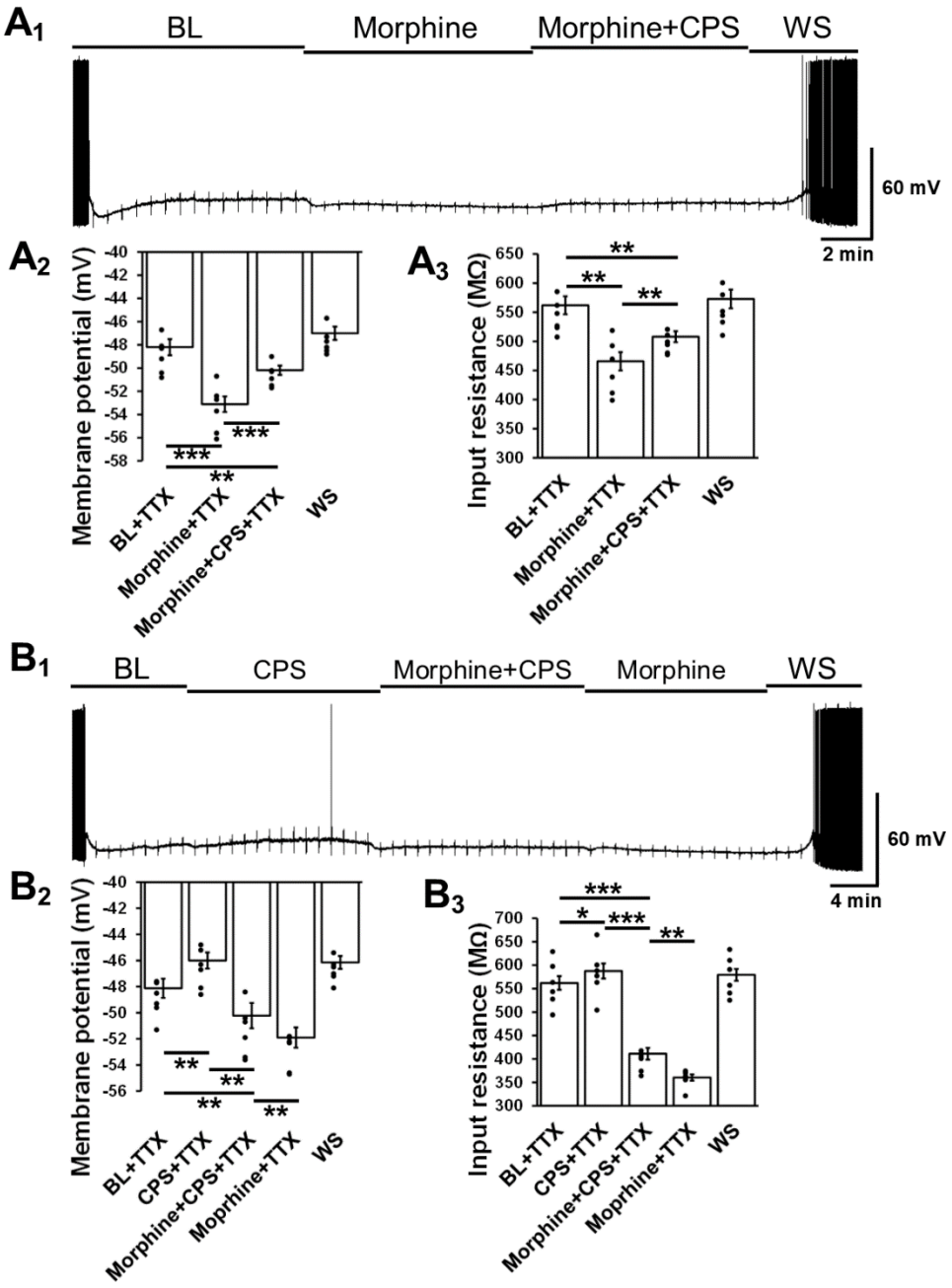

Figure 6.5 Effects of morphine / CPS on LC firing activities with TTX application.

A_1, B_1, whole-cell current clamp recording traces of drug treatment. A_2, A_3, B_2, B_3, analyzed membrane properties. We applied the perfusion system with 0.5 μM TTX to block the neuronal transmission. With morphine treatment before CPS: Morphine still hyperpolarized LC cell

membrane potential from -48.2±0.7mV to -53.1±0.7mV, with a changing level of 4.9±0.3mV (p=0.000101); input resistance decreased from 562.0±15.5ΩM to 465.7±15.7ΩM, with a changing level of 96.2±19.3ΩM (p=0.00158). Then we gave CPS together with morphine, the membrane potential depolarized from -53.1±0.7mV to -50.2±0.4mV, with a changing level of 2.9±0.4mV (p=0.000687); input resistance increased from 465.7±15.7ΩM to 507.9±9.3ΩM, with a changing level of 42.2±10.0ΩM (p=0.00389, N=8). When treated with CPS before morphine: CPS depolarized membrane potential from -48.1±0.7mV to -46.0±0.6mV, with a changing level of 2.1±0.3mV (p=0.00114); input resistance was increased from 562.0±14.7ΩM to 587.6±16.0ΩM, with a changing level of 25.6±5.9ΩM (p=0.0337). Then we gave CPS with morphine, the membrane potential changed from -46.0±0.6mV to -50.2±1.0mV, with a changing level of 4.2±0.6mV (p=0.00245); input resistance changed from 587.6±16.0ΩM to 411.2±12.6ΩM, with a changing level of 176.4±14.0ΩM (p=0.000466). After that, we gave only morphine after this morphine+CPS to test the maximum morphine effect, the membrane potential was further hyperpolarized from 50.2±1.0mV to -51.9±0.8mV, with a changing level of 1.7±0.4mV (p=0.00257); input resistance further decreased from 411.2±12.6ΩM to 360.4±6.6ΩM, with a changing level of 50.8±11.9ΩM (p=0.00366, N=8). There were statistically significant differences between group means as determined by one-way ANOVA: $F(3, 36) = 16.974$, $p= 0.000147$. (*, $p\leq0.05$; **, $p\leq0.01$; ***, $p\leq0.001$; Bonferroni's post hoc test). Since the TTX eliminated all action potential, we did not use firing frequency for data analysis.

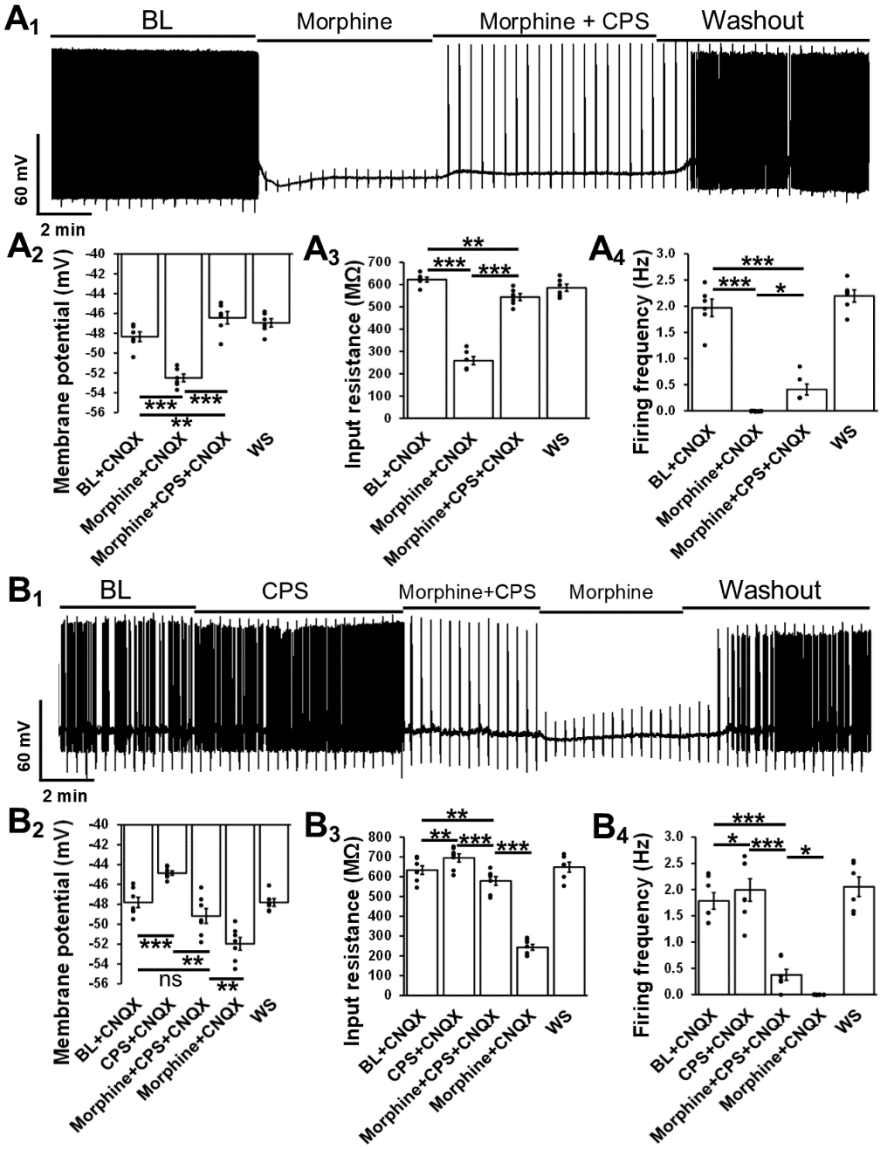

Figure 6.6 Effects of morphine / CPS on LC membrane properties with CNQX administration.

A_1, B_1, whole-cell current clamp recording traces of drug treatment. A_2, A_3, A_4, B_2, B_3, B_4, analyzed membrane properties. We gave 20μM CNQX in the perfusion solution to block the AMPA receptor. With morphine treatment before CPS: Morphine hyperpolarized membrane potential of LC cell from -48.4±0.5mV to -52.5±0.4mV, with a changing level of 4.2±0.4mV (p=0.000152); input resistance was reduced from 622.6±11.1ΩM to 258.6±18.1ΩM, with a changing level of 364.0±13.8ΩM (p=0.000144); and the firing frequency decreased from

2.0±0.2Hz to 0Hz, with a changing level of 2.0±0.2Hz (p=0.000766). Then we gave morphine+CPS after the morphine treatment, the membrane potential was depolarized from -52.0±0.4mV to -46.4±0.6mV, with a changing level of 6.1±0.7mV (p=0.000275); input resistance was increased from 258.6±18.1ΩM to 543.8±15.6ΩM, with a changing level of 285.2±25.8ΩM (p=0.000105); the firing frequency increased from 0Hz to 0.4±0.1Hz, with a changing level of 0.4±0.1Hz (p=0.0115, N=7). With the CPS treatment before morphine: The CPS depolarized membrane potential from -47.8±0.5mV to -44.9±0.2mV, with a changing level of 3.0±0.5mV (p=0.000668); input resistance increased from 633.1±21.9ΩM to 694.8±20.9ΩM, with a changing level of 61.6±9.2ΩM (p=0.00529); firing frequency increased from 1.8±0.2Hz to 2.0±0.2Hz, with a changing level of 0.3±0.0Hz (p=0.0387). Then we gave morphine+CPS after this CPS treatment, the membrane potential was hyperpolarized from -44.9±0.2mV to -49.2±0.8mV, with a changing level of 4.3±0.8mV (p=0.00155); input resistance decreased from 694.8±20.9ΩM to 578.7±21.7ΩM, with a changing level of 116.1±4.8ΩM (p=0.000329); firing frequency decreased from 2.0±0.2Hz to 0.4±0.1Hz, with a changing level of 1.6±0.2Hz (p=0.000396). We also gave only morphine treatment after this morphine+CPS treatment to test the maximum morphine effects, the membrane potential was further hyperpolarized from -49.2±0.8mV to -52.0±0.6mV, with a changing level of 2.8±0.4mV (p=0.00216); input resistance even decreased from 578.7±21.7ΩM to 243.2±14.8ΩM, with a changing level of 335.5±12.4ΩM (p=0.000168); firing frequency decreased from 0.4±0.1Hz to 0Hz, with a changing level of 0.4±0.1Hz (p=0.0116, N=7). There were statistically significant differences between group means as determined by one-way ANOVA: $F(3, 21) = 128.421$, $p = 0.000184$. (*, $p \leq 0.05$; **, $p \leq 0.01$; ***, $p \leq 0.001$; Bonferroni's post hoc test).

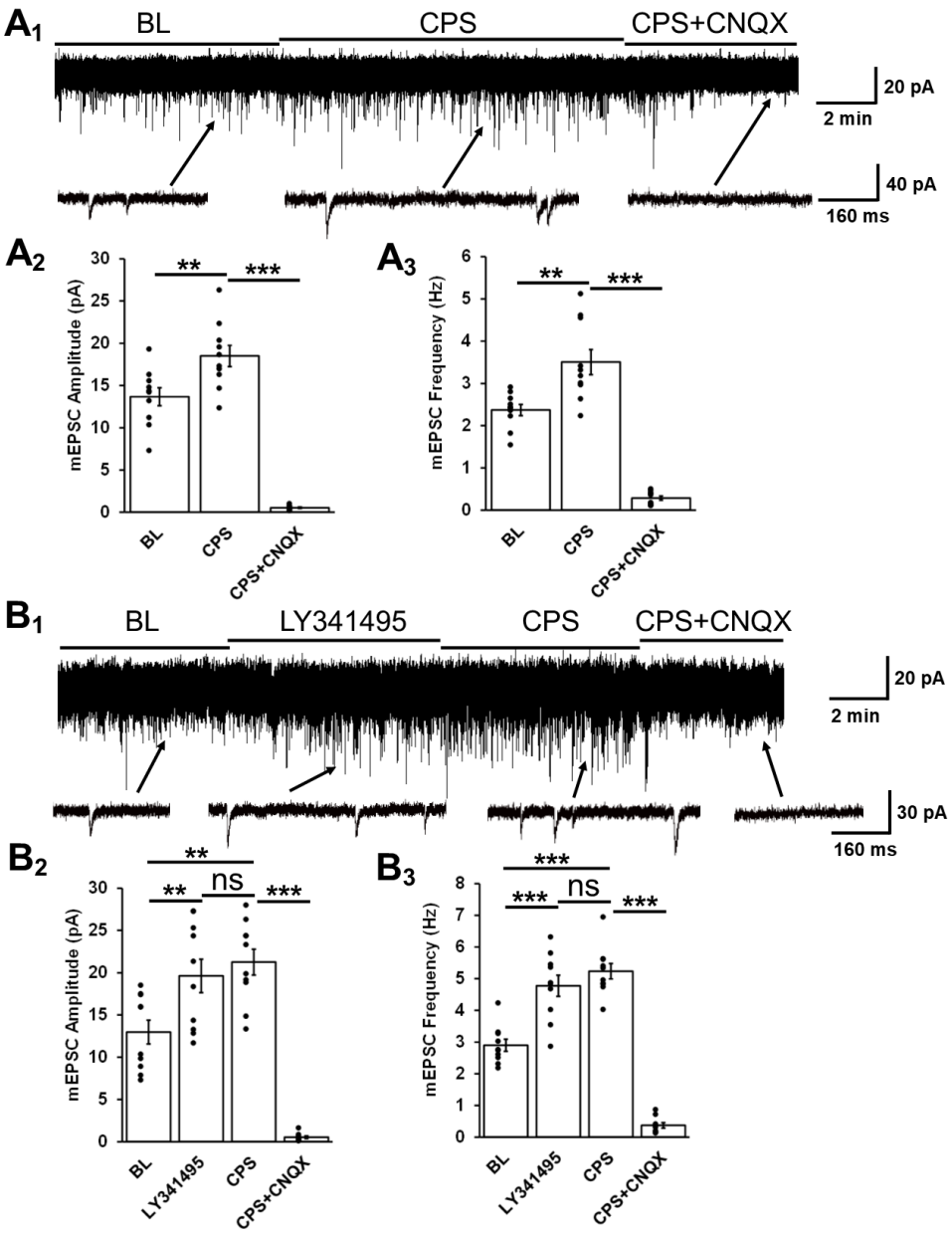

Figure 6.7 CPS affected mEPSCs on LC via regulating presynaptic GIRK channels.

A_1, B_1, whole-cell voltage clamp recording traces of drug treatment. A_2, A_3, B_2, B_3, analyzed mEPSCs amplitude and frequency. When we applied the recording slice with CPS, the mEPSCs amplitude was increased from 13.7±1.1pA to 18.5±1.3pA, with a changing level of 4.8±0.5pA (p=0.00625); mEPSCs frequency increased from 2.4±0.1Hz to 3.5±0.3Hz, with a changing level

of 1.1±0.2Hz (p=0.00290). Then we gave CPS+CNQX after the CPS treatment, we fine mEPSCs amplitude was reduced from 18.5±1.3pA to 0.5±0.1pA, with a changing level of 18.0±1.2pA (p=0.000143); and the mEPSCs frequency was reduced from 3.5±0.3Hz to 0.3±0.1Hz, with a changing level of 3.2±0.3Hz (p=0.000798, N=10) We also gave 20μM LY341495 before CPS treatment. LY341495 increased mEPSCs amplitude from 13.0±1.4pA to 19.6±2.0pA, with a changing level of 6.7±0.8pA (p=0.00203); the frequency increased from 2.9±0.2Hz to 4.8±0.3Hz, with a changing level of 1.9±0.2Hz (p=0.000807). As we gave CPS after this LY341495 treatment, the mEPSCs amplitude slightly increased from 19.6±2.0pA to 21.3±1.5pA, with a changing level of 2.9±1.1pA (p=0.249); and the mEPSCs frequency increased from 4.8±0.3Hz to 5.2±0.2Hz, with a changing level of 0.6±0.2Hz (p=0.0920). After the CPS treatment, we applied CNQX together with CPS, the mEPSCs amplitude was reduced from 21.3±1.5pA to 0.5±0.2pA, with a changing level of 21.4±1.5pA (p=0.000692); and the mEPSCs frequency reduced from 5.2±0.2Hz to 0.4±0.1Hz, with a changing level of 4.9±0.3Hz (p=0.000612, N=10). There were statistically significant differences between group means as determined by one-way ANOVA: $F(3, 35) = 52.903$, $p = 0.000196$. (*, $p \leq 0.05$; **, $p \leq 0.01$; ***, $p \leq 0.001$; Bonferroni's post hoc test).

Table 6.1 Plethysmography data after drug treatment

	BL	20min	40min	60min	N
Tidal V (ml·100g^{-1})					
CPS	0.39±0.02	0.38±0.02	0.38±0.02	0.38±0.02	5
Morphine	0.35±0.05	0.25±0.01	0.22±0.01	0.23±0.01	12
Morphine+CPS	0.37±0.02	0.28±0.01	0.28±0.01	0.29±0.01	11
Frequency (Hz)					
CPS	1.8±0.0	1.8±0.0	1.8±0.0	1.8±0.0	5
Morphine	2.0±0.1	0.6±0.0	0.5±0.0	0.5±0.0	12
Morphine+CPS	2.1±0.0	1.0±0.0	1.1±0.0	1.5±0.0	11
Minute V (ml·min^{-1}·100g^{-1})					
CPS	41.69±2.52	40.96±2.68	40.87±3.21	40.93±2.66	5
Morphine	42.09±2.40	8.67±0.54	6.05±0.36	7.35±0.40	12
Morphine+CPS	46.82±2.89	16.40±0.71	18.25±0.93	26.08±0.97	11

Table 6.2 Survival data after chemical treatment

	Morphine dose (mg/kg)	**48**	**68**	**88**	**108**	**128**	**140**	**150**	**170**
Group	**Outcome**								
CPS + morphine	Survived	7	7	9	8	6	3	1	0
	Dead	0	0	1	2	4	4	6	7
Saline + morphine	Survived	7	6	7	5	2	0	0	0
	Dead	0	1	3	5	8	7	7	7
Sum		7	7	10	10	10	7	7	7

Table 6.3 K^+ Current in transfected HEK cell

	BL	Morphine	CPS	Morphine+CPS	Δ BL/Morphine	Δ BL/CPS	Δ BL/Morphine +CPS	N
Amplitude (pA)								
Morphine 1st	208.8±24.1	488.7±42.1		160.5±17.7	+279.8±33.8		-48.3±19.6	6
CPS 1st	215.2±24.1		67.8±7.5	176.5±26.7		-147.3±23.2	-69.3±16.1	6

Table 6.4 Whole-cell current clamp membrane properties

	BL	Morphine	CPS	Morphine+CPS	Δ BL/Morphine	Δ BL/CPS	N
Membrane potential (mV)							
No blocker	-56.0±1.8	-67.8±1.3		-50.4±1.1	-11.8±1.4		11
TTX	-48.2±0.7	-53.1±0.7		-50.2±0.4	-4.9±0.3		8
CNQX	-48.4±0.5	-52.5±0.4		-46.4±0.6	-4.2±0.4		7
No blocker	-55.0±2.2		-48.4±1.8	-50.4±1.5		+6.6±1.6	11
TTX	-48.1±0.7	-51.9±0.8	-46.0±0.6	-50.2±1.0	-3.8±0.4	+2.1±0.8	8
CNQX	-47.8±0.5	-52.0±0.6	-44.9±0.2	-49.2±0.8	-4.2±0.6	+3.0±0.5	7
Input resistance (ΩM)							
No blocker	475.9±43.5	601.7±25.0		778.6±40.1	+174.5±27.4		11
TTX	562.0±15.5	465.7±15.7		507.9±9.3	-96.2±19.3		8
CNQX	622.6±11.1	258.6±18.1		543.8±15.6	-364.0±13.8		7
No blocker	467.2±66.7		639.3±65.7	708.7±61.8		+172.2±31.6	11
TTX	562.0±14.7	360.4±6.6	587.6±16.0	411.2±12.6	-201.6±13.4	+25.6±5.9	8
CNQX	633.1±21.9	243.2±14.8	694.8±20.9	578.7±21.7	-390.0±9.1	+61.6±9.2	7
Firing frequency (Hz)							
No blocker	2.5±0.4	0		0.5±0.1	-2.5±0.4		11
TTX	0	0		0	0		8
CNQX	2.0±0.2	0		0.4±0.1	-2.0±0.2		7
No blocker	2.5±0.4		3.6±0.5	0.5±0.1		+1.1±0.2	11
TTX	0	0	0	0	0	0	8
CNQX	1.8±0.2	0	2.0±0.2	0.4±0.1	-1.8±0.2	+0.3±0.0	7

Table 6.5 Whole-cell voltage clamp mEPSCs

	BL	LY341495	CPS	CPS+CNQX	Δ BL/LY341495	Δ BL/CPS	N
Amplitude (pA)							
CPS	13.7±1.1		18.5±1.3	0.5±0.1		+4.8±0.5	10
LY341495 / CPS	13.0±1.4	19.6±2.0	21.3±1.5	0.5±0.2	+6.7±0.8	+8.3±1.3	10
Frequency (Hz)							
CPS	2.4±0.1		3.5±0.3	0.3±0.1		+1.1±0.2	10
LY341495 / CPS	2.9±0.2	4.8±0.3	5.2±0.2	0.4±0.1	+1.9±0.2	+2.3±0.2	10

7 GENERAL DISCUSSIONS

We sought to discover certain common mechanisms of CRD from two animal models involving abnormalities in specific neurotransmission and neuronal excitability and tested the effectiveness of a novel treatment method to alleviate CRD. We have found that *Mecp2*^{R168X} male mice shows an overall decrease in inhibitory synaptic signaling in XII/DMNV neurons. We have also found that the reduction of $GABA_A$ergic inhibition is significantly greater than glycinergic signaling. Thus, the RTT mice rely more on glycine than GABA to maintain the inhibitory system. In rats, morphine-induced CRD is obvious when measuring breathing activity. In the rats, LC neurons are strongly inhibited due to both hyperpolarization of the cells and lack of sufficient presynaptic glutamatergic input. Remarkably, the morphine-induced CRD and alterations of LC neuronal excitability caused by morphine treatment are treatable by the over-the-counter cough medicine CPS. The CPS alleviates the morphine-induced CRD by blockade of GIRK channels in LC neurons and presynaptic glutamatergic cells. The CPS also increases glutamate release from presynaptic terminals by blocking presynaptic metabolic glutamate receptors. All these helps to ease neuronal hypo excitability during morphine exposure.

Our results indicate that the CRD found in the RTT model and the morphine treated rats share similar behavioral and cellular phenotypes. Behaviorally, we have shown that both CRD models have decreased breathing tidal volume, reduced minute ventilation, and increased breathing frequency variation. Both types of CRD involve abnormalities in neurotransmission and neuronal excitability. Despite these similarities, specific cellular mechanisms are playing a part in these two CRD models. In the RTT model, the inhibitory synaptic signals are defective in XII/DMNV neurons, while lack of the excitatory neurotransmission and postsynaptic inhibition are predominant in LC cells in morphine-induced CRD. Therefore, these results indicate that

respiration regulation depends on an elaborate balance of excitation vs inhibition of brainstem neurons, and the CRD can take place when either is disrupted.

Both inhibitory and excitatory neurotransmissions, together with the altered neuronal excitability, are known to be critical during CRD development. With respect to the inhibitory neurotransmission, it is known that defects in both GABA and glycine signaling are attributable to the CRD symptom in RTT mice (Mesuret, Dannenberg et al. 2018, Lozovaya, Nardou et al. 2019). In comparison of these two, we have found that the glycine system seems better reserved in brainstem neurons than the GABA system. The presence of higher levels of endogenous glycine neurotransmitter and glycine receptors in RTT brainstem neurons than those for GABA signaling is encouraging as the glycine system seems to be an ideal target for correction of synaptic inhibition when the GABA system is badly impaired. It is possible that targeting on the glycine signaling provides a promising addition to current therapeutic strategy focusing on the GABA system.

These dissertation studies have allowed us to identify several potential targets for pharmacological intervention. In the RTT model, deficiency of inhibitory neurotransmission is critical. At present, several potential counteractions are being attempted, mainly focusing on the GABA system (Abdala, Dutschmann et al. 2010, Voituron and Hilaire 2011, Zhong, Cui et al. 2015, Zhong, Johnson et al. 2016, Zhong, Johnson et al. 2017). In addition to the GABA system, our new finding in this dissertation indicates that the glycine mediated neurotransmission seems to be another promising target for CRD treatment in RTT. Our results have shown that glycine signaling is impaired to a much less degree in RTT mice than the GABA system. The existing glycine and glycine receptor may allow brainstem neurons to maintain decent synaptic inhibition in the RTT condition. This finding is particularly important as we have shown that the same

inhibitory neurons release both GABA and glycine with each excitation or firing. Such a co-localization of two inhibitory neurotransmitters tends to enable the host neurons to perform their inhibitory function when one of the neurotransmitter systems is defective, which is not a surprise because such a conservational arrangement in the brainstem neurons is vital for systemic survival. By taking the advantage of the conservational arrangement in brainstem neurons, glycine seems more likely to be manipulated in RTT under CRD condition for several reasons: 1) The glycine content is higher than GABA in the RTT model; 2) glycine is found sparsely in other brain areas; 3) there are selective agents acting on glycine uptake and receptor binding; 4) the GABA agonist-induced sedation may be avoided. It is possible that by focusing on enhancing glycinergic neurotransmission instead of GABA, more effective therapeutical modalities can be formulated to achieve better breathing improvement and avoid the side effects of the treatment such as sedation.

The abnormal excitatory glutamatergic system is known to play a role in opioid-induced CRD. In this current study, we have found that blockade of GIRK channels with CPS improves morphine-induced CRD and alleviates the depression of LC neuronal excitability with morphine treatment. Such GIRK channel inhibition not only results in an increase in LC neuronal excitability, but also raises excitatory synaptic input by depolarization of excitatory presynaptic neurons. Thus, CPS appears to counteract morphine-induced LC cell inhibition by both pre- and postsynaptic mechanisms.

A recent study from our lab suggests that CPS improves breathing dysfunction in *Mecp2*-null mice, where brainstem neurons tend to be overly excitable. The hyperexcitability of LC neurons can be improved with CPS. This is mediated by blocking GIRK channels in synaptic terminals leading to enhanced GABA release, an effect that overwhelms the excitatory effect of GIRK

channel inhibition on LC neurons (Johnson, Cui et al. 2020). Unlike glutamatergic neurons, the presynaptic GABAergic neurons in the dorsal tegmental nucleus (DTN) do not have functional GIRK channels (Johnson, Cui et al. 2020). As a result, the observed effect of CPS on LC neurons is inhibitory in the RTT model. Although the general effect of CPS is to depolarize individual neurons, its overall effect on a specific neuronal network depends on where in the soma, dendrites and/or synaptic terminals these cells express the GIRK channels, and whether or not the excitatory effect of CPS on a neuron is greater than the inhibitory synaptic input to the cell.

It is worth noting that CPS seems to facilitate excitation more than inhibition in morphine-induced CRD, and vice versa in the RTT model. How these apparently opposite effects take place is unclear. One possible mechanism would be that CPS has different affinity for various synaptic isoforms of GIRK channels on different types of neurons, which does not seem to be the case as our previous study has shown that CPS blocks $GABA_B$ receptors in presynaptic terminals, and facilitates GABA release (Johnson, Cui et al. 2020). Another possibility is that the proportion of active synaptic outputs from the excitatory and inhibitory neuronal networks becomes different after GIRK channel blockade. Supporting evidence for this scenario can be found in our previous studies showing that CPS causes inhibition of GABAergic neurons in the DTN instead of excitation, as these neurons do not show functional GIRK channel activity (Johnson, Cui et al. 2020). Furthermore, it is possible that the effect of GIRK channel inhibition depends on the state of membrane excitability, which is subject to each condition of RTT and morphine overdose. In the case of the hyperexcitability in a neuron from the RTT model, further excitatory input might have limited effect on the cell when its excitability has reached the ceiling or extreme level. Consequently, the inhibitory effect becomes predominant. Indeed, there is evidence supporting the ceiling excitability of norepinephrinergic neurons in RTT models

(Zhang, Johnson et al. 2016). In the case of morphine-induced CRD, on the other hand, brainstem neuronal inhibition is intensive and overwhelming. Under this condition, extra inhibitory input may not be as effective as the recruitment of additional excitatory input. Nevertheless, future studies are needed to reveal how CPS acts selectively on the excitatory and inhibitory systems in brainstem neurons.

Although our studies suggest a potential approach to alleviate morphine-induced CRD via the GIRK channel mechanism, we must keep all potential side effects into consideration. Taking several medications along with CPS could potentially be at risk of developing adverse side effects. There are reports indicating that patients show dystonia when taking CPS together with different medicines (Linazasoro, Garmendia et al. 2000). Another study shows that CPS inhibits hERG channels to prolong the QT interval (Snyders 1999). In our preliminary studies, intraperitoneal injections of CPS (30 mg/kg) and morphine (10mg/kg) caused suspicious seizure attack in 2 of 7 rats, suggesting that a mixture of CPS and morphine should be used with precautions. Future dose-dependent and pharmacokinetic studies of CPS are necessary. Our use of CPS to treat CRD is one of a few studies that have tested the drug effects on behaviors other than cough. Clearly, all that we have found about CPS in these studies are still at the early stage, and more studies are warranted before preclinical and clinical trials. Overall, these results indicate that CPS seems to be an alternative drug for the treatment and prevention of opioid-induced CRD, as respiratory stimulants that are now the only available agents for opioid overdose other than naloxone have been shown ineffective to treat opioid-induced CRD.

8 CONCLUSION

These dissertation studies were aimed at addressing mechanisms of CRD. Our results from the RTT study indicate both GABA and glycine signaling co-exist in equal quantity in the presynaptic cells of XII and DMNV neurons from control mice. These presynaptic neurons were previously known as GABAergic. In the mouse model of RTT, an overall reduction of inhibitory neurotransmission is found in XII and DMNV neurons, while such a defect is much less severe in the glycinergic system as indicated by optogenetics, pharmacological electrophysiology and glycinergic synaptic currents. Thus, these two medullary neurons rely more on glycine than GABA in their inhibitory synaptic transmission. It is possible that GABA and glycine act in a mutual compensational way to maintain the inhibitory synaptic transmissions in the brainstem neurons. When one of them is deficient, the other can compensate. This is an evolutional strategy ensuring system survival, which is necessary for the brainstem where several vital functions are housed. The morphine-induced CRD study reveals that morphine treatment leads to CRD that can be alleviated by CPS. Examining cellular mechanisms, we have found that CPS blocks GIRK channels in LC neurons and their presynaptic glutamatergic neurons. These pre- and postsynaptic effects allow CPS to dampen morphine-induced depression in LC neuronal excitability. These studies in the RTT model and morphine-overdose model indicate that CRD occurs with impair in either neurotransmission or neuronal excitability in brainstem neuronal networks. So does it with either hyper- or hypo excitability of the brainstem neurons that are involved in respiratory regulations. The understanding of the cellular and molecular basis of CRD has a profound impact on the therapeutical designs for CRD treatment.

REFERENCES

Abdala, A. P., M. Dutschmann, J. M. Bissonnette and J. F. Paton (2010). "Correction of respiratory disorders in a mouse model of Rett syndrome." Proc Natl Acad Sci U S A **107**(42): 18208-18213.

Abdala, A. P., M. A. Toward, M. Dutschmann, J. M. Bissonnette and J. F. Paton (2016). "Deficiency of GABAergic synaptic inhibition in the Kolliker-Fuse area underlies respiratory dysrhythmia in a mouse model of Rett syndrome." J Physiol **594**(1): 223-237.

Alheid, G. F., W. K. Milsom and D. R. McCrimmon (2004). "Pontine influences on breathing: an overview." Respir Physiol Neurobiol **143**(2-3): 105-114.

Amir, R. E., I. B. Van den Veyver, M. Wan, C. Q. Tran, U. Francke and H. Y. Zoghbi (1999). "Rett syndrome is caused by mutations in X-linked MECP2, encoding methyl-CpG-binding protein 2." Nat Genet **23**(2): 185-188.

Anderson, T. M., A. J. Garcia, 3rd, N. A. Baertsch, J. Pollak, J. C. Bloom, A. D. Wei, K. G. Rai and J. M. Ramirez (2016). "A novel excitatory network for the control of breathing." Nature **536**(7614): 76-80.

Anderson, T. M. and J. M. Ramirez (2017). "Respiratory rhythm generation: triple oscillator hypothesis." F1000Res **6**: 139.

Armstrong, D., J. K. Dunn, B. Antalffy and R. Trivedi (1995). "Selective dendritic alterations in the cortex of Rett syndrome." J Neuropathol Exp Neurol **54**(2): 195-201.

Bacci, A., J. R. Huguenard and D. A. Prince (2004). "Long-lasting self-inhibition of neocortical interneurons mediated by endocannabinoids." Nature **431**(7006): 312-316.

Baer, K., H. J. Waldvogel, R. L. Faull and M. I. Rees (2009). "Localization of glycine receptors in the human forebrain, brainstem, and cervical spinal cord: an immunohistochemical review." Front Mol Neurosci **2**: 25.

Balakrishnan, S. and S. L. Mironov (2018). "Regenerative glutamate release in the hippocampus of Rett syndrome model mice." PLoS One **13**(9): e0202802.

Banerjee, A., R. V. Rikhye, V. Breton-Provencher, X. Tang, C. Li, K. Li, C. A. Runyan, Z. Fu, R. Jaenisch and M. Sur (2016). "Jointly reduced inhibition and excitation underlies circuit-wide changes in cortical processing in Rett syndrome." Proc Natl Acad Sci U S A **113**(46): E7287-E7296.

Barbour, S. J., C. A. Vandebeek and J. M. Ansermino (2004). "Increased tidal volume variability in children is a better marker of opioid-induced respiratory depression than decreased respiratory rate." J Clin Monit Comput **18**(3): 171-178.

Barker-Haliski, M. and H. S. White (2015). "Glutamatergic Mechanisms Associated with Seizures and Epilepsy." Cold Spring Harb Perspect Med **5**(8): a022863.

Betz, H. and B. Laube (2006). "Glycine receptors: recent insights into their structural organization and functional diversity." J Neurochem **97**(6): 1600-1610.

Blue, M. E., S. Naidu and M. V. Johnston (1999). "Development of amino acid receptors in frontal cortex from girls with Rett syndrome." Ann Neurol **45**(4): 541-545.

Boland, J., E. Boland and D. Brooks (2013). "Importance of the correct diagnosis of opioid-induced respiratory depression in adult cancer patients and titration of naloxone." Clin Med (Lond) **13**(2): 149-151.

Bongianni, F., D. Mutolo, E. Cinelli and T. Pantaleo (2010). "Respiratory responses induced by blockades of GABA and glycine receptors within the Botzinger complex and the pre-Botzinger complex of the rabbit." Brain Res **1344**: 134-147.

Bongianni, F., D. Mutolo and T. Pantaleo (1997). "Depressant effects on inspiratory and expiratory activity produced by chemical activation of Botzinger complex neurons in the rabbit." Brain Res **749**(1): 1-9.

Boom, M., M. Niesters, E. Sarton, L. Aarts, T. W. Smith and A. Dahan (2012). "Non-analgesic effects of opioids: opioid-induced respiratory depression." Curr Pharm Des **18**(37): 5994-6004.

Brandes, I. F., G. M. Stettner, M. Morschel, L. Kubin and M. Dutschmann (2011). "REM sleep-like episodes of motoneuronal depression and respiratory rate increase are triggered by pontine carbachol microinjections in in situ perfused rat brainstem preparation." Exp Physiol **96**(5): 548-555.

Bubier, J. A., H. He, V. M. Philip, T. Roy, C. M. Hernandez, R. Bernat, K. D. Donohue, B. F. O'Hara and E. J. Chesler (2020). "Genetic variation regulates opioid-induced respiratory depression in mice." Sci Rep **10**(1): 14970.

Burke, D. S. (2016). "Forecasting the opioid epidemic." Science **354**(6312): 529.

Calfa, G., W. Li, J. M. Rutherford and L. Pozzo-Miller (2015). "Excitation/inhibition imbalance and impaired synaptic inhibition in hippocampal area CA3 of Mecp2 knockout mice." Hippocampus **25**(2): 159-168.

Carlton, S. M. and E. S. Hayes (1990). "Light microscopic and ultrastructural analysis of GABA-immunoreactive profiles in the monkey spinal cord." J Comp Neurol **300**(2): 162-182.

Catania, M. A. and S. Cuzzocrea (2011). "Pharmacological and clinical overview of cloperastine in treatment of cough." Ther Clin Risk Manag **7**: 83-92.

Chao, H. T., H. Chen, R. C. Samaco, M. Xue, M. Chahrour, J. Yoo, J. L. Neul, S. Gong, H. C. Lu, N. Heintz, M. Ekker, J. L. Rubenstein, J. L. Noebels, C. Rosenmund and H. Y. Zoghbi (2010). "Dysfunction in GABA signalling mediates autism-like stereotypies and Rett syndrome phenotypes." Nature **468**(7321): 263-269.

Chen, C. Y., J. Di Lucente, Y. C. Lin, C. C. Lien, M. A. Rogawski, I. Maezawa and L. W. Jin (2018). "Defective GABAergic neurotransmission in the nucleus tractus solitarius in Mecp2-null mice, a model of Rett syndrome." Neurobiol Dis **109**(Pt A): 25-32.

Christenson, J., O. Shupliakov, S. Cullheim and S. Grillner (1993). "Possible morphological substrates for GABA-mediated presynaptic inhibition in the lamprey spinal cord." J Comp Neurol **328**(4): 463-472.

Corey, S., G. Krapivinsky, L. Krapivinsky and D. E. Clapham (1998). "Number and stoichiometry of subunits in the native atrial G-protein-gated K+ channel, IKACh." J Biol Chem **273**(9): 5271-5278.

Crook, J., A. Hendrickson and F. R. Robinson (2006). "Co-localization of glycine and gaba immunoreactivity in interneurons in Macaca monkey cerebellar cortex." Neuroscience **141**(4): 1951-1959.

Cruz, H. G., F. Berton, M. Sollini, C. Blanchet, M. Pravetoni, K. Wickman and C. Luscher (2008). "Absence and rescue of morphine withdrawal in GIRK/Kir3 knock-out mice." J Neurosci **28**(15): 4069-4077.

Cummings, C. J., E. J. Dahle and H. Y. Zoghbi (1998). "Analysis of the genomic structure of the human glycine receptor alpha2 subunit gene and exclusion of this gene as a candidate for Rett syndrome." Am J Med Genet **78**(2): 176-178.

Dahan, A., R. van der Schrier, T. Smith, L. Aarts, M. van Velzen and M. Niesters (2018). "Averting Opioid-induced Respiratory Depression without Affecting Analgesia." Anesthesiology **128**(5): 1027-1037.

Dani, V. S., Q. Chang, A. Maffei, G. G. Turrigiano, R. Jaenisch and S. B. Nelson (2005). "Reduced cortical activity due to a shift in the balance between excitation and inhibition in a mouse model of Rett syndrome." Proc Natl Acad Sci U S A **102**(35): 12560-12565.

De Filippis, B., P. Nativio, A. Fabbri, L. Ricceri, W. Adriani, E. Lacivita, M. Leopoldo, F. Passarelli, A. Fuso and G. Laviola (2014). "Pharmacological stimulation of the brain serotonin receptor 7 as a novel therapeutic approach for Rett syndrome." Neuropsychopharmacology **39**(11): 2506-2518.

Del Negro, C. A., N. Koshiya, R. J. Butera, Jr. and J. C. Smith (2002). "Persistent sodium current, membrane properties and bursting behavior of pre-botzinger complex inspiratory neurons in vitro." J Neurophysiol **88**(5): 2242-2250.

Del Negro, C. A., C. Morgado-Valle and J. L. Feldman (2002). "Respiratory rhythm: an emergent network property?" Neuron **34**(5): 821-830.

Del Negro, C. A., C. Morgado-Valle, J. A. Hayes, D. D. Mackay, R. W. Pace, E. A. Crowder and J. L. Feldman (2005). "Sodium and calcium current-mediated pacemaker neurons and respiratory rhythm generation." J Neurosci **25**(2): 446-453.

Devenyi, P., A. Mitwalli and W. Graham (1982). "Clonidine therapy for narcotic withdrawal." Can Med Assoc J **127**(10): 1009-1011.

Dutschmann, M. and T. E. Dick (2012). "Pontine mechanisms of respiratory control." Compr Physiol **2**(4): 2443-2469.

Einhorn, L. C. and G. S. Oxford (1993). "Guanine nucleotide binding proteins mediate D2 dopamine receptor activation of a potassium channel in rat lactotrophs." J Physiol **462**: 563-578.

El-Khoury, R., N. Panayotis, V. Matagne, A. Ghata, L. Villard and J. C. Roux (2014). "GABA and glutamate pathways are spatially and developmentally affected in the brain of Mecp2-deficient mice." PLoS One **9**(3): e92169.

Enikanolaiye, A., J. Ruston, R. Zeng, C. Taylor, M. Schrock, C. M. Buchovecky, J. Shendure, E. Acar and M. J. Justice (2020). "Suppressor mutations in Mecp2-null mice implicate the DNA damage response in Rett syndrome pathology." Genome Res **30**(4): 540-552.

Enman, N. M., B. A. S. Reyes, Y. Shi, R. J. Valentino and E. J. Van Bockstaele (2019). "Sex differences in morphine-induced trafficking of mu-opioid and corticotropin-releasing factor receptors in locus coeruleus neurons." Brain Res **1706**: 75-85.

Ezure, K., I. Tanaka and M. Kondo (2003). "Glycine is used as a transmitter by decrementing expiratory neurons of the ventrolateral medulla in the rat." J Neurosci **23**(26): 8941-8948.

Fatemi, S. H., A. R. Halt, J. M. Stary, R. Kanodia, S. C. Schulz and G. R. Realmuto (2002). "Glutamic acid decarboxylase 65 and 67 kDa proteins are reduced in autistic parietal and cerebellar cortices." Biol Psychiatry **52**(8): 805-810.

Feldman, J. L., C. A. Del Negro and P. A. Gray (2013). "Understanding the rhythm of breathing: so near, yet so far." Annu Rev Physiol **75**: 423-452.

Fogarty, M. J., K. L. Smallcombe, Y. Yanagawa, K. Obata, M. C. Bellingham and P. G. Noakes (2013). "Genetic deficiency of GABA differentially regulates respiratory and non-respiratory motor neuron development." PLoS One **8**(2): e56257.

Gantz, S. C., C. P. Ford, K. A. Neve and J. T. Williams (2011). "Loss of Mecp2 in substantia nigra dopamine neurons compromises the nigrostriatal pathway." J Neurosci **31**(35): 12629-12637.

Gautier, H. and F. Bertrand (1975). "Respiratory effects of pneumotaxic center lesions and subsequent vagotomy in chronic cats." Respir Physiol **23**(1): 71-85.

Gerrits, P. O. and G. Holstege (1996). "Pontine and medullary projections to the nucleus retroambiguus: a wheat germ agglutinin-horseradish peroxidase and autoradiographic tracing study in the cat." J Comp Neurol **373**(2): 173-185.

Glaze, D. G., J. D. Frost, Jr., H. Y. Zoghbi and A. K. Percy (1987). "Rett's syndrome. Correlation of electroencephalographic characteristics with clinical staging." Arch Neurol **44**(10): 1053-1056.

Gold, W. A., R. Krishnarajy, C. Ellaway and J. Christodoulou (2018). "Rett Syndrome: A Genetic Update and Clinical Review Focusing on Comorbidities." ACS Chem Neurosci **9**(2): 167-176.

Gomes, T., D. N. Juurlink, T. Antoniou, M. M. Mamdani, J. M. Paterson and W. van den Brink (2017). "Gabapentin, opioids, and the risk of opioid-related death: A population-based nested case-control study." PLoS Med **14**(10): e1002396.

Grudzinska, J., R. Schemm, S. Haeger, A. Nicke, G. Schmalzing, H. Betz and B. Laube (2005). "The beta subunit determines the ligand binding properties of synaptic glycine receptors." Neuron **45**(5): 727-739.

Guy, J., J. Gan, J. Selfridge, S. Cobb and A. Bird (2007). "Reversal of neurological defects in a mouse model of Rett syndrome." Science **315**(5815): 1143-1147.

Hajiha, M., M. A. DuBord, H. Liu and R. L. Horner (2009). "Opioid receptor mechanisms at the hypoglossal motor pool and effects on tongue muscle activity in vivo." J Physiol **587**(Pt 11): 2677-2692.

Haverkamp, S., U. Muller, H. U. Zeilhofer, R. J. Harvey and H. Wassle (2004). "Diversity of glycine receptors in the mouse retina: localization of the alpha2 subunit." J Comp Neurol **477**(4): 399-411.

He, C., F. Chen, B. Li and Z. Hu (2014). "Neurophysiology of HCN channels: from cellular functions to multiple regulations." Prog Neurobiol **112**: 1-23.

Hill, R., R. Santhakumar, W. Dewey, E. Kelly and G. Henderson (2020). "Fentanyl depression of respiration: Comparison with heroin and morphine." Br J Pharmacol **177**(2): 254-266.

Hong, S., T. J. Morrow, P. E. Paulson, L. L. Isom and J. W. Wiley (2004). "Early painful diabetic neuropathy is associated with differential changes in tetrodotoxin-sensitive and -resistant sodium channels in dorsal root ganglion neurons in the rat." J Biol Chem **279**(28): 29341-29350.

Hu, H. J., Y. Carrasquillo, F. Karim, W. E. Jung, J. M. Nerbonne, T. L. Schwarz and R. W. t. Gereau (2006). "The kv4.2 potassium channel subunit is required for pain plasticity." Neuron **50**(1): 89-100.

Hulsmann, S., G. Mesuret, J. Dannenberg, M. Arnoldt and M. Niebert (2016). "GlyT2-Dependent Preservation of MECP2-Expression in Inhibitory Neurons Improves Early Respiratory Symptoms but Does Not Rescue Survival in a Mouse Model of Rett Syndrome." Front Physiol **7**: 385.

Hwang, C. K., K. Y. Song, C. S. Kim, H. S. Choi, X. H. Guo, P. Y. Law, L. N. Wei and H. H. Loh (2009). "Epigenetic programming of mu-opioid receptor gene in mouse brain is regulated by MeCP2 and Brg1 chromatin remodelling factor." J Cell Mol Med **13**(9B): 3591-3615.

Imam, M. Z., A. Kuo, S. Ghassabian and M. T. Smith (2018). "Progress in understanding mechanisms of opioid-induced gastrointestinal adverse effects and respiratory depression." Neuropharmacology **131**: 238-255.

Imam, M. Z., A. Kuo and M. T. Smith (2020). "Countering opioid-induced respiratory depression by non-opioids that are respiratory stimulants." F1000Res **9**.

Imani, F. (2011). "Postoperative pain management." Anesth Pain Med **1**(1): 6-7.

Inquimbert, P., J. L. Rodeau and R. Schlichter (2007). "Differential contribution of GABAergic and glycinergic components to inhibitory synaptic transmission in lamina II and laminae III-IV of the young rat spinal cord." Eur J Neurosci **26**(10): 2940-2949.

Ito-Ishida, A., K. Ure, H. Chen, J. W. Swann and H. Y. Zoghbi (2015). "Loss of MeCP2 in Parvalbumin-and Somatostatin-Expressing Neurons in Mice Leads to Distinct Rett Syndrome-like Phenotypes." Neuron **88**(4): 651-658.

Ito, S. (2016). "GABA and glycine in the developing brain." J Physiol Sci **66**(5): 375-379.

Ivanina, T., D. Varon, S. Peleg, I. Rishal, Y. Porozov, C. W. Dessauer, T. Keren-Raifman and N. Dascal (2004). "Galphai1 and Galphai3 differentially interact with, and regulate, the G protein-activated K+ channel." J Biol Chem **279**(17): 17260-17268.

Jalal, H., J. M. Buchanich, M. S. Roberts, L. C. Balmert, K. Zhang and D. S. Burke (2018). "Changing dynamics of the drug overdose epidemic in the United States from 1979 through 2016." Science **361**(6408).

Janczewski, W. A., A. Tashima, P. Hsu, Y. Cui and J. L. Feldman (2013). "Role of inhibition in respiratory pattern generation." J Neurosci **33**(13): 5454-5465.

Jelacic, T. M., M. E. Kennedy, K. Wickman and D. E. Clapham (2000). "Functional and biochemical evidence for G-protein-gated inwardly rectifying K+ (GIRK) channels composed of GIRK2 and GIRK3." J Biol Chem **275**(46): 36211-36216.

Jeong, H. J., S. H. Han, B. I. Min and Y. W. Cho (2001). "5-HT1A receptor-mediated activation of G-protein-gated inwardly rectifying K+ current in rat periaqueductal gray neurons." Neuropharmacology **41**(2): 175-185.

Jiang, C. and J. Lipski (1990). "Extensive monosynaptic inhibition of ventral respiratory group neurons by augmenting neurons in the Botzinger complex in the cat." Exp Brain Res **81**(3): 639-648.

Jin, X., N. Cui, W. Zhong, X. T. Jin and C. Jiang (2013). "GABAergic synaptic inputs of locus coeruleus neurons in wild-type and Mecp2-null mice." Am J Physiol Cell Physiol **304**(9): C844-857.

Jin, X. T., N. Cui, W. Zhong, X. Jin, Z. Wu and C. Jiang (2013). "Pre- and postsynaptic modulations of hypoglossal motoneurons by alpha-adrenoceptor activation in wild-type and Mecp2(-/Y) mice." Am J Physiol Cell Physiol **305**(10): C1080-1090.

Johnson, C. M., N. Cui, H. Xing, Y. Wu and C. Jiang (2020). "The antitussive cloperastine improves breathing abnormalities in a Rett Syndrome mouse model by blocking presynaptic GIRK channels and enhancing GABA release." Neuropharmacology **176**: 108214.

Johnson, C. M., N. Cui, W. Zhong, M. F. Oginsky and C. Jiang (2015). "Breathing abnormalities in a female mouse model of Rett syndrome." J Physiol Sci **65**(5): 451-459.

Jonkman, K., E. van Rijnsoever, E. Olofsen, L. Aarts, E. Sarton, M. van Velzen, M. Niesters and A. Dahan (2018). "Esketamine counters opioid-induced respiratory depression." Br J Anaesth **120**(5): 1117-1127.

Jordan, D. (2001). "Central nervous pathways and control of the airways." Respir Physiol **125**(1-2): 67-81.

Jung, S., T. D. Jones, J. N. Lugo, Jr., A. H. Sheerin, J. W. Miller, R. D'Ambrosio, A. E. Anderson and N. P. Poolos (2007). "Progressive dendritic HCN channelopathy during epileptogenesis in the rat pilocarpine model of epilepsy." J Neurosci **27**(47): 13012-13021.

Katz, D. M., M. Dutschmann, J. M. Ramirez and G. Hilaire (2009). "Breathing disorders in Rett syndrome: progressive neurochemical dysfunction in the respiratory network after birth." Respir Physiol Neurobiol **168**(1-2): 101-108.

Kawano, T., P. Zhao, S. Nakajima and Y. Nakajima (2004). "Single-cell RT-PCR analysis of GIRK channels expressed in rat locus coeruleus and nucleus basalis neurons." Neurosci Lett **358**(1): 63-67.

Kerr, A. M., Y. Nomura, D. Armstrong, M. Anvret, P. V. Belichenko, S. Budden, H. Cass, J. Christodoulou, A. Clarke, C. Ellaway, M. d'Esposito, U. Francke, M. Hulten, P. Julu, H. Leonard, S. Naidu, C. Schanen, T. Webb, I. W. Engerstrom, Y. Yamashita and M. Segawa (2001). "Guidelines for reporting clinical features in cases with MECP2 mutations." Brain Dev **23**(4): 208-211.

Kim, D. Y., B. W. Carey, H. Wang, L. A. Ingano, A. M. Binshtok, M. H. Wertz, W. H. Pettingell, P. He, V. M. Lee, C. J. Woolf and D. M. Kovacs (2007). "BACE1 regulates voltage-gated sodium channels and neuronal activity." Nat Cell Biol **9**(7): 755-764.

Kim, K. Y., E. Hysolli and I. H. Park (2011). "Neuronal maturation defect in induced pluripotent stem cells from patients with Rett syndrome." Proc Natl Acad Sci U S A **108**(34): 14169-14174.

Klausberger, T., P. J. Magill, L. F. Marton, J. D. Roberts, P. M. Cobden, G. Buzsaki and P. Somogyi (2003). "Brain-state- and cell-type-specific firing of hippocampal interneurons in vivo." Nature **421**(6925): 844-848.

Kline, D. D., A. Ramirez-Navarro and D. L. Kunze (2007). "Adaptive depression in synaptic transmission in the nucleus of the solitary tract after in vivo chronic intermittent hypoxia: evidence for homeostatic plasticity." J Neurosci **27**(17): 4663-4673.

Knoflach, F. and J. A. Kemp (1998). "Metabotropic glutamate group II receptors activate a G protein-coupled inwardly rectifying K+ current in neurones of the rat cerebellum." J Physiol **509 (Pt 2)**: 347-354.

Kobelt, P., K. Burke and P. Renker (2014). "Evaluation of a standardized sedation assessment for opioid administration in the post anesthesia care unit." Pain Manag Nurs **15**(3): 672-681.

Kofuji, P., N. Davidson and H. A. Lester (1995). "Evidence that neuronal G-protein-gated inwardly rectifying K+ channels are activated by G beta gamma subunits and function as heteromultimers." Proc Natl Acad Sci U S A **92**(14): 6542-6546.

Koontz, M. A., L. E. Hendrickson, S. T. Brace and A. E. Hendrickson (1993). "Immunocytochemical localization of GABA and glycine in amacrine and displaced amacrine cells of macaque monkey retina." Vision Res **33**(18): 2617-2628.

Kuwana, S., N. Tsunekawa, Y. Yanagawa, Y. Okada, J. Kuribayashi and K. Obata (2006). "Electrophysiological and morphological characteristics of GABAergic respiratory neurons in the mouse pre-Botzinger complex." Eur J Neurosci **23**(3): 667-674.

Lai, Y. T., C. K. Su, S. T. Jiang, Y. J. Chang, A. C. Lai and Y. S. Huang (2016). "Deficiency of CPEB2-Confined Choline Acetyltransferase Expression in the Dorsal Motor Nucleus of Vagus Causes Hyperactivated Parasympathetic Signaling-Associated Bronchoconstriction." J Neurosci **36**(50): 12661-12676.

Lesage, F., E. Guillemare, M. Fink, F. Duprat, C. Heurteaux, M. Fosset, G. Romey, J. Barhanin and M. Lazdunski (1995). "Molecular properties of neuronal G-protein-activated inwardly rectifying K+ channels." J Biol Chem **270**(48): 28660-28667.

Levitt, E. S., A. P. Abdala, J. F. Paton, J. M. Bissonnette and J. T. Williams (2015). "mu opioid receptor activation hyperpolarizes respiratory-controlling Kolliker-Fuse neurons and suppresses post-inspiratory drive." J Physiol **593**(19): 4453-4469.

Li, W., X. Xu and L. Pozzo-Miller (2016). "Excitatory synapses are stronger in the hippocampus of Rett syndrome mice due to altered synaptic trafficking of AMPA-type glutamate receptors." Proc Natl Acad Sci U S A **113**(11): E1575-1584.

Liang, X., Z. Yong and R. Su (2018). "Inhibition of protein kinase A and GIRK channel reverses fentanyl-induced respiratory depression." Neurosci Lett **677**: 14-18.

Liao, D., H. Lin, P. Y. Law and H. H. Loh (2005). "Mu-opioid receptors modulate the stability of dendritic spines." Proc Natl Acad Sci U S A **102**(5): 1725-1730.

Liao, Y. J., Y. N. Jan and L. Y. Jan (1996). "Heteromultimerization of G-protein-gated inwardly rectifying K+ channel proteins GIRK1 and GIRK2 and their altered expression in weaver brain." J Neurosci **16**(22): 7137-7150.

Linazasoro, G., M. T. Garmendia and X. Lizaso (2000). "Acute dystonia in a young schizophrenic patient associated with ingestion of a cloperastine containing cough syrup." Parkinsonism Relat Disord **6**(1): 57-58.

Llamosas, N., L. Ugedo and M. Torrecilla (2017). "Inactivation of GIRK channels weakens the pre- and postsynaptic inhibitory activity in dorsal raphe neurons." Physiol Rep **5**(3).

Lorier, A. R., G. D. Funk and J. J. Greer (2010). "Opiate-induced suppression of rat hypoglossal motoneuron activity and its reversal by ampakine therapy." PLoS One **5**(1): e8766.

Lotsch, J., C. Skarke, A. Schneider, T. Hummel and G. Geisslinger (2005). "The 5-hydroxytryptamine 4 receptor agonist mosapride does not antagonize morphine-induced respiratory depression." Clin Pharmacol Ther **78**(3): 278-287.

Lozovaya, N., R. Nardou, R. Tyzio, M. Chiesa, A. Pons-Bennaceur, S. Eftekhari, T. T. Bui, M. Billon-Grand, J. Rasero, P. Bonifazi, D. Guimond, J. L. Gaiarsa, D. C. Ferrari and Y. Ben-Ari (2019). "Early alterations in a mouse model of Rett syndrome: the GABA developmental shift is abolished at birth." Sci Rep **9**(1): 9276.

Luoni, M., S. Giannelli, M. T. Indrigo, A. Niro, L. Massimino, A. Iannielli, L. Passeri, F. Russo, G. Morabito, P. Calamita, S. Gregori, B. Deverman and V. Broccoli (2020). "Whole brain delivery of an instability-prone Mecp2 transgene improves behavioral and molecular pathological defects in mouse models of Rett syndrome." Elife **9**.

Luscher, C., L. Y. Jan, M. Stoffel, R. C. Malenka and R. A. Nicoll (1997). "G protein-coupled inwardly rectifying K+ channels (GIRKs) mediate postsynaptic but not presynaptic transmitter actions in hippocampal neurons." Neuron **19**(3): 687-695.

Luscher, C. and P. A. Slesinger (2010). "Emerging roles for G protein-gated inwardly rectifying potassium (GIRK) channels in health and disease." Nat Rev Neurosci **11**(5): 301-315.

Mansour, A., H. Khachaturian, M. E. Lewis, H. Akil and S. J. Watson (1987). "Autoradiographic differentiation of mu, delta, and kappa opioid receptors in the rat forebrain and midbrain." J Neurosci **7**(8): 2445-2464.

Mantegazza, M., A. Gambardella, R. Rusconi, E. Schiavon, F. Annesi, R. R. Cassulini, A. Labate, S. Carrideo, R. Chifari, M. P. Canevini, R. Canger, S. Franceschetti, G. Annesi, E. Wanke and A. Quattrone (2005). "Identification of an Nav1.1 sodium channel (SCN1A) loss-of-function mutation associated with familial simple febrile seizures." Proc Natl Acad Sci U S A **102**(50): 18177-18182.

Manzke, T., M. Dutschmann, G. Schlaf, M. Morschel, U. R. Koch, E. Ponimaskin, O. Bidon, P. M. Lalley and D. W. Richter (2009). "Serotonin targets inhibitory synapses to induce modulation of network functions." Philos Trans R Soc Lond B Biol Sci **364**(1529): 2589-2602.

Manzke, T., M. Niebert, U. R. Koch, A. Caley, S. Vogelgesang, A. M. Bischoff, S. Hulsmann, E. Ponimaskin, U. Muller, T. G. Smart, R. J. Harvey and D. W. Richter (2011). "[Serotonin receptor 1A-modulated dephosphorylation of glycine receptor alpha3: a new molecular mechanism of breathing control for compensation of opioid-induced respiratory depression without loss of analgesia]." Schmerz **25**(3): 272-281.

Marchetto, M. C., C. Carromeu, A. Acab, D. Yu, G. W. Yeo, Y. Mu, G. Chen, F. H. Gage and A. R. Muotri (2010). "A model for neural development and treatment of Rett syndrome using human induced pluripotent stem cells." Cell **143**(4): 527-539.

Marron Fernandez de Velasco, E., L. Zhang, N. V. B, M. Tipps, S. Farris, Z. Xia, A. Anderson, N. Carlblom, C. D. Weaver, S. M. Dudek and K. Wickman (2017). "GIRK2 splice variants and neuronal G protein-gated K(+) channels: implications for channel function and behavior." Sci Rep **7**(1): 1639.

May, C. N., M. R. Dashwood, C. J. Whitehead and C. J. Mathias (1989). "Differential cardiovascular and respiratory responses to central administration of selective opioid agonists in conscious rabbits: correlation with receptor distribution." Br J Pharmacol **98**(3): 903-913.

McMenamin, C. A., L. Anselmi, R. A. Travagli and K. N. Browning (2016). "Developmental regulation of inhibitory synaptic currents in the dorsal motor nucleus of the vagus in the rat." J Neurophysiol **116**(4): 1705-1714.

Medrano, M. C., M. T. Santamarta, P. Pablos, Z. Aira, I. Buesa, J. J. Azkue, A. Mendiguren and J. Pineda (2017). "Characterization of functional mu opioid receptor turnover in rat locus coeruleus: an electrophysiological and immunocytochemical study." Br J Pharmacol **174**(16): 2758-2772.

Medrihan, L., E. Tantalaki, G. Aramuni, V. Sargsyan, I. Dudanova, M. Missler and W. Zhang (2008). "Early defects of GABAergic synapses in the brain stem of a MeCP2 mouse model of Rett syndrome." J Neurophysiol **99**(1): 112-121.

Mellios, N., D. A. Feldman, S. D. Sheridan, J. P. K. Ip, S. Kwok, S. K. Amoah, B. Rosen, B. A. Rodriguez, B. Crawford, R. Swaminathan, S. Chou, Y. Li, M. Ziats, C. Ernst, R. Jaenisch, S. J. Haggarty and M. Sur (2018). "MeCP2-regulated miRNAs control early human neurogenesis through differential effects on ERK and AKT signaling." Mol Psychiatry **23**(4): 1051-1065.

Mercadante, S., E. Arcuri and A. Santoni (2019). "Opioid-Induced Tolerance and Hyperalgesia." CNS Drugs **33**(10): 943-955.

Merriam, E. B., M. Millette, D. C. Lumbard, W. Saengsawang, T. Fothergill, X. Hu, L. Ferhat and E. W. Dent (2013). "Synaptic regulation of microtubule dynamics in dendritic spines by calcium, F-actin, and drebrin." J Neurosci **33**(42): 16471-16482.

Mesuret, G., J. Dannenberg, M. Arnoldt, A. A. Grutzner, M. Niebert and S. Hulsmann (2018). "Breathing disturbances in a model of Rett syndrome: A potential involvement of the glycine receptor alpha3 subunit?" Respir Physiol Neurobiol **248**: 43-47.

Mitrovic, I., M. Margeta-Mitrovic, S. Bader, M. Stoffel, L. Y. Jan and A. I. Basbaum (2003). "Contribution of GIRK2-mediated postsynaptic signaling to opiate and alpha 2-adrenergic analgesia and analgesic sex differences." Proc Natl Acad Sci U S A **100**(1): 271-276.

Montandon, G., W. Qin, H. Liu, J. Ren, J. J. Greer and R. L. Horner (2011). "PreBotzinger complex neurokinin-1 receptor-expressing neurons mediate opioid-induced respiratory depression." J Neurosci **31**(4): 1292-1301.

Montandon, G., J. Ren, N. C. Victoria, H. Liu, K. Wickman, J. J. Greer and R. L. Horner (2016). "G-protein-gated Inwardly Rectifying Potassium Channels Modulate Respiratory Depression by Opioids." Anesthesiology **124**(3): 641-650.

Morgado-Valle, C., S. M. Baca and J. L. Feldman (2010). "Glycinergic pacemaker neurons in preBotzinger complex of neonatal mouse." J Neurosci **30**(10): 3634-3639.

North, R. A., J. T. Williams, A. Surprenant and M. J. Christie (1987). "Mu and delta receptors belong to a family of receptors that are coupled to potassium channels." Proc Natl Acad Sci U S A **84**(15): 5487-5491.

O'Dell, T. J., R. D. Hawkins, E. R. Kandel and O. Arancio (1991). "Tests of the roles of two diffusible substances in long-term potentiation: evidence for nitric oxide as a possible early retrograde messenger." Proc Natl Acad Sci U S A **88**(24): 11285-11289.

Oertel, B. G., L. Felden, P. V. Tran, M. H. Bradshaw, M. S. Angst, H. Schmidt, S. Johnson, J. J. Greer, G. Geisslinger, M. A. Varney and J. Lotsch (2010). "Selective antagonism of opioid-

induced ventilatory depression by an ampakine molecule in humans without loss of opioid analgesia." Clin Pharmacol Ther **87**(2): 204-211.

Oertel, B. G., A. Schneider, M. Rohrbacher, H. Schmidt, I. Tegeder, G. Geisslinger and J. Lotsch (2007). "The partial 5-hydroxytryptamine1A receptor agonist buspirone does not antagonize morphine-induced respiratory depression in humans." Clin Pharmacol Ther **81**(1): 59-68.

Oginsky, M. F., N. Cui, W. Zhong, C. M. Johnson and C. Jiang (2014). "Alterations in the cholinergic system of brain stem neurons in a mouse model of Rett syndrome." Am J Physiol Cell Physiol **307**(6): C508-520.

Oginsky, M. F., N. Cui, W. Zhong, C. M. Johnson and C. Jiang (2017). "Hyperexcitability of Mesencephalic Trigeminal Neurons and Reorganization of Ion Channel Expression in a Rett Syndrome Model." J Cell Physiol **232**(5): 1151-1164.

Ohno, K., Y. Saito, R. Ueda, M. Togawa, T. Ohmae, E. Matsuda, M. Fujiyama and Y. Maegaki (2016). "Effect of Serotonin 1A Agonists and Selective Serotonin Reuptake Inhibitors on Behavioral and Nighttime Respiratory Symptoms in Rett Syndrome." Pediatr Neurol **60**: 54-59 e51.

Oranje, P., R. Gouka, L. Burggraaff, M. Vermeer, C. Chalet, G. Duchateau, P. van der Pijl, M. Geldof, N. de Roo, F. Clauwaert, T. Vanpaeschen, J. Nicolai, T. de Bruyn, P. Annaert, I. J. AP and G. J. P. van Westen (2019). "Novel natural and synthetic inhibitors of solute carriers SGLT1 and SGLT2." Pharmacol Res Perspect **7**(4): e00504.

Ornung, G., O. Shupliakov, H. Linda, O. P. Ottersen, J. Storm-Mathisen, B. Ulfhake and S. Cullheim (1996). "Qualitative and quantitative analysis of glycine- and GABA-immunoreactive nerve terminals on motoneuron cell bodies in the cat spinal cord: a postembedding electron microscopic study." J Comp Neurol **365**(3): 413-426.

Ozawa, Y. and N. Okado (2002). "Alteration of serotonergic receptors in the brain stems of human patients with respiratory disorders." Neuropediatrics **33**(3): 142-149.

Paterson, D. S., E. G. Thompson, R. A. Belliveau, B. A. Antalffy, F. L. Trachtenberg, D. D. Armstrong and H. C. Kinney (2005). "Serotonin transporter abnormality in the dorsal motor nucleus of the vagus in Rett syndrome: potential implications for clinical autonomic dysfunction." J Neuropathol Exp Neurol **64**(11): 1018-1027.

Pejhan, S., V. M. Siu, L. C. Ang, M. R. Del Bigio and M. Rastegar (2020). "Differential brain region-specific expression of MeCP2 and BDNF in Rett Syndrome patients: a distinct grey-white matter variation." Neuropathol Appl Neurobiol **46**(7): 735-750.

Pepper, C. M. and G. Henderson (1980). "Opiates and opioid peptides hyperpolarize locus coeruleus neurons in vitro." Science **209**(4454): 394-395.

Petukhova, E., D. Ponomareva, M. Mukhamedyarov, G. Maleeva and P. Bregestovski (2018). "Developmental Changes in the Inhibition of Glycinergic Synaptic Currents by Niflumic Acid in Hypoglossal Motoneurons." Front Mol Neurosci **11**: 416.

Ponce, A., E. Bueno, C. Kentros, E. Vega-Saenz de Miera, A. Chow, D. Hillman, S. Chen, L. Zhu, M. B. Wu, X. Wu, B. Rudy and W. B. Thornhill (1996). "G-protein-gated inward rectifier K+ channel proteins (GIRK1) are present in the soma and dendrites as well as in nerve terminals of specific neurons in the brain." J Neurosci **16**(6): 1990-2001.

Poria, D. and N. K. Dhingra (2015). "Spontaneous oscillatory activity in rd1 mouse retina is transferred from ON pathway to OFF pathway via glycinergic synapse." J Neurophysiol **113**(2): 420-425.

Pourzitaki, C., G. Tsaousi, G. Papazisis, A. Kyrgidis, C. Zacharis, A. Kritis, F. Malliou and D. Kouvelas (2018). "Fentanyl and naloxone effects on glutamate and GABA release rates from anterior hypothalamus in freely moving rats." Eur J Pharmacol **834**: 169-175.

Purcell, A. E., O. H. Jeon, A. W. Zimmerman, M. E. Blue and J. Pevsner (2001). "Postmortem brain abnormalities of the glutamate neurotransmitter system in autism." Neurology **57**(9): 1618-1628.

Quaresma, P. G. F., P. D. S. Teixeira, F. Wasinski, A. M. P. Campos, E. O. List, J. J. Kopchick and J. Donato, Jr. (2020). "Cholinergic neurons in the hypothalamus and dorsal motor nucleus of the vagus are directly responsive to growth hormone." Life Sci **259**: 118229.

Racke, K., U. R. Juergens and S. Matthiesen (2006). "Control by cholinergic mechanisms." Eur J Pharmacol **533**(1-3): 57-68.

Ramirez, J. M., N. J. Burgraff, A. D. Wei, N. A. Baertsch, A. G. Varga, H. A. Baghdoyan, R. Lydic, K. F. Morris, D. C. Bolser and E. S. Levitt (2021). "Neuronal mechanisms underlying opioid-induced respiratory depression: our current understanding." J Neurophysiol **125**(5): 1899-1919.

Ren, J., X. Ding, G. D. Funk and J. J. Greer (2009). "Ampakine CX717 protects against fentanyl-induced respiratory depression and lethal apnea in rats." Anesthesiology **110**(6): 1364-1370.

Ren, J., X. Ding and J. J. Greer (2015). "5-HT1A receptor agonist Befiradol reduces fentanyl-induced respiratory depression, analgesia, and sedation in rats." Anesthesiology **122**(2): 424-434.

Ren, J., X. Ding and J. J. Greer (2019). "Activating alpha4beta2 Nicotinic Acetylcholine Receptors Alleviates Fentanyl-induced Respiratory Depression in Rats." Anesthesiology **130**(6): 1017-1031.

Ren, J., X. Ding and J. J. Greer (2020). "Countering Opioid-induced Respiratory Depression in Male Rats with Nicotinic Acetylcholine Receptor Partial Agonists Varenicline and ABT 594." Anesthesiology **132**(5): 1197-1211.

Ren, J., B. Y. Poon, Y. Tang, G. D. Funk and J. J. Greer (2006). "Ampakines alleviate respiratory depression in rats." Am J Respir Crit Care Med **174**(12): 1384-1391.

Ribeiro, M. C. and J. L. MacDonald (2020). "Sex differences in Mecp2-mutant Rett syndrome model mice and the impact of cellular mosaicism in phenotype development." Brain Res **1729**: 146644.

Richter, D. W. and J. C. Smith (2014). "Respiratory rhythm generation in vivo." Physiology (Bethesda) **29**(1): 58-71.

Roozekrans, M., R. van der Schrier, P. Okkerse, J. Hay, J. F. McLeod and A. Dahan (2014). "Two studies on reversal of opioid-induced respiratory depression by BK-channel blocker GAL021 in human volunteers." Anesthesiology **121**(3): 459-468.

Roux, J. C., N. Panayotis, E. Dura and L. Villard (2010). "Progressive noradrenergic deficits in the locus coeruleus of Mecp2 deficient mice." J Neurosci Res **88**(7): 1500-1509.

Saito, Y., M. Ito, Y. Ozawa, T. Matsuishi, K. Hamano and S. Takashima (2001). "Reduced expression of neuropeptides can be related to respiratory disturbances in Rett syndrome." Brain Dev **23 Suppl 1**: S122-126.

Salpietro, V., C. L. Dixon, H. Guo, O. D. Bello, J. Vandrovcova, S. Efthymiou, R. Maroofian, G. Heimer, L. Burglen, S. Valence, E. Torti, M. Hacke, J. Rankin, H. Tariq, E. Colin, V. Procaccio, P. Striano, K. Mankad, A. Lieb, S. Chen, L. Pisani, C. Bettencourt, R. Mannikko, A. Manole, A. Brusco, E. Grosso, G. B. Ferrero, J. Armstrong-Moron, S. Gueden, O. Bar-Yosef, M. Tzadok, K. G. Monaghan, T. Santiago-Sim, R. E. Person, M. T. Cho, R. Willaert,

Y. Yoo, J. H. Chae, Y. Quan, H. Wu, T. Wang, R. A. Bernier, K. Xia, A. Blesson, M. Jain, M. M. Motazacker, B. Jaeger, A. L. Schneider, K. Boysen, A. M. Muir, C. T. Myers, R. H. Gavrilova, L. Gunderson, L. Schultz-Rogers, E. W. Klee, D. Dyment, M. Osmond, M. Parellada, C. Llorente, J. Gonzalez-Penas, A. Carracedo, A. Van Haeringen, C. Ruivenkamp, C. Nava, D. Heron, R. Nardello, M. Iacomino, C. Minetti, A. Skabar, A. Fabretto, S. S. Group, M. Raspall-Chaure, M. Chez, A. Tsai, E. Fassi, M. Shinawi, J. N. Constantino, R. De Zorzi, S. Fortuna, F. Kok, B. Keren, D. Bonneau, M. Choi, B. Benzeev, F. Zara, H. C. Mefford, I. E. Scheffer, J. Clayton-Smith, A. Macaya, J. E. Rothman, E. E. Eichler, D. M. Kullmann and H. Houlden (2019). "AMPA receptor GluA2 subunit defects are a cause of neurodevelopmental disorders." Nat Commun **10**(1): 3094.

Sanabria, E. R., H. Su and Y. Yaari (2001). "Initiation of network bursts by Ca2+-dependent intrinsic bursting in the rat pilocarpine model of temporal lobe epilepsy." J Physiol **532**(Pt 1): 205-216.

Saugstad, J. A., T. P. Segerson and G. L. Westbrook (1996). "Metabotropic glutamate receptors activate G-protein-coupled inwardly rectifying potassium channels in Xenopus oocytes." J Neurosci **16**(19): 5979-5985.

Sbardella, D., G. R. Tundo, V. Cunsolo, G. Grasso, R. Cascella, V. Caputo, A. M. Santoro, D. Milardi, A. Pecorelli, C. Ciaccio, D. Di Pierro, S. Leoncini, L. Campagnolo, V. Pironi, F. Oddone, P. Manni, S. Foti, E. Giardina, C. De Felice, J. Hayek, P. Curatolo, C. Galasso, G. Valacchi, M. Coletta, G. Graziani and S. Marini (2020). "Defective proteasome biogenesis into skin fibroblasts isolated from Rett syndrome subjects with MeCP2 non-sense mutations." Biochim Biophys Acta Mol Basis Dis **1866**(7): 165793.

Scain, A. L., H. Le Corronc, A. E. Allain, E. Muller, J. M. Rigo, P. Meyrand, P. Branchereau and P. Legendre (2010). "Glycine release from radial cells modulates the spontaneous activity and its propagation during early spinal cord development." J Neurosci **30**(1): 390-403.

Schmidt, A., H. Zhang and M. C. Cardoso (2020). "MeCP2 and Chromatin Compartmentalization." Cells **9**(4).

Schreihofer, A. M., R. L. Stornetta and P. G. Guyenet (1999). "Evidence for glycinergic respiratory neurons: Botzinger neurons express mRNA for glycinergic transporter 2." J Comp Neurol **407**(4): 583-597.

Schwarzacher, S. W., J. C. Smith and D. W. Richter (1995). "Pre-Botzinger complex in the cat." J Neurophysiol **73**(4): 1452-1461.

Shah, M. M., A. E. Anderson, V. Leung, X. Lin and D. Johnston (2004). "Seizure-induced plasticity of h channels in entorhinal cortical layer III pyramidal neurons." Neuron **44**(3): 495-508.

Shah, R. R. and A. P. Bird (2017). "MeCP2 mutations: progress towards understanding and treating Rett syndrome." Genome Med **9**(1): 17.

Shannon, R. and B. G. Lindsey (1987). "Expiratory neurons in the region of the retrofacial nucleus: inhibitory effects of intercostal tendon organs." Exp Neurol **97**(3): 730-734.

Signorini, S., Y. J. Liao, S. A. Duncan, L. Y. Jan and M. Stoffel (1997). "Normal cerebellar development but susceptibility to seizures in mice lacking G protein-coupled, inwardly rectifying K+ channel GIRK2." Proc Natl Acad Sci U S A **94**(3): 923-927.

Simat, M., F. Parpan and J. M. Fritschy (2007). "Heterogeneity of glycinergic and gabaergic interneurons in the granule cell layer of mouse cerebellum." J Comp Neurol **500**(1): 71-83.

Smith, J. C., A. P. Abdala, A. Borgmann, I. A. Rybak and J. F. Paton (2013). "Brainstem respiratory networks: building blocks and microcircuits." Trends Neurosci **36**(3): 152-162.

Smith, J. C., H. H. Ellenberger, K. Ballanyi, D. W. Richter and J. L. Feldman (1991). "Pre-Botzinger complex: a brainstem region that may generate respiratory rhythm in mammals." Science **254**(5032): 726-729.

Snyders, D. J. (1999). "Structure and function of cardiac potassium channels." Cardiovasc Res **42**(2): 377-390.

Soeda, F., Y. Fujieda, M. Kinoshita, T. Shirasaki and K. Takahama (2016). "Centrally acting non-narcotic antitussives prevent hyperactivity in mice: Involvement of GIRK channels." Pharmacol Biochem Behav **144**: 26-32.

Song, G. and C. S. Poon (2004). "Functional and structural models of pontine modulation of mechanoreceptor and chemoreceptor reflexes." Respir Physiol Neurobiol **143**(2-3): 281-292.

Song, G., Y. Yu and C. S. Poon (2006). "Cytoarchitecture of pneumotaxic integration of respiratory and nonrespiratory information in the rat." J Neurosci **26**(1): 300-310.

Squillaro, T., N. Alessio, M. Cipollaro, M. A. Melone, G. Hayek, A. Renieri, A. Giordano and U. Galderisi (2012). "Reduced expression of MECP2 affects cell commitment and maintenance in neurons by triggering senescence: new perspective for Rett syndrome." Mol Biol Cell **23**(8): 1435-1445.

Steinecker, B., C. Rosker and W. Schreibmayer (2007). "The GIRK1 brain variant GIRK1d and its functional impact on heteromultimeric GIRK channels." J Recept Signal Transduct Res **27**(5-6): 369-382.

Stettner, G. M., P. Huppke, C. Brendel, D. W. Richter, J. Gartner and M. Dutschmann (2007). "Breathing dysfunctions associated with impaired control of postinspiratory activity in Mecp2-/y knockout mice." J Physiol **579**(Pt 3): 863-876.

Stotzner, P., V. Spahn, M. O. Celik, D. Labuz and H. Machelska (2018). "Mu-Opioid Receptor Agonist Induces Kir3 Currents in Mouse Peripheral Sensory Neurons - Effects of Nerve Injury." Front Pharmacol **9**: 1478.

Subramaniam, N. S., C. S. Bawden, H. Waldvogel, R. M. L. Faull, G. S. Howarth and R. G. Snell (2018). "Emergence of breath testing as a new non-invasive diagnostic modality for neurodegenerative diseases." Brain Res **1691**: 75-86.

Sultan, P., M. C. Gutierrez and B. Carvalho (2011). "Neuraxial morphine and respiratory depression: finding the right balance." Drugs **71**(14): 1807-1819.

Sun, J., S. R. Chen, H. Chen and H. L. Pan (2019). "mu-Opioid receptors in primary sensory neurons are essential for opioid analgesic effect on acute and inflammatory pain and opioid-induced hyperalgesia." J Physiol **597**(6): 1661-1675.

Sun, L., C. Grutzner, S. Bolte, M. Wibral, T. Tozman, S. Schlitt, F. Poustka, W. Singer, C. M. Freitag and P. J. Uhlhaas (2012). "Impaired gamma-band activity during perceptual organization in adults with autism spectrum disorders: evidence for dysfunctional network activity in frontal-posterior cortices." J Neurosci **32**(28): 9563-9573.

Takigawa, T. and C. Alzheimer (1999). "G protein-activated inwardly rectifying K+ (GIRK) currents in dendrites of rat neocortical pyramidal cells." J Physiol **517 (Pt 2)**: 385-390.

Tan, W., S. Pagliardini, P. Yang, W. A. Janczewski and J. L. Feldman (2010). "Projections of preBotzinger complex neurons in adult rats." J Comp Neurol **518**(10): 1862-1878.

Tan, Z. Y., D. F. Donnelly and R. H. LaMotte (2006). "Effects of a chronic compression of the dorsal root ganglion on voltage-gated Na+ and K+ currents in cutaneous afferent neurons." J Neurophysiol **95**(2): 1115-1123.

Taneja, P., M. Ogier, G. Brooks-Harris, D. A. Schmid, D. M. Katz and S. B. Nelson (2009). "Pathophysiology of locus ceruleus neurons in a mouse model of Rett syndrome." J Neurosci **29**(39): 12187-12195.

Tatetsu, M., J. Kim, S. Kina, H. Sunakawa and C. Takayama (2012). "GABA/glycine signaling during degeneration and regeneration of mouse hypoglossal nerves." Brain Res **1446**: 22-33.

Thomas, J., N. I. Corson, A. Meinhold and C. P. Both (2019). "Neurological excitation in a 6-week-old male infant after morphine overdose." Paediatr Anaesth **29**(10): 1060-1061.

Torrecilla, M., C. L. Marker, S. C. Cintora, M. Stoffel, J. T. Williams and K. Wickman (2002). "G-protein-gated potassium channels containing Kir3.2 and Kir3.3 subunits mediate the acute inhibitory effects of opioids on locus ceruleus neurons." J Neurosci **22**(11): 4328-4334.

Torrecilla, M., N. Quillinan, J. T. Williams and K. Wickman (2008). "Pre- and postsynaptic regulation of locus coeruleus neurons after chronic morphine treatment: a study of GIRK-knockout mice." Eur J Neurosci **28**(3): 618-624.

Treiman, D. M. (2001). "GABAergic mechanisms in epilepsy." Epilepsia **42 Suppl 3**: 8-12.

Turovsky, E., A. Karagiannis, A. P. Abdala and A. V. Gourine (2015). "Impaired CO2 sensitivity of astrocytes in a mouse model of Rett syndrome." J Physiol **593**(14): 3159-3168.

van der Schier, R., M. Roozekrans, M. van Velzen, A. Dahan and M. Niesters (2014). "Opioid-induced respiratory depression: reversal by non-opioid drugs." F1000Prime Rep **6**: 79.

Varga, A. G., B. T. Reid, B. L. Kieffer and E. S. Levitt (2020). "Differential impact of two critical respiratory centres in opioid-induced respiratory depression in awake mice." J Physiol **598**(1): 189-205.

Viemari, J. C., J. C. Roux, A. K. Tryba, V. Saywell, H. Burnet, F. Pena, S. Zanella, M. Bevengut, M. Barthelemy-Requin, L. B. Herzing, A. Moncla, J. Mancini, J. M. Ramirez, L. Villard and G. Hilaire (2005). "Mecp2 deficiency disrupts norepinephrine and respiratory systems in mice." J Neurosci **25**(50): 11521-11530.

Vivekanandarajah, A., K. A. Waters and R. Machaalani (2019). "Cigarette smoke exposure effects on the brainstem expression of nicotinic acetylcholine receptors (nAChRs), and on cardiac, respiratory and sleep physiologies." Respir Physiol Neurobiol **259**: 1-15.

Voituron, N. and G. Hilaire (2011). "The benzodiazepine Midazolam mitigates the breathing defects of Mecp2-deficient mice." Respir Physiol Neurobiol **177**(1): 56-60.

Voituron, N., C. Menuet, M. Dutschmann and G. Hilaire (2010). "Physiological definition of upper airway obstructions in mouse model for Rett syndrome." Respir Physiol Neurobiol **173**(2): 146-156.

Waldvogel, H. J., F. M. Biggins, A. Singh, C. J. Arasaratnam and R. L. M. Faull (2019). "Variable colocalisation of GABAA receptor subunits and glycine receptors on neurons in the human hypoglossal nucleus." J Chem Neuroanat **97**: 99-111.

Wang, I. T., A. R. Reyes and Z. Zhou (2013). "Neuronal morphology in MeCP2 mouse models is intrinsically variable and depends on age, cell type, and Mecp2 mutation." Neurobiol Dis **58**: 3-12.

Wang, J. G., J. A. Strong, W. Xie and J. M. Zhang (2007). "Local inflammation in rat dorsal root ganglion alters excitability and ion currents in small-diameter sensory neurons." Anesthesiology **107**(2): 322-332.

Wang, J. M., P. B. Johnston, B. G. Ball and R. D. Brinton (2005). "The neurosteroid allopregnanolone promotes proliferation of rodent and human neural progenitor cells and regulates cell-cycle gene and protein expression." J Neurosci **25**(19): 4706-4718.

Ward, C. S., E. M. Arvide, T. W. Huang, J. Yoo, J. L. Noebels and J. L. Neul (2011). "MeCP2 is critical within HoxB1-derived tissues of mice for normal lifespan." J Neurosci **31**(28): 10359-10370.

Weese-Mayer, D. E., S. P. Lieske, C. M. Boothby, A. S. Kenny, H. L. Bennett and J. M. Ramirez (2008). "Autonomic dysregulation in young girls with Rett Syndrome during nighttime in-home recordings." Pediatr Pulmonol **43**(11): 1045-1060.

Wei, J., M. E. Hodes, R. Piva, Y. Feng, Y. Wang, B. Ghetti and S. R. Dlouhy (1998). "Characterization of murine Girk2 transcript isoforms: structure and differential expression." Genomics **51**(3): 379-390.

Wetherington, J. P. and N. A. Lambert (2002). "GABA(B) receptor activation desensitizes postsynaptic GABA(B) and A(1) adenosine responses in rat hippocampal neurones." J Physiol **544**(2): 459-467.

Williams, J. T., M. J. Christie and O. Manzoni (2001). "Cellular and synaptic adaptations mediating opioid dependence." Physiol Rev **81**(1): 299-343.

Wilson, R. I. and R. A. Nicoll (2001). "Endogenous cannabinoids mediate retrograde signalling at hippocampal synapses." Nature **410**(6828): 588-592.

Winter, S. M., J. Fresemann, C. Schnell, Y. Oku, J. Hirrlinger and S. Hulsmann (2009). "Glycinergic interneurons are functionally integrated into the inspiratory network of mouse medullary slices." Pflugers Arch **458**(3): 459-469.

Wu, Y., W. Zhong, N. Cui, C. M. Johnson, H. Xing, S. Zhang and C. Jiang (2016). "Characterization of Rett Syndrome-like phenotypes in Mecp2-knockout rats." J Neurodev Disord **8**: 23.

Wydeven, N., E. Marron Fernandez de Velasco, Y. Du, M. A. Benneyworth, M. C. Hearing, R. A. Fischer, M. J. Thomas, C. D. Weaver and K. Wickman (2014). "Mechanisms underlying the activation of G-protein-gated inwardly rectifying K+ (GIRK) channels by the novel anxiolytic drug, ML297." Proc Natl Acad Sci U S A **111**(29): 10755-10760.

Yamanouchi, H., M. Kaga and M. Arima (1993). "Abnormal cortical excitability in Rett syndrome." Pediatr Neurol **9**(3): 202-206.

Yousefifard, M., M. H. Vazirizadeh-Mahabadi, A. M. Neishaboori, S. N. R. Alavi, M. Amiri, A. Baratloo and P. Saberian (2020). "Intranasal versus Intramuscular/Intravenous Naloxone for Pre-hospital Opioid Overdose: A Systematic Review and Meta-analysis." Adv J Emerg Med **4**(2): e27.

Zhang, L., J. He, D. G. Jugloff and J. H. Eubanks (2008). "The MeCP2-null mouse hippocampus displays altered basal inhibitory rhythms and is prone to hyperexcitability." Hippocampus **18**(3): 294-309.

Zhang, S., C. M. Johnson, N. Cui, H. Xing, W. Zhong, Y. Wu and C. Jiang (2016). "An optogenetic mouse model of rett syndrome targeting on catecholaminergic neurons." J Neurosci Res **94**(10): 896-906.

Zhang, W. and D. J. Linden (2003). "The other side of the engram: experience-driven changes in neuronal intrinsic excitability." Nat Rev Neurosci **4**(11): 885-900.

Zhang, X., N. Cui, Z. Wu, J. Su, J. S. Tadepalli, S. Sekizar and C. Jiang (2010). "Intrinsic membrane properties of locus coeruleus neurons in Mecp2-null mice." Am J Physiol Cell Physiol **298**(3): C635-646.

Zhang, X., J. Su, N. Cui, H. Gai, Z. Wu and C. Jiang (2011). "The disruption of central CO2 chemosensitivity in a mouse model of Rett syndrome." Am J Physiol Cell Physiol **301**(3): C729-738.

Zhang, X., J. Su, A. Rojas and C. Jiang (2010). "Pontine norepinephrine defects in Mecp2-null mice involve deficient expression of dopamine beta-hydroxylase but not a loss of catecholaminergic neurons." Biochem Biophys Res Commun **394**(2): 285-290.

Zhilenko, V. N., N. V. Khoroshilova and V. M. Efremova (1989). "[Hygienic evaluation of atactic polypropylene]." Gig Sanit(12): 86-87.

Zhong, W., N. Cui, X. Jin, M. F. Oginsky, Y. Wu, S. Zhang, B. Bondy, C. M. Johnson and C. Jiang (2015). "Methyl CpG Binding Protein 2 Gene Disruption Augments Tonic Currents of gamma-Aminobutyric Acid Receptors in Locus Coeruleus Neurons: IMPACT ON NEURONAL EXCITABILITY AND BREATHING." J Biol Chem **290**(30): 18400-18411.

Zhong, W., C. M. Johnson, N. Cui, H. Xing, Y. Wu and C. Jiang (2017). "Effects of chronic exposure to low dose THIP on brainstem neuronal excitability in mouse models of Rett syndrome: Evidence from symptomatic females." Neuropharmacology **116**: 288-299.

Zhong, W., C. M. Johnson, Y. Wu, N. Cui, H. Xing, S. Zhang and C. Jiang (2016). "Effects of early-life exposure to THIP on phenotype development in a mouse model of Rett syndrome." J Neurodev Disord **8**: 37.

Zhou, X., D. Han, R. Xu, H. Wu, C. Qu, F. Wang, X. Wang and Y. Zhao (2016). "Glycine protects against high sucrose and high fat-induced non-alcoholic steatohepatitis in rats." Oncotarget **7**(49): 80223-80237.

APPENDIX:

US Patent

- **Hao Xing**, Christopher M Johnson, Chun Jiang. *WO2020236693 - Morphine-induced respiratory depression: behavioral, phrenic and brainstem respiratory neuronal evidence*. App. No. PCT/US2020/033360. November 26, 2020.

Publications

1. **Hao Xing**, Ningren Cui, Hongmin Yao, Christopher M. Johnson, Chun Jiang. Cloperastine reduces morphine-induced respiratory depression in rats: Potential mechanisms for GIRK channel inhibition in locus coeruleus neurons. J Cell Physiol. Under review.
2. Yang Wu, Ningren Cui, **Hao Xing**, Weiwei Zhong, Colin Arrowood, Christopher M Johnson, Chun Jiang. *In vivo* evidence for the cellular basis of central hypoventilation of Rett syndrome and pharmacological correction in the rat model. J Cell Physiol. 2021 Jun 2. doi: 10.1002/jcp.30462. Online ahead of print.
3. **Hao Xing**, Ningren Cui, Christopher M. Johnson, Zaakir Faisthalab, Chun Jiang. Functional consequences of GABA/glycine onto hypoglossal and dorsal motor nucleus of vagus with/without *Mecp2* gene disruption. J Cell Physiol. 2021 May;236(5):3615-3628.
4. Christopher M Johnson, Ningren Cui, **Hao Xing**, Yang Wu, Chun Jiang. The antitussive cloperastine improves breathing abnormalities in a Rett Syndrome mouse model by blocking presynaptic GIRK channels and enhancing GABA release. Neuropharmacology. 2020 Jul 3; 176: 108214.

5. Wu Y, Cui N, **Xing H**, Zhong W, Arrowood C, Johnson CM, Jiang C. *Mecp2* Disruption in Rats Causes Reshaping in Firing Activity and Patterns of Brainstem Respiratory Neurons. Neuroscience. 2019 Jan 15;397:107-115.
6. Zhong W, Johnson CM, Cui N, **Xing H**, Wu Y, Jiang C. Effects of chronic exposure to low dose THIP on brainstem neuronal excitability in mouse models of Rett syndrome: Evidence from symptomatic females. Neuropharmacology. 2017 Jan 6; 116: 288-299.
7. Zhong W, Johnson CM, Wu Y, Cui N, **Xing H**, Zhang S, Jiang C. Effects of early-life exposure to THIP on phenotype development in a mouse model of Rett syndrome. J Neurodev Disord. 2016 Oct 19; 8: 37.
8. Johnson CM, Zhong W, Cui N, Wu Y, **Xing H**, Zhang S, Jiang C. Defects in brainstem neurons associated with breathing and motor function in the *Mecp2*$^{R168-/Y}$ mouse model of Rett syndrome. Am J Physiol Cell Physiol. 2016 Dec 1; 311 (6): C895-C909.
9. Zhang S, Johnson CM, Cui N, **Xing H**, Zhong W, Wu Y, Jiang C. An optogenetic mouse model of rett syndrome targeting on catecholaminergic neurons. J Neurosci Res. 2016 Oct; 94 (10): 896-906.
10. Wu Y, Zhong W, Cui N, Johnson CM, **Xing H**, Zhang S, Jiang C. Characterization of Rett Syndrome-like phenotypes in *Mecp2*-knockout rats. J Neurodev Disord. 2016 Jun 16; 8: 23.
11. Wang S, Cao W, **Xing H**, Chen YL, Li Q, Shen T, Jiang C, Zhu D, Activation of ERK pathway is required for 15-HETE-induced angiogenesis in human umbilical vascular endothelial cells. J Recept Signal Transduct Res. 2016;36:225-32.
12. Yan Xing, Xiaodong Zheng, Guixia Li, Lin Liao, Weiwei Cao, **Hao Xing**, Tingting Shen, Lihua Sun, Baofeng Yang, Daling Zhu. MicroRNA-30c contributes to the development

of hypoxia pulmonary hypertension by decreasing PDGFRβ expression. Int J Biochem Cell Biol. 2015 Jul;64:155-66.

13. Wei L, Zhang B, Cao W, **Xing Hao**, Yu X, Zhu D. Inhibition of CXCL12/CXCR4 suppresses pulmonary arterial smooth muscle cell proliferation and cell cycle progression via PI3K/Akt pathway under hypoxia. J Recept Signal Transduct Res. 2014 Nov 25:1-11.
14. Song S, Wang S, Jun M, Lan Y, **Hao Xing**, Lei Zhang, Lin Liao, Daling Zhu. Biliverdin reductase/bilirubin mediates the anti-apoptotic effect of hypoxia in pulmonary arterial smooth muscle cells through ERK1/2 pathway. Exp Cell Res. 2013 Aug 1; 319(13):1973-87.